Port Gamble S'Klallam Tribe Coastal Analysis: Shoreline Change and Extreme Water Levels

Mitchell Hatfield

A report prepared in partial fulfillment of
the requirements for the degree of

Master of Science
Earth and Space Sciences: Applied Geosciences

University of Washington

March 2020

Project mentor:
Ian Miller, Washington Sea Grant

Internship coordinator:
Kathy Troost

Reading committee:
Ian Miller
Kathy Troost
Juliet Crider

MESSAGe Technical Report Number: 087

Executive Summary

The Port Gamble S'Klallam Tribe (PGST) relies on coastal resources for recreation, cultural enrichment, spiritual enhancement, and food. Shoreline change and extreme water levels associated with climate change will impact the future of the PGST. As part of their effort to create a coastal management plan, PGST contracted with our project team to assess geologic aspects of coastal risk and provide recommendations for future monitoring.

There is limited information on coastal geomorphology, sediment transportation, and accurate water levels for the PGST coast (Ladd et al., 2016; McCollum et al., 2016). This report addresses shoreline changes, extreme water levels, and coastal hazards associated with climate change along the PGST coastline. I designed a sediment transport monitoring system and conducted water level measurement and analyses.

For the first Phase of this project, I assessed historical coastal bluff and shoreline changes using aerial photographs, historical maps and photographs, shoreline topographic surveys, LiDAR analysis, and time-lapse photography. I established shoreline transects for future monitoring of the PGST shoreline and collected baseline data. Using historical T-sheet survey data with modern LiDAR, I found the PGST bluff erosion rates to be less than 3.7 ± 2.8 in/yr over a 162-yr period from 1856 to 2018, with the highest rate along the Tribal Center bluff. Overall, the beach face appears to be relatively stable with little evidence of change from our GNSS beach transect surveys.

To evaluate extreme water levels, I collected water level data along the PGST coast and compared our local water level measurements to long-term water level records at Port Townsend and Seattle. Water level data at PGST suggest that using longer water level records from Seattle and Port Townsend would reliably predict flood magnitude and frequency at PGST. Our data show bluffs currently undergo frequent interaction with sea water. During our study, time-lapse photography showed small (< 1 ft) waves with limited wave run-up. However, while not entirely common along the PGST coastline, the combination of larger storm events with high tides may cause flooding of Point Julia and increase bluff erosion rates.

Lastly, I assessed the response of coastal flooding to climate change along the PGST coastline. Extreme water levels will flood most of Point Julia under different climate change scenarios. We created a series of inundation maps at Point Julia based on recent sea level rise projections for the area (Miller et al., 2018). Climate change and sea level rise will impact the coastline and how the tribe interacts with it.

The development of detailed sediment budgets and shoreline change models requires long-term, high-resolution datasets. While our data provide a baseline, continued study and additional data are recommended to make informed coastal management decisions. I recommend performing frequent (2-3 years, seasonally, or event-aligned) repeat surveys of the established shoreline transects. I recommend yearly surveying for transects in areas of highest erosion (i.e. near the Tribal Center). Flooding and bluff erosion may be mitigated by projects which support large woody debris and increased sediment on beaches. Coastal inundation maps may be helpful for planning and management strategies, considering the time frame and likelihood of each scenario.

Table of Contents

List of Figures

List of Tables

1. Introduction and Motivation

The coastline of Port Gamble S'Klallam Tribal land is shaped by a dynamic marine environment and diverse geologic conditions. Natural coastal hazards, especially erosion and flooding, are the consequences of these conditions. Climate change is likely to exacerbate both hazards. The Port Gamble S'Klallam Tribe (PGST) relies on coastal resources for recreation, cultural enrichment, spiritual enhancement, and food. The future of the PGST is interconnected with the coastal area and the effects of climate change.

There is limited information and only low-resolution data on coastal geomorphology and sediment transportation for the PGST coast (Ladd et al., 2016; McCollum et al., 2016). Accurate water elevation and tidal fluctuation data for the PGST coastline are also lacking. As part of their effort to create a coastal management plan, PGST contracted with our project team to assess geologic aspects of coastal risk and provide recommendations for future monitoring. Members of the project team include Ian Miller, Kathy Troost, Sam Angel, and Crystal Lambert. We divided this work into three phases:

- PHASE 1: Evaluating coastal sediment transport and current beach conditions
- PHASE 2: Evaluating bluff stability
- PHASE 3: Evaluating the impacts of sea level rise on the beach and bluffs

This report focuses on Phases 1 and 3 of the study, for which I have primary responsibility. Separate reports address bluff stability and possible impacts to bluff stability from sea level rise.

I divided Phase 1 of the study into 4 tasks:

- TASK 1: Evaluate historical shoreline change
- TASK 2: Design sediment transport monitoring
- TASK 3: Conduct water level measurement and analyses
- TASK 4: Provide recommendations for PGST for their coastal management plan

For Phase 3 I assessed the impacts of sea level rise. I used recently published sea level rise projections for the State of Washington (Miller et al., 2018) and created inundation maps for the PGST coastline (NOAA Office of Coastal Management, 2017).

2. Background

PGST lands are located near the northern end of the Kitsap Peninsula in the central basin of Puget Sound (Figure 1). The PGST coastline consists of bluff-backed beaches, a cuspate foreland (Point Julia), and stream fan deltas (Figure 2). The near surface geology of the area consists primarily of Glaciomarine Drift; Vashon Stade recessional outwash deposits; till, advance outwash sands; and Pre-Vashon sand, silt, clay, till, and glaciomarine deposits (Polenz et al., 2015). Irregular, discontinuous glacial and interglacial stratigraphy is typical of the Puget Lowland as successive glaciers eroded and deposited material (Garling and Molenaar, 1965). Since deglaciation, Kitsap Peninsula coastal beaches and bluffs have continued to erode from wave action (Garling and Molenaar, 1965).

The bluffs on PGST land consist of predominantly glacially overridden deposits capped by some looser, not overridden deposits. Glacially overridden deposits are dense to very dense granular and very stiff to hard fine-grained sediment. PGST coastal bluffs are steep with interbedded coarse, fine-grained, and mixed material. Springs and seeps can also be found on the coastal bluffs. PGST bluffs are subject to landsliding. Some of the coarse deposits are easily eroded due to low cohesion, despite being glacially overridden. Weathering (from wave action, tree roots, freeze-thaw, groundwater, rain, and chemical weathering) of the deposits produces colluvium which contributes to shallow slope failures, especially in wet weather.

Subglacial scour in the Puget Lowland left steep bluffs (Booth, 1994). Rivers formed to drain the saturated sediments and transport precipitation from the uplands into the Puget Sound. Sea level rise at the end of the Vashon Glaciation (~13,000 years ago (Thorson, 1980)) contributed to bluff retreat and erosion. Rapid sea level rise until about 6000 ka contributed to significant erosion and the development of landslides and feeder bluffs (Troost, 1994). The rate of sea level rise then slowed, resulting in beach aggradation and the development of spits, deltas, and points (like Point Julia) from long-shore drift (Troost and Stein, 1995).

Bluff retreat is a major concern in the Puget Lowland where homes and other structures are built near Puget Sound. Armoring the base of bluffs can mitigate bluff erosion caused by wave action. Armoring of bluffs in the Elwha drift cell on the Strait of Juan de Fuca reduced bluff recession rates by 50% (Kaminsky et al., 2014). However, armoring has negative impacts on the nearshore ecosystem and the adjacent beaches and bluffs (Heerhartz et al., 2016). Armoring reduces beach wrack and sediment fluxes to the intertidal beach. Bluffs are the primary source of sediment to beaches in the Puget Lowland where rivers are not present (Keuler, 1988) and play a key role in supporting a healthy nearshore ecosystem. Some marine organisms (such as forage fish) rely on sediment delivered from bluffs. Shoreline armoring disrupts the transport of bluff-derived sediment to beaches, leads to larger and more variable beach sediment in the intertidal zone, and lowers ecological function of beaches (Parks et al., 2013).

Where some form of armoring is necessary to protect homes, roads and other structures, alternative armoring methods can be used in place of traditional bulkheads by considering site conditions and risk tolerance (Gerstel and Brown, 2006; Gerstel et al., 2012). Alternatives to shoreline armoring may include beach nourishment, artificial beach berms, shaped beach slopes, or large woody debris (anchored or unanchored) and may see varying levels of success. Attempts to supplement sediment to beaches in Puget Lowland through beach nourishment projects have also seen varying levels of success (Shipman, 2001).

Many bluffs adjacent to Puget Sound are considered feeder bluffs. Shipman et al. (2014) defined a feeder bluff as “an eroding coastal bluff that delivers a significant amount of sediment to the beach over an extended period of time and contributes to the local littoral sediment budget” (p. iv). Monitoring local littoral (or drift) cell sediment budgets is an important component of a coastal management plan. Taggart (1984) identified two drift cells along the PGST coast (Figure 3): one to the north and one to the south of Point Julia, a cuspate foreland built by the convergence of these two drift cells. As sediment is transported, relatively stable and unstable zones form on the beach face. Beach profile transects and sampling of beach materials can be used to assess how sediment is transported and sorted along a beach (Self, 1977).

Ladd et al. (2016) broadly identified three main coastal geomorphic and sediment transport zones along PGST coast:

1. North of Point Julia with high energy waves and larger sediment
2. At Point Julia with accumulating sandy beaches and tidal wetland
3. South of Point Julia with a more protected shoreline area of mostly fine sand, silt and clay

They also reported little degradation of coastal landforms and ecological function with bluffs contributing sediment and vegetation to the beaches.

3. Shoreline Change

3.1. Introduction

For Phase 1, I assessed historical coastal bluff and shoreline changes using aerial photographs, historical maps and photographs, shoreline topographic surveys, LiDAR analysis, and time-lapse photography. I also adopted a sediment transport monitoring program and started the long-term collection of monitoring data. I identified target areas for long-term monitoring of bluff and shoreline changes.

3.2. Background

Shoreline form is a function of the inherited geology and topography of the coast and how the land interacts with sea level change as physical processes redistribute sediment (Shipman, 2008). Shoreline change is influenced by many factors including wind, waves, currents, streams, climate, shoreline geology and geomorphology, and human influence. Wind and waves erode shorelines, transport sediment, and deposit sediment in new areas, reworking the shoreline. Local geologic and geomorphic heterogeneity create relatively stable and less stable areas of the shoreline. Vegetation, woody debris, and armoring of the shoreline add stability to the shoreline. This variation of shoreline characteristics and redistribution of sediment creates erosional (bluffs) or depositional (points, spits, and estuaries) shorelines (Shipman, 2008).

The PGST shoreline consists of predominantly bluff-backed beaches. Wind waves transport sediment at the base of bluffs. This wave action destabilizes bluffs through debuttressing and oversteepening. Beaches provide natural protection of bluffs from wave erosion as wave energy is dissipated over the beach face (Dean, 1991). The amount of bluff/wave exposure varies with the tide. High tides reduce the amount of beach available to dissipate energy, thus allowing waves to undercut and transport sediment at the base of bluffs.

Observations at Cama Beach, WA showed dominant storms are the most important sediment transport events in a low-wave energy environment like Puget Sound (Finlayson, 2006). Dominant storms are storms that are strong enough to initiate sediment transport and occur frequently enough to have a cumulative effect on beach geomorphology. Dominant storms in Puget Sound generally occur every several years or more but are more frequent than 50- and 100-year storms (Finlayson, 2006). Longshore drift sediment transport rates are relatively low in beaches adjacent to Puget Sound because of the mostly low wave-energy environment (Shipman et al., 2014).

Wallace (1988) quantified sediment transport rates at twenty-six different sites in the Puget Lowland. Of these twenty-six sites, the Port Gamble mill site was among the lowest five drift cell rates he measured (105 yd^3/yr). For comparison, the average net shore-drift rate for the six East-Central Region sites (including Port Gamble) was 1,960 yd^3/yr (Wallace, 1988). Wallace determined the major factors influencing net shore-drift rates are fetch (the distance over water the wave-generating wind blows), availability of sediment, and drift cell length. Taggart (1984) mapped two drift cells converging at Point Julia (Figure 3).

Little work has been done to quantify change rates along the PGST shoreline. Ladd et al. (2016) identified that grain size on PGST beaches is likely associated with different sediment transport

regimes along the PGST coast. They characterized the PGST coastline south of Point Julia as a low energy environment and north of Point Julia as a higher energy environment.

3.3. Methods

I used a variety of data sets to evaluate shoreline change along the PGST coast (Table 1).

Table 1. Sources used for evaluating PGST shoreline change

Source	Bluff Erosion Analysis	Shoreline Change Analysis	Beach Grain Size Mapping
T-sheet (T-585)	✓	✓	
2018 LiDAR	✓		
Aerial photos (vertical)		✓	
Aerial photos (oblique)	✓	✓	
GNSS survey		✓	✓
LiDAR (DTM) differencing	✓	✓	
Time-lapse photography		✓	
Drone photography			✓
Citizen survey	✓		

3.3.1. Coastal Bluff Erosion Analysis

The bluffs backing most of PGST's beaches are eroding at varying rates. As bluffs erode, they contribute sediment to PGST beaches and are important for the health of the PGST shoreline. However, valuable property like homes and invaluable property such as the tribe cemetery are near the bluffs. To help understand rates of bluff erosion, I estimated historical bluff erosion rates using a historical survey map and modern LiDAR data.

In the 1850s, surveyors used a plane-board system to map the shorelines of the Port Gamble Bay area and created maps known as T-sheets. I used an 1856 surveyed T-sheet map (T-585) to calculate historical erosion rates (Puget Sound River History Project, 2003). I used the digitized version of this T-sheet to compare historical bluff crest position with modern bluff crest position using 2018 LiDAR data (Quantum Spatial, 2018). The T-sheet showed four stretches of surveyed bluffs along PGST's coast (Figure 4). To map the modern bluff crest, I used a 2018 LiDAR-derived digital terrain model (DTM), with 3-foot horizontal resolution and estimated 0.184-foot vertical resolution (Quantum Spatial, 2018). This LiDAR was served on Washington DNR's LiDAR Portal in Washington State Plane Zone South Coordinates in units of U.S. Survey Feet. Using LiDAR, I digitized the bluff crest along PGST bluffs using hillshade and slope maps in ArcMap 10.5.1 (Figure 5). Specifically, I used the maximum break in slope to trace the bluff crest.

Digitizing and georeferencing maps and images introduces some uncertainty into the estimate of the position of a feature like a bluff crest. To estimate potential error in the mapped location of the bluff crests, I used methods like those outlined by Morton et al. (2004) and MacLennan et al. (2018).

I used a modified equation from Morton et al. (2004) and MacLennan et al. (2018) to calculate the maximum position error and maximum cumulative uncertainty associated with our mapping of shoreline features (Equation 1; Table 2). I calculated *maximum* uncertainty values. Actual error of the mapped shoreline features may be smaller than values in Table 2. The sources of error addressed in this equation include uncertainty introduced during the georeferencing process (rectification error), the digitization of shoreline features (digitizing error), surveying the shoreline (survey error), and LiDAR positioning (LiDAR position error). Table 3 describes these uncertainty terms and how I assigned values in greater detail.

Equation 1: $$E_{sp} = \sqrt{E_r^2 + E_d^2 + E_t^2 + E_{tr}^2 + E_l^2}$$

Table 2. Bluff crest mapping uncertainty values

Measurement error (ft)	**1856 T-sheet**	**2018 Lidar**
Digitizing error (E_d)	6.56	—
T-sheet survey error (E_t)	27.9	—
T-sheet rectification error (E_{tr})	13.1	—
LiDAR position error (E_l)	—	6
Maximum total shoreline position error (E_{sp})	31.5	6
Maximum cumulative uncertainty (ft)	**37.5**	
Maximum annualized error (ft/yr)	0.232	
Maximum annualized error (in/yr)	2.78	

Table 3. Description of terms used to assess mapped shoreline features

Term	Error value	Description
Rectification error (E_r)	Average RMS Error	The rectification error is quantified in ArcMap using root mean square error values (RMSE). ArcMap calculates RMSE during the georeferencing processes. ArcMap uses the distance between selected points on the georeferenced image and the corresponding point on the base image to quantify the RMSE. I used the average RMSE for each aerial photo I digitized. I omitted this error value for images I did not need to digitize/georeference.
Digitizing error (E_d)	Average pixel size	The digitizing error is meant to capture uncertainty introduced during the digitizing of shoreline features. The exact position of shoreline features can be difficult to determine, especially with images of lower quality resolution. Since this digitizing error is closely associated with image resolution, I used the pixel size as the error value. Pixel size is considered in the LiDAR position error, so I did not use this term for 2018 LiDAR error calculation.
T-sheet survey error (E_t)	Maximum survey error	I determined the maximum T-sheet survey error based on National Map Accuracy Standards. According to NOAA, hard copies of historical T-sheets should "meet or exceed current National Map Accuracy Standards" (shoreline.noaa.gov/data/datasheets/t-sheets.html). This T-sheet was mapped at a scale of 1:10,000. According to National Map Accuracy Standards, this means the sheet should be horizontally accurate within 27.9 ft (U. S. Geological Survey, 1999).
T-sheet rectification error (E_{tr})	T-sheet horizontal accuracy	This T-sheet (T-585) was digitized by the UW River History Project. This project digitized and georeferenced the T-sheet hard copy and digitized shoreline features. I used the estimated maximum horizontal accuracy of this T-sheet as determined by the River History Project as our error value. More details of the T-sheet digitization process and data quality can be found at: http://riverhistory.ess.washington.edu/tsheets/nad27/t0585_meta.html.
LiDAR position error (E_l)	2x the grid spacing	I used 2018 LiDAR data for digitizing the bluff crest. To account for the error introduced during this process, I used 2x the LiDAR grid spacing as the LiDAR positional error value.

I measured the difference in coastal bluff crest position along established shoreline transects (section 3.3.2.3. Shoreline Changes from Survey Data) and calculated an average erosion rate for each area over the 162-year period. I used this long-term bluff retreat rate rather than comparing more recent LiDAR datasets because of (a) poor horizontal resolution in earlier LiDAR datasets and (b) short-term timescales may represent localized events rather than long-term, spatially representative, sustained bluff retreat.

Finally, I used water level data in conjunction with LiDAR data to perform a simple bluff-water interaction evaluation (section 4.3.1. Water Level Data Collection). I mapped the base of the bluff from 2018 LiDAR using the hillshade and slope maps as described above. By taking the average base of bluff elevation on bluff-backed beaches from 2018 LiDAR along the established shoreline transects (section 3.3.2.3. Shoreline Changes from Survey Data), I calculated the percentage of time water level was above the base of bluff elevation during our water logger deployment period.

3.3.2. Historical Shoreline Change Analysis

3.3.2.1. Shoreline Changes from Aerial Photos

I compared shoreline position estimated from aerial photographs from different years to evaluate the extent of shoreline change at PGST. Different features can be used as a proxy for shoreline position when looking at historical shoreline changes. Some of these features may include: the high-water line, beach berms, the base of bluffs, or vegetation line or wrack lines. For this study, I used the vegetation line visible in aerial photographs as a proxy for shoreline to assess shoreline change because it is the most distinguishable feature along PGST beaches in historical aerial photos.

For historical shoreline change analysis, I used aerial photos from August 1942, June 1965, April 1995, July 2003, and July 2017 (all available at the University of Washington library). These aerial photos vary in resolution and include grayscale and color photographs. I scanned, imported, and georeferenced non-digital images in ArcMap 10.5.1. I also incorporated the mapped shoreline (high-water line) from an 1865 NOAA historical survey (T-sheet) (Puget Sound River History Project, 2003).

I used the same equation and methods described above (section 3.3.1. Historical Coastal Bluff Erosion Analysis) to address uncertainty in the shoreline vegetation change mapping. Table 4 shows the maximum total shoreline position error for sources used and the maximum cumulative uncertainty.

Table 4. Shoreline change mapping uncertainty values

Measurement error (ft)	1856 T-sheet	1944	1965	1995	2003	2017
Rectification error (E_r)	—	40.15	5.81E-10	2.61	1.01	—
Digitizing error (E_d)	6.56	2.76	0.72	1.86	1.80	3.28
T-sheet survey error (E_t)	27.9	—	—	—	—	—
T-sheet rectification error (E_{tr})	13.1	—	—	—	—	—
LiDAR position error (E_l)	—	—	—	—	—	—
Maximum total shoreline position error (E_{sp})	31.5	40.2	0.72	3.21	2.06	3.28
Maximum cumulative uncertainty (ft)			**81**			

3.3.2.2. Shoreline Changes from Historical Oblique Photographs

To supplement aerial photographs, I also incorporated historical aerial oblique photographs to assess shoreline change. These photographs are published by Washington State Department of Ecology and date back to 1977 (Washington State Department of Ecology, 2019). The ability to quantify shoreline change rates is limited using oblique photos. However, oblique photos are helpful for qualitatively assessing changes to beaches and bluffs and identifying possible focus areas for monitoring. I compared oblique photo sets from 1977, 1990, 2000, 2006, and 2016.

3.3.2.3. Shoreline Changes from Survey Data

I surveyed beach elevations using centimeter grade Global Navigation Satellite System (GNSS) receivers. Using this surveying equipment, I can repeat surveys on established transects along PGST beaches to evaluate short- (i.e. weeks) and mid-term (i.e. years) changes. I worked with Dr. Ian Miller to establish a total of 65 transects spaced approximately 200 ft apart with closer spacing of transects on Point Julia (Figure 6). I occupied each of these transects at least once during our study to establish baseline conditions. Of these shoreline transects, I established a "focus reach" of 18 transects for more frequent surveying. I chose these transects based on regular spacing intervals but adjusted the spacing to capture areas of interest. For this study, I gathered profiles along these transects in the summer, early fall, and late fall of 2019 to look for seasonal dynamics and establish baseline conditions for future monitoring.

I surveyed these transects from the water up toward the bluff, collecting points on 1-second intervals using a Trimble Geo7x GNSS receiver. These GNSS data were post-processed using Trimble Pathfinder Office to increase the accuracy of the survey. To assess the error of the GNSS system used, I performed repeat surveys along the Point Julia road and at a benchmark near the hatchery. Post-processed precision based on these control surveys was exceptional (Std Dev = 0.03 feet), but our surveyed control elevations were consistently lower than the control elevation at the hatchery benchmark (12.95 ft NAVD 88; Wnek Engineering, 2014; Table 5). The source of this bias was not clear, but I applied a 5.94-inch manual vertical correction to our survey data in order to establish consistency with the published survey control on Point Julia.

Table 5. Difference between our surveyed elevations and benchmark control elevation

Date	Our surveyed elevation (ft NAVD 88)	Inches below published elevation
7/14/2019	12.50	5.43
8/4/2019	12.43	6.18
8/31/2019	12.48	5.63
10/21/2019	12.45	5.94
10/21/2019	12.46	5.91
10/21/2019	12.41	6.46
10/21/2019	12.48	5.59
10/25/2019	12.46	5.83
10/25/2019	12.41	6.46
Average	**12.45**	**5.94**
Std. deviation	0.03	0.35

3.3.2.4. Shoreline Changes from DTM-Differencing Analysis

I used publicly available aerial LiDAR-derived DTMs from February 2005, March 2014, September 2014 and February 2018 (Table 6) to evaluate spatially explicit changes in beaches and bluffs. I converted DTM raster values to uniform units using the raster calculator tool in ArcMAP 10.5.1. I then clipped the DTMs to the study area and reprojected them to a uniform coordinate system (NAD 1983 State Plane Washington North FIPS 4601; NAVD 1988). Using the raster calculator and "con" tools, I calculated the difference of raster values between datasets to show areas of apparent erosion and deposition. To assess the DTM quality, I used the stack profiles tool on transect lines to extract LiDAR profiles.

I assessed quality of these LiDAR DTMs and determined the 2005 LiDAR to be of too low resolution to use in our study to detect shoreline and bluff changes. DTM-differencing and shoreline profiling using LiDAR over a relatively short period of time requires a certain level of horizontal and vertical resolution to assess changes. The 2014 and 2018 LiDAR datasets provide some context for shoreline change but given the resolution (3 ft horizontal), they do not accurately detect small changes over this short period. These airborne LiDAR datasets are especially unreliable for vertical surface differencing of the bluffs.

Table 6. LiDAR metadata

Survey date	Survey type	Grid spacing (ft)	Surveyor
February 2005	Airborne	6.0	Terrapoint *for* Puget Sound Regional Council
March 2014	Boat-based topobathy	3.28	Washington State Department of Ecology
September 2014	Airborne topobathy (CZMIL)	3.0	OCM Partners, USACE *for* USGS
February 2018	Airborne	3.0	Quantum Spatial *for USGS*

3.3.2.5. Shoreline Changes from Time-Lapse Photography

I deployed a time-lapse camera to assess event-driven shoreline changes and sediment transport processes on Point Julia. I used a Wingscapes TimelapseCam Pro camera. I placed the camera about 30 ft high on a light pole near the south boat ramp of Point Julia (Figure 2). This camera was aimed north, taking pictures of the beach near the north boat ramp on Point Julia. The camera took one photo at least every 30 minutes from November 2019 to mid-February 2020. I compiled photos into time-lapse videos and visually analyzed them, looking for changes and dominant patterns. As of the writing of this report, the camera was still in place.

3.3.3. Beach Grain Size Mapping

To establish baseline conditions of the beach, I mapped beach sediment grain size (Figure 7). I classified grain sizes visually and using field techniques. I mapped grain size in the field using a high resolution (~0.79 in) orthomosaic image from drone photography as the base map (Figure 8). I used Agisoft PhotoScan 1.2.6 to create the orthomosaic from 2,514 photos captured with a DJI Phantom 3 drone FC300X camera flown at 100-165 ft above the beach surface (Appendix A). To increase the spatial accuracy of the orthomosaic, I used 13 ground control points (GCP) captured using a Trimble Geo7x GNSS receiver.

3.4. Findings

3.4.1. Historical Coastal Bluff Erosion Analysis

Using the bluff crest surveyed in 1856 and the bluff crest from 2018 LiDAR I calculated historical bluff erosion rates for four areas along the PGST coast: north of Shipbuilders Creek, near the Tribal Center, south of the community garden, and near Middle Creek (Table 7). I limited historical bluff erosion rates to these four areas because they were the only areas showing bluff crest position on the 1856 T-sheet (Figure 4).

Table 7. PGST coastal bluff crest erosion rates between 1856 and 2018

Area	Mean bluff change (ft)	Mean erosion rate (in/yr)	Number of transects
North of Shipbuilders Creek	23.0	1.7 ± 2.8	11
Tribal Center bluffs	49.9	3.7 ± 2.8	9
South of community garden	29.9	2.2 ± 2.8	1
Near Middle Creek	30.8	2.3 ± 2.8	2

Based on these erosion rates, I estimated the volume of sediment contributed to PGST beaches from the bluffs (Table 8). I calculated these sediment volumes using average bluff height and length of the bluff segment in each area. I also normalized these volumes for foot sections of the bluff to make relevant sediment flux comparisons.

Table 8. Sediment flux to beaches from PGST coastal bluffs from 1856 to 2018

Area	Segment length (ft)	Sediment flux to the beaches (yd^3/yr)	Normalized sediment flux to beaches ($ft^3/ft/yr$)
North of Shipbuilders creek	2,210	520 ± 860	6.4 ± 11
Tribal Center bluffs	1,600	980 ± 740	35 ± 27
South of community garden	215	39 ± 50	5.0 ± 6.4
Near Middle Creek	465	170 ± 210	9.9 ± 12

Based on our simple bluff-water interaction analysis from water logger data and LiDAR data, from August 3, 2019 to December 18, 2019, water was at or above the base of the bluff for an average of about 50 minutes per day. However, given the nature of tidal fluctuations, bluffs may be exposed to water much longer or shorter than this on any given day.

3.4.2. Historical Shoreline Change Analysis

On Point Julia, historical aerial photos and T-sheet analysis of proxy shorelines suggest possible landward migration trends around the southern perimeter of Point Julia (Figure 9). Trends on the northern side of Point Julia are less clear, possibly from the north boat ramp acting as a groin. At the tip of Point Julia, historical aerial photos between 1965 and 2017 suggest landward movement of the shoreline of approximately 45 ft, though it is not clear if this is due to erosion, sea level rise, or other processes. The shoreline at the tip of Point Julia appears to have moved seaward between 1865 and 1965, but I assign low confidence to this observation based on the uncertainty in mapped shoreline positions (Table 4).

North of Point Julia near Shipbuilders Creek, historical aerial photos and the T-sheet suggest an overall landward movement of the vegetation line, though the processes driving this erosion may be associated with creek mouth dynamics (Figure 10). Further north of Point Julia and south of Point Julia, shoreline change from aerial photography is not detectable.

Oblique photographs showed signs of bluff instability along the PGST coast (Figure 11). Bluff failures often seem to be associated with tree removal along the bluffs (Figures 12, 13), and tree removal on bluffs appears to have been common, especially between 1977 and 1990 (Figure 14).

Between 2000 and 2006, there appeared to be an increase in the frequency of bluff failures (Figures 15, 16). Oblique photos showed sediment delivery to the upper beach face along the PGST coastline through dry ravel, tree topple, and shallow landslides.

Our GNSS survey data coupled with LiDAR suggest little in the way of seasonal shoreline dynamics, Most short-term shoreline change observed during our study is generally associated with creek mouths to the north of Point Julia (Figure 10). The LiDAR in particular does not appear to have adequate resolution to detect small changes on the bluff face, and possible changes in the intertidal zone are rarely larger than the uncertainty. Overall, the shoreline appears to be relatively stable over the last 5 years (Appendix B). However, the shoreline profile on the tip of Point Julia shows measurable scallop of about 1 m in the upper intertidal zone between 2014 and 2018 (Figure 17).

Analysis of time-lapse photos suggested a dominant wind wave direction from north to south with occasional waves from the south-southwest on the north side of Point Julia in November and December 2019. While the wave directions suggest a dominant north to south sediment transport pattern on the north side of Point Julia, I could not detect any significant shoreline changes in the time-lapse photographs or survey data during this time period.

3.4.3. Beach Grain Size Mapping

PGST beaches are generally divided into fines (fine sand, silt, and clay) south of Point Julia, sands (fine to coarse) around Point Julia and north to Shipbuilders Creek, and gravel/cobbles north of Shipbuilders Creek (Figure 7). It should be noted that grain size map shows the *predominan*t grain size on the beach face. Much of PGST beaches have mixed grain sizes and grain size may vary with seasons and storms. Table 9 has a more detailed description of mapped grain sizes.

Table 9. Grain size descriptions

Mapped grain size	Description	Predominant grain size
Fines	Predominantly mixed fine sand, silt, and clay. Some sand, gravel, and shells.	< #40 sieve (0.0165 in)
Sand	Predominantly sand (fine to coarse) with some gravel and shells.	#200 (0.0029 in) – #4 sieve (0.197 in)
Mixed sand and gravel	Predominantly mixed sand (fine to coarse) and gravel (fine to coarse). Areas near the base of the bluffs tend to have gravel surface armoring with some cobbles.	#200 sieve - 3 in
Mixed gravel and cobbles	Predominantly gravel and cobbles with some boulders. Armored surface (lag deposit).	0.75 – 12 in

3.5. Discussion

3.5.1. Historical Coastal Bluff Erosion Analysis

Our data show small (<3.7 ± 2.8 in/yr) rates of bluff erosion, with the highest retreat rates to the south of Point Julia (Figure 18). Average bluff erosion rates along the PGST coastline range from 1.7 to 3.7 ± 2.8 in/yr (Table 7) between 1856 and 2018. The estimated erosion rate for bluffs north of Shipbuilders Creek, south of the community garden, and near Middle Creek are smaller than the annualized uncertainty. Therefore, with these data, erosion is not detectable along these three bluff areas. However, these erosion rates are comparable to other published erosion rates in the area giving us some confidence (MacLennan et al., 2018). These rates are slightly lower than the 4.32 in/yr rate found by MacLennan et al. (2018) at a site approximately 3 miles north of Point Julia. Rates found by MacLennan et al. (2018) may be higher because of greater fetch or because the composition to the north is more erodible. PGST bluff erosion rates are highest at 3.7 ± 2.8 in/yr near the Tribal Center. Tribal members have reported higher incidence of landslides on the bluff near the Tribal Center. There are a number of factors that may be contributing to heightened erosion rates on the bluffs just south of Point Julia including: strong south wind effects, vegetation, increased runoff from development, and bluff composition.

The area contributing the most sediment to PGST beaches based on historical erosion rates and bluff height is the Tribal Center bluff. This bluff contributes approximately 980 ± 740 yd^3/yr or about 35 ± 27 ft^3/ft/yr to the intertidal beach based on the 162-yr data set. Kaminsky et al. (2014) calculated sediment volumes from the Dungeness and Elwha bluffs to be about 80 ft^3/ft/yr and 45 ft^3/ft/yr, respectively for an eleven-year data set from 2001 to 2012. The Elwha and Dungeness bluffs along the Strait of Juan de Fuca are generally taller, exposed to longer fetch, and have different compositions.

Based on an overall average erosion rate, overall average bluff height, and approximate length of bluff-backed beaches on the PGST coast, coastal bluffs contribute approximately 2,800 ± 3900 yd^3 of sediment to PGST beaches per year. This is enough sediment to fill approximately 220 dump trucks each year. This is a rough estimate for sediment input from PGST bluffs and temporal/spatial variability of bluff erosion is expected.

I was not able to supplement our assessment of long-term erosion rates using more recent LiDAR datasets because of poor resolution of airborne LiDAR on vertical surfaces. However, I was able to supplement our findings of historical bluff erosion rates with qualitative assessments from the aerial oblique photographs and a survey of residents conducted by PGST in 2016. Our findings from the oblique photographs support higher bluff erosion rates along the bluff near the Tribal Center. Photos from these bluffs show frequent bluff failure with exposed soil, lacking in vegetation and loss of trees (Figure 19). In the survey conducted in 2016, the residents in this area consistently reported the highest erosion rates of all the residents along the PGST coast.

I found the oblique photographs seemed to show bluffs most commonly failing by tree topple, dry ravel, and shallow landslides. Residents in the 2016 survey noted trees falling and pulling off bluff material. One of the major concerns noted by many residents was a steepening of the bluffs over the years. They noted slides and failures generally associated with heavy rain events.

To assess areas of greatest concern for bluff and shoreline change, I compiled our findings for each area based on historical change rates, historical oblique photographs, the resident survey, and bluff geologic composition (Table 10). I assigned ratings (1-very low hazard, 2-low hazard, 3-medium

hazard, 4-high hazard, 5-very high hazard) based on hazard for each variable. The sum of the values for each area was used to create a total hazard rating relative to other areas of the PGST coast. Figure 20 shows this assessment and the relative concern for each stretch of bluff.

Table 10. Parameters used to rate areas of greatest concern for bluff and shoreline change

Area	Historical bluff erosion rate	Oblique photos	2016 survey of residents	Geology	**Total rating**
North of Shipbuilders Creek	2	3	2	3	**10**
Point Julia	N/D	1	1	3	**5**
Tribal Center	4	5	5	4	**18**
Near community garden	3	4	2	3	**12**
Near Middle Creek	3	3	4	3	**13**

3.5.2. Historical Shoreline Change Analysis

I saw a slight trend of landward migration of vegetation on the south side of Point Julia (Figure 9). Our mapped vegetation line on Point Julia from historical aerial photographs seem more consistent with possible impacts of sea level rise rather than a migration of Point Julia. The relatively landward position of the April 1995 vegetation line compared to the 2017 vegetation line may be due to seasonal vegetation dynamics. Overall, we may be seeing a pattern of feature growth through 1965 and subsequent erosion or impact of sea level rise since 1965. Sea level trend at the Port Townsend tide gauge since 1972 shows an average of 0.07 in/yr relative sea level rise from 1972 to 2019 (NOAA, 2019). This relative sea level rise since 1972 is likely similar at Point Julia and may be contributing to some of the change in the vegetation line on Point Julia.

As identified by Ladd et al. (2016), beach grain size is likely associated with different sediment transport regimes along the PGST coast. However, beach grain size is also related to the composition and armoring of bluffs within drift cells. Generally, beaches are lower energy south of Point Julia with increasing energy north of the point. We might expect lower energy areas south of Point Julia to be relatively more stable zones with finer sediment. Our survey data do confirm relatively stable beach faces south of Point Julia, but I also found the intertidal beach to be relatively stable north of Point Julia. Historical aerial photos and GNSS survey data show the most dynamic sediment transport zones are areas with sediment transport influenced by creek mouths and at the tip of Point Julia. Creek mouths and the tip of Point Julia show evidence of migrating vegetation lines and beach profile variation.

I made a simple conceptual model of a sediment budget for PGST beaches (Figure 21). This model illustrates sediment sources, sediment transport, sediment storage, and sediment deposition/sinks along PGST's coast.

Primary sediment sources along PGST coasts include updrift beaches, bluffs, and streams. Sediment is delivered to the beaches as bluffs erode. Primary mechanisms for bluff erosion at PGST include wind and wave erosion, dry ravel, rainwash, shallow landslides, and tree topple. Sediment from the uplands is delivered to the beaches from creeks and streams. There are six main streams draining

the PGST uplands (Figure 2). Most of the sediment from streams comes from Shipbuilders Creek, Little Boston Creek, and Middle Creek.

Sediment is transported and stored along the beaches of the PGST. Sediment transport on PGST beaches is dominated by swash-zone processes driven by wind waves and tidal fluctuations. Time-lapse photos showed a dominant north to south sediment transport regime north of Point Julia. These findings support net drift cell mapping of the area with converging drift cells at Point Julia (Figure 3). However, time-lapse photos showed that this longshore drift pattern may shift during individual storms. Our GNSS survey data suggest relatively low sediment transport rates on PGST beaches, showing little change in the beach profiles and surface armoring in much of the upper beach shoreface.

Sediment sinks along PGST coasts include sediment transported to deep water and the convergence of sediment at Point Julia. Sediment is transported off the tidal platform and into deep water where it is essentially lost out of the system. Longshore drift transports the remaining sediment on beaches until it reaches Point Julia where it is stored indefinitely.

3.5.3. Beach Grain Size Mapping

The beaches on PGST coast vary in grain size. The beaches consist of clay to boulder size material. These grain sizes are typical of glacial sediment which tends to vary in composition. Beaches of the PGST reflect the grain size and composition of the adjacent bluffs delivering material to the beaches. PGST beaches include lag deposits of cobbles/boulders that are deposited on the beach from eroding bluffs. Cobbles and boulders are left in place, since waves in this low-energy environment are unable to mobilized them. PGST beaches also have areas of gravel surface armoring in the upper beach face near the toe of bluffs. I assume this gravel surface armoring represents relatively stable areas of the beach since the gravel also has dense barnacle covering.

3.6. Conclusions and Monitoring Recommendations

The development of detailed sediment budgets based on quantitative shoreline change and bluff erosion rates require long-term, high-resolution datasets. While our data provide a baseline and give an idea for shoreline processes and dynamics along PGST, continued study and additional data are recommended to make informed coastal management decisions. Additional LiDAR will be especially valuable for bluff monitoring and sediment transport studies. Boat-based or terrestrial LiDAR are recommended for monitoring of bluff faces because they provide more accurate detail of topographic relief on vertical faces (Kaminsky et al., 2014). I found the PGST bluff erosion rates to be less than 3.7 in/yr. The Tribal Center bluffs have the highest erosion rate of 3.7 ± 2.8 in/yr over a 162-yr period from 1856 to 2018. Areas of greatest concern for bluff erosion based on historical bluff erosion rates, historical oblique photographs, a survey of residents, and bluff composition are shown in Figure 20. Overall, the beach face appears to be relatively stable with little evidence of change over the short monitoring period of our GNSS beach profiles. Point Julia and beach areas near creek mouths are relatively less stable with some evidence of change based on historic aerial photographs and GNSS beach profile data.

I have several recommendations for continued monitoring of the beach and bluff:

> I established shoreline transects with eighteen “focus” transects for future monitoring of the PGST shoreline. I recommend performing repeat surveys of the established shoreline transects every 2-3 years or more frequently as required. More frequent, seasonal or event-

aligned surveying of these transects may show interesting shoreline change processes and dynamics. Areas with greatest change (i.e. near the Tribal Center) should be monitored seasonally.
I recommend yearly photo monitoring of the bluff. Crystal Lambert is developing a baseline set of photos to accompany our Phase 2 report.

In addition, obtaining yearly drone-based orthomosaics would be worthwhile for comparing grain size changes on the beach over time.

Images should be downloaded from the time-lapse camera and reviewed on a regular basis to qualitatively evaluated waves and water levels during extreme events.

All of my digital files will be provided to the PGST as baselines for continued monitoring.

4. Extreme Water Level

4.1. Introduction

The ability to predict extreme water level magnitudes and frequencies is critical to evaluating coastal flooding and effective coastal management. To evaluate extreme water levels, I collected water level data along the PGST coast, compared our local water level measurements to long-term water level records in Puget Sound, and assessed wave run-up and total water level.

4.2. Background

The observed water level at a particular location is the sum of the sea level due to tidal (astronomical) forces and non-tidal residuals (NTR) forced by pressure variability and climate cycles (Pugh and Vassie, 1978). This NTR is generalized as the meteorological component of the water level and is often referred to as "surge" or "storm surge" (Pugh and Vassie, 1978). For example, low atmospheric pressure combined with high winds have been found to raise observed sea level by as much as 4.9 ft above the astronomical tide near Toke Point, WA (Serafin et al., 2017). Atmospheric pressure changes of 1 mb produce a 0.76-inch anomaly in sea level in Puget Sound (Finlayson, 2006). During El Nino years, winter sea levels can rise 3.9-7.9 in due to a variety of interacting processes in the North Pacific Ocean (Finlayson, 2006). The most extreme flooding can occur when storm surges coincide with high tides (Pugh and Vassie, 1978).

Astronomical tides are predictable, but NTRs are not. Local tides are modelled and there are many programs to predict tides in an area. However, during a storm surge, NTR's are less readily modelled and may be a critical component to understanding extreme water levels and their potential impact on the coastline. Our goal for this project, therefore, was to compare the NTRs measured near the Port Gamble shoreline with longer NTR records from Seattle and Port Townsend. If NTRs at Port Gamble followed the pattern and magnitude of those measured at Port Townsend and Seattle, I would have greater confidence in predicting flood magnitude and frequency at PGST by applying the extreme water level return frequency curves derived for those locations.

Washington State Department of Ecology produces risk maps to assess flood risk and wave hazard using the Federal Emergency Management Agency's (FEMA) risk assessment tool, Hazus (Washington State Department of Ecology, 2015). These maps show base flood elevation (BFE) or the 1% annual chance of flooding. The BFE for PGST coastline shows flooding up to about 13 ft (NAVD 88), inundating all of Point Julia (Figure 22). WA Department of Ecology (2015) also mapped moderate wave hazard (waves heights <3 ft) for most of PGST shoreline with high wave hazard (wave heights >3 ft) for the northern shoreline (Figure 23). These maps represent extreme events but show the potential for extreme water levels and wave hazard during flooding along the PGST coast.

Waves around Puget Sound have little to no energy component from ocean swell and are generated by local winds, limited by fetch (Finlayson, 2006). Nearby geomorphic features like Teekalet Bluff create a wind shadow for much of PGST coast (Figure 2). Teekalet Bluff limits the fetch for southwesterly winds building on Hood Canal. Fain Environmental modelled wave height in Port Gamble Bay for PGST's FLUPSY facility in 2016 using wind data collected over an approximately 75-

year period at McChord Air Force Base and Bremerton National Airport (Fain Environmental, 2016). Based on that record they modelled waves for a peak windspeed of 76 mph with a southerly fetch. They found the maximum significant wave heights to be about 4.2 ft with a breaking wave height of approximately 6.3 ft at the FLUPSY facility (Figure 2).

At the mouth of Port Gamble Bay, maximum fetch is 14 miles to the north-northwest (Fain Environmental, 2016). Historical wind records show the dominant wind directions are from the northeast and south-southwest. However, fetch is limited to the northeast and south-southwest, so these winds typically do not generate large waves. Disregarding the storm of record, Fain Environmental modelled significant wave and breaking wave heights at the mouth of Port Gamble Bay (Table 11), suggesting maximum significant wave height at Point Julia to be about 3.8 ft, resulting in breaking wave heights on the shoreline of about 5.7 ft (Fain Environmental, 2016). However, average significant and breaking wave heights at Point Julia are only about 0.2 ft and 0.3 ft, respectively. Larger waves are possible, but winds rarely blow from the direction of maximum fetch.

Table 11. Significant and breaking wave height at Point Julia as modelled by Fain Environmental

		Based on Bremerton National Airport Winds	Based on McChord Air Force Base Winds
Significant wave height (ft)	Maximum	3.8	3.2
	Mean	0.2	0.2
	Median	0.2	0.1
Breaking wave height (ft)	Maximum	5.7	4.8
	Mean	0.3	0.3
	Median	0.3	0.2

4.3. Methods

4.3.1. Water Level Data Collection

To collect water level data at Port Gamble, I deployed three Onset HOBO 30-ft titanium water level loggers from August 3, 2019 to December 18, 2019 (Figure 24). I placed these loggers on the north side of Point Julia, on the south side of Point Julia near the hatchery, and near the community garden. Using a logger placed on land (outside of the Natural Resources Department at the Trible Center) to correct for variation in barometric pressure, I calculated the depth of water at each location in the intertidal zone. I measured the water logger elevations (and coordinates), relative to NAVD 88, using a Trimble Geo7x cm grade GNSS receiver (Table 12).

Table 12. Water logger locations and elevations

Location	Date	Elevation (ft NAVD 88)	Latitude	Longitude
North side of Point Julia	10/25/2019 to 11/6/2019	5.18	47.857141333	-122.5742213
	11/6/2019 to 12/18/2019	5.39	47.85714121	-122.5742214
	12/18/2019 to 2/17/2020	5.36	47.85714117	-122.5742216
Near the hatchery	8/3/2019 to 8/31/2019	-3.42	47.85226951	-122.5733867
	8/31/2019 to 10/25/2019	-3.58	47.85226997	-122.5733868
	10/25/2019 to 12/18/2019	4.33	47.85254407	-122.5715162
	12/18/2019 to 2/17/2020	4.40	47.852545386	-122.571517325
South of the community garden	10/25/2019 to 12/18/2019	3.93	47.84598689	-122.568982
	12/18/2019 to 2/17/2020	4.04	47.845986756	-122.568982196

Water level elevations were then converted into a tidal datum by adding the water depth above each water logger and the water logger elevation relative to MLLW at Port Gamble (1.854 ft). I excluded datum when the water level was at or below the water logger.

I accessed both predicted and measured water level data from tide gauges in Port Townsend and Seattle from the NOAA Tides and Currents website (NOAA, 2019). I downloaded six-minute water level observations from August 2019 through December 2019, corresponding with our period of measurement at Port Gamble.

Finally, I used photos taken on December 26, 2018 during a "king" tide event to get an idea for flooding during an exceptionally high tide (Figure 25). Using these photos, I surveyed the elevation of flooding during this event.

4.3.2. Calculating the NTR

At Port Townsend and Seattle, we calculated the NTR using NOAA's tide gauge predicted and measured water levels (predicted levels consider tidal forces but not NTR). For PGST, we differenced our water level measurements with tidal water levels predicted for Bangor, WA, about 13 miles SW into Hood Canal from the PGST (Figure 1), using t_tide (Pawlowicz et al., 2002), implemented in Matlab. Predicted tides for PGST were not available in t_tide, Bangor was the nearest site available.

4.3.3. Wave Run-Up and Total Water Level

Our ability to analyze wave run-up for this study was limited given our time frame and scope of work. However, I used BFE, time-lapse photographs, and a previously conducted wave height analysis study (Fain Environmental, 2016) to get an idea of wave run-up potential during extreme events. I also used time-lapse photography as described above (3.3.2.5. Shoreline Changes from Time-Lapse Photography) to access dominant wave direction and wave height.

4.4. Findings

I found differences in tidal ranges between Port Townsend, Seattle, and Port Gamble (Figure 27). I recorded a maximum water level of 12.19 ft MLLW from August 3, 2019 to December 18, 2019 along the PGST coast. The maximum water levels for this time period at Port Townsend and Seattle were 10.11 ft MLLW and 12.9 ft MLLW, respectively (NOAA, 2019). This is not surprising given tidal range generally increases moving further into Puget Sound (MacLennan et al., 2018).

The difference between the predicted and measured water levels at PGST I estimated were, on average, well within ± 1.5 ft (Figure 27). The estimated NTR at PGST showed more variance than the NTR at Seattle and Port Townsend. The bottom panel of Figure 27 compares the non-tidal residual (NTR) of water levels at each site and shows the NTR pattern from the 3 sites align well. A storm at the end of October 2019 showed an elevated NTR of similar magnitude and pattern at all 3 sites.

From the “king” tide event photos, I found the average flood depth to be 10.5 ft (NAVD 88). The water levels during this event covered the beach face and flooded much of Point Julia (Figure 25). The time-lapse camera also showed significant high tides flooding much of the northern beach on Point Julia (Figure 26).

During deployment of the time-lapse camera in November and December of 2019, I saw dominant north-south wind waves, while occasional storms brought waves from the south-southwest on the north side of Point Julia. These waves had a significant wave height of <1 ft (Figure 28). Based on these photos, I did not see significant wave run-up.

4.5. Discussion

Tides are important to sediment erosion and transport in coastal environments. Diurnal tides at PGST constantly change the area of beach face exposed to the swash zone. This has implications for wave processes on the beach, infiltration/exfiltration, and the beach groundwater table (Finlayson, 2006). Tides are a major component of the total water level (TWL). The ability to predict TWL is integral to coastal hazard analysis.

TWL is a sum of the still water level (tide and NTR) and wave run-up (Serafin et al., 2017). Our data show the upper beach face of PGST is frequently exposed to extreme water levels. The base of the PGST bluffs were exposed to water an average of 50 minutes per day during Fall 2019, however, the average exposure may be higher during stormy periods with significant wave run-up.

The overall NTR signal pattern is consistent with the NTR patterns at Seattle and Port Townsend (Figure 27). This suggests the ability to predict flood frequency at Port Gamble based on Port Townsend and Seattle water level, NTR, and flood frequency predictions. The NTR pattern would

likely be even more similar if we could model predicted tide levels at Port Gamble rather than at Bangor, WA (Figure 1). Water levels at Bangor, WA will be similar but different than at Port Gamble.

Given the time frame for this study and the relatively calm Fall and Winter, I did not see large storm events producing large NTRs. Comparing the NTR magnitude and patterns during large storm events would increase the confidence of our ability to predict PGST flood magnitude and frequency based on Seattle and Port Townsend records.

Time-lapse photos and photos taken during the December 2018 "king" tide event show that much of Point Julia's beaches flood at high tide (Figure 25; Figure 26). If these high tide events were to coincide with a storm producing breaking waves 4.8-5.7 ft high, Point Julia would experience significant flooding. PGST would also likely see significant coastal erosion and impact to the bluffs along the shoreline. Even more impactful would be a storm event with significant waves during a 1% annual probability flood event as shown in the BFE map (Figure 22). Uncommon extreme water level events like this would have serious impacts on the PGST shoreline.

4.6. Conclusions and Monitoring Recommendations

Water level data at PGST suggest using longer water level records from Seattle and Port Townsend would reliably predict flood magnitude and frequency at PGST. Extreme water levels impact much of PGST beaches and bluffs causing flooding and bluff erosion. Our data show bluffs currently undergo frequent interaction with sea water. While large storms are not entirely common in this area of the Puget Lowland, the combination of storm events with high tides may cause flooding of Point Julia and increase bluff erosion rates.

As part of the effort to provide robust sea level rise and storm impact projections for local planners, the USGS has been working to develop a model to predict coastal flooding. This coastal storm modeling system (CoSMoS) has been developed by USGS for coastal areas in California and is currently expanding to provide more coverage. The USGS is working to release CoSMoS for the Puget Sound coastline in the near future (estimated 2020). This numerical model combines sea level rise scenarios, storm impacts, and river flooding to project coastal flooding extent, depth, elevation, maximum wave height, currents, and ecosystem impacts (Barnard et al., 2009). Once Puget Sound CoSMoS is released, we recommend using it to see if it will be a helpful tool for future coastal management and hazard projections. We also recommend downloading images from the time-lapse camera and reviewing them on a regular basis to qualitatively evaluate waves and water levels. Water level data should also be collected from the data loggers on a regular basis to quantitatively evaluate water levels and the duration of bluff/water interaction, particularly during extreme events.

5. Coastal Hazards and Climate Change

5.1. Introduction

The PGST coastline will likely be negatively impacted by sea level rise. To understand the magnitude and timing of some of these changes, we assessed the response of coastal flooding to climate change. Sea level rise will increase flooding of the PGST coastline and will likely increase bluff erosion rates. Our goal is to provide water level information under some sea level rise scenarios and to describe the effects climate change may have on the PGST coastline.

5.2. Background

PGST is concerned with sea level rise and its potential impacts on the near-shore environment. Rising sea level may increase coastal hazards impacting bluff retreat rates, sediment transport, and sediment storage along the coast. By 2100, likely projections (83-17% probability) for relative sea level rise near Port Gamble are 1 to 2.6 ft under a low greenhouse gas scenario (RCP 4.5) and 1.4 to 3.1 ft for a high greenhouse gas scenario (RCP 8.5) (Miller et al., 2018). These local relative sea level rise projections are based on global absolute sea level rise projections published by Kopp et al. (2014) and local estimates of vertical land movement (subsidence or uplift). The rise of sea level will impact the shorelines along Puget Sound, changing the sediment delivery system rates and stressing many components of the ecosystem (Fresh et al., 2011).

We used sea level rise projections from Miller et al. (2018). These sea level rise projections take into account global sea level rise projections and incorporate vertical land movement estimation and uncertainty (1 standard deviation) for this area. The PGST coastline has an estimated subsidence rate of 0.2 ± 0.5 ft/century (Miller et al., 2018). However, based on seismic deformation models, a subduction zone earthquake may cause additional subsidence of PGST of 0 to 0.2 ft, resulting in an even more dramatic relative rise in sea level (Miller et al., 2018).

5.3. Methods

One consequence of climate change and sea level rise is increased flooding of coastal areas. To assess the impacts of sea level rise and show potential for inundation of Point Julia, we used methods outlined by NOAA's Coastal Inundation Mapping Guidebook (2017). We used 2018 LiDAR-derived 3-foot horizontal resolution DTM as our elevation layer (Quantum Spatial, 2018). We then registered elevation data from NAVD 88 US Survey feet to MHHW US Survey feet using an offset of 8.44 ft. We then used "raster calculator" in ArcMap to generate a uniform water surface at MHHW and at +1-foot increments. We then used the "con" tool to difference water surface layers and the DTM.

5.4. Findings

We created a set of nine inundation maps (Appendix C). These maps show inundation at and above current mean higher high water (MHHW), at 1ft intervals. For example, Map A shows inundation when water level is at current MHHW or the daily average high tide (8.446 ft NAVD 88). Subsequent maps (B-I) show expected flooding when water level is 1 ft above MHHW.

The maps are intended to convey the extent of inundation associated with both sea level rise and extreme water level events.

There are two general steps to interpret these maps and use them for planning purposes:

1) Use Table 13 (Coastal water level map key) to identify the water level that corresponds to a particular sea level scenario and extreme water level magnitude. In most cases, the table also identifies a map that corresponds to the selected scenario. This step should answer the question: *How do sea level rise and extreme water level events combine to drive flooding at the PGST?*

2) Use Table 14 (Percent likelihood sea level rise scenario will be reached by a given year) to assess the likelihood or percent chance that sea level will reach or exceed a given magnitude (expressed in feet relative to contemporary MHHW). The values that populate this table are for two different greenhouse gas emission scenarios (RCP 4.5 and RCP 8.5). This step should answer the question: *For a given sea level scenario that has been selected in Step 1, how likely is that sea level scenario by a particular year in the future?*

Table 13. Coastal water level map key

Sea Level Rise Scenario	Daily Average High Tide	Extreme Water Level (Sea level rise scenario + Still water level magnitudes, relative to mean higher high water, across a range of return frequencies)					
		1 -yr	2-yr	5-yr	20-yr	50-yr	100-yr
MHHW+0 (Existing Conditions)	0 (Map A)	1.2 (Map B)	2.2 (Map C)	2.6	2.9 (Map D)	3.1 (Map D)	3.2 (Map D)
MHHW+1	1 (Map B)	2.2 (Map C)	3.2 (Map D)	3.6	3.9 (Map E)	4.1 (Map E)	4.2 (Map E)
MHHW+2	2 (Map C)	3.2 (Map D)	4.2 (Map E)	4.6	4.9 (Map F)	5.1 (Map F)	5.2 (Map F)
MHHW+3	3 (Map D)	4.2 (Map E)	5.2 (Map F)	5.6	5.9 (Map G)	6.1 (Map G)	6.2 (Map G)
MHHW+4	4 (Map E)	5.2 (Map F)	6.2 (Map G)	6.6	6.9	7.1	7.2
MHHW+5	5 (Map F)	6.2 (Map G)	7.2	7.6	7.9 (Map H)	8.1 (Map H)	8.2 (Map H)
MHHW+6	6 (Map G)	7.2	8.2 (Map H)	8.6	8.9	9.1	9.2
MHHW+7	7	8.2 (Map H)	9.2	9.6	9.9 (Map I)	10.1 (Map I)	10.2 (Map I)
MHHW+8	8 (Map H)	9.2	10.2 (Map I)	10.6	10.9	11.1	11.2
MHHW+9	9	10.2 (Map I)	11.2	11.6	11.9	12.1	12.2
MHHW+10	10 (Map I)	11.2	12.2	12.6	12.9	13.1	13.2

For example, Map D shows the expected inundation at MHHW plus 3 ft. This particular scenario represents inundation expected either:

a) During the expected still water flooding that would be exceeded currently, on average, at least once every 20 years
b) During the expected still water flooding that would be exceeded on average, at least once every other year after 1 ft of sea level rise
c) During the expected still water flooding that would be exceeded on average, at least once every year after 2 ft of sea level rise
d) During the expected daily high tide flooding after 3 ft of sea level rise

These maps help to visualize potential inundation scenarios. However, it should be noted that these maps are drawn on the existing landscape and DO NOT represent how the shoreline may evolve as sea level rises.

Table 14. Percent likelihood sea level rise scenario will be reached or exceeded by a given year

Sea Level Rise Scenario	Assessed Likelihood by (RCP 4.5/8.5)				
	2030	**2050**	**2070**	**2090**	**2150**
MHHW+0 (Existing Conditions)	100/100	100/100	100/100	100/100	100/100
MHHW+1	0/0	19/24	60/72	79/90	92/98
MHHW+2	0/0	0/0	5/8	25/43	72/90
MHHW+3	0/0	0/0	0/1	3/8	44/70
MHHW+4	0/0	0/0	0/0	1/1	21/43
MHHW+5	0/0	0/0	0/0	0/0	9/22
MHHW+6	0/0	0/0	0/0	0/0	4/10
MHHW+7	0/0	0/0	0/0	0/0	2/5
MHHW+8	0/0	0/0	0/0	0/0	1/3
MHHW+9	0/0	0/0	0/0	0/0	1/2

5.5. Discussion

One of the major hazards associated with climate change and PGST coasts is coastal bluff erosion. Bluff erosion is affected by several factors including waves, wind, rain, and groundwater. While just a part of the story, wave-induced erosion will likely increase bluff erosion rates as sea level rises (Shipman et al., 2014). Waves move sediment at the base of bluffs, debuttressing, oversteepening, and destabilizing bluffs. Kaminsky et al. (2014) found that sea level rise may increase bluff retreat rates along the Elwha and Dungeness bluffs in Clallam County, WA by up to 0.3 ft/yr by 2050. While calculating future bluff retreat rates based on sea level rise at our site is outside of the scope of work for this project, I assume sea level rise and climate change will indeed increase the rate of bluff retreat along PGST's coast. Johannessen and MacLennan (2007) recommend the use of soft shore protection to mitigate the effects of sea level rise on coastal erosion. Soft shore protection strategies include beach nourishment (gravelling), planting vegetation, and anchoring large woody debris on the beaches.

Climate change is also predicted to increase extreme precipitation events (Dalton et al., 2013). Increased storm intensity may increase bluff erosion directly from wind and rain and indirectly by decreasing the stability of the bluffs. Rain infiltrates into bluff material, increasing pore pressure, resulting in a decreased effective normal stress, thus lowering the "strength" of the bluff. Depending on the local geology, water in bluff material either from groundwater or rain may be a major factor for bluff stability on the PGST coast.

Beaches help provide protection from wave erosion by dissipating wave energy over the beach face (Dean, 1991). However, as sea level rises, loss of exposed beach will result in bluffs being more

frequently exposed to wave action. This increased erosion of bluffs, however, will also provide increased sediment to the beaches, potentially raising the elevation of the beach face to some equilibrium as sea level rises. It is unclear how this negative feedback will impact coastal bluff erosion at PGST.

While flooding of coastal areas, specifically Point Julia is likely to be a major concern for the PGST coastline, increased bluff erosion may help to reduce the effects of sea level rise on coastal flooding. Natural systems and feedbacks may work to keep the beach and bluff profile in equilibrium as sea level rises (Dean, 1991). While we cannot be sure of the timing and magnitude of this rise of the beach face with sea level rise, it will likely be delayed enough for coastal flooding to occur similar to the maps produced for this project (Appendix C). The geomorphic evolution of the PGST coast will likely be a delayed response to sea level rise. The effects of sea level rise and inundation should be expected, and planning should be done to mitigate risk.

5.6. Conclusions and Monitoring Recommendations

The PGST coastline is an important cultural and economic resource for the tribe. Climate change and sea level rise will impact the coastline and change how the tribe interacts with it. Bluff erosion rates will likely increase, sediment transport and storage on beaches will change, marine and nearshore habitat areas will shift, and flooding will likely increase.

Point Julia is the most vulnerable area to climate change and sea level rise. Point Julia may already be exhibiting signs of sea level rise. I recommend continued monitoring of Point Julia with shoreline surveying. Flooding and bluff erosion may be mitigated by projects which support large woody debris and sediment on beaches. Coastal inundation maps may be helpful for planning and management strategies, considering the time frame and likelihood of each scenario.

6. References and Data Sources

Barnard, P.L., et al., 2009, The framework of a coastal hazards model; a tool for predicting the impact of severe storms: U.S. Geological Survey Open-File Report 2009-1073, 21 p., https://pubs.usgs.gov/of/2009/1073/.

Booth, D.B., 1994, Glaciofluvial infilling and scour of the Puget Lowland, Washington, during ice-sheet glaciation: Geology, v. 22, no. 8, p. 695-698.

Dalton, M.M., Mote, P.W., and Snover, A.K., eds., 2013, Climate Change in the Northwest: Implications for Our Landscapes, Waters, and Communities: Washington, DC, Island Press, 230 p.

Dean, R.G., 1991, Equilibrium beach profiles: characteristics and applications: Journal of Coastal Research, v. 7, no. 1, p. 53-84.

Fain Environmental, 2016, Wave height analysis for Port Gamble Bay FLUPSY Facility, Port Gamble, WA, for Port Gamble S'Klallam Tribe, 7 p.

Finlayson, D., 2006, The geomorphology of Puget Sound beaches, for Puget Sound Nearshore Partnership: Technical Report 2006-02, 55 p., http://pugetsoundnearshore.org.

Fresh K., et al., 2011, Implications of observed anthropogenic changes to the nearshore ecosystems in Puget Sound, for Puget Sound Nearshore Ecosystem Restoration Project: Technical Report 2011-03, 30 p.

Garling, M.E., and Molenaar, D., 1965, Water resources and geology of the Kitsap Peninsula and certain adjacent islands: Washington Division of Water Resources, Water Supply Bulletin, no. 18, 309 p.

Gerstel, W., and Brown, J., 2006, Alternative shoreline stabilization evaluation project, for Puget Sound Action Team, 43 p.

Gerstel, W., Small, J., and Schlenger, P., 2012, Restoration feasibility and prioritization analysis of sediment sources in Kitsap County, for Kitsap Regional Shoreline Restoration Feasibility and Prioritization Study Demonstration Project, 66 p.

Heerhartz, S.M., Toft, J.D., Cordell, J.R., Dethier, M.N., and Ogston, A.S., 2016, Shoreline armoring in an estuary constrains wrack-associated invertebrate communities: Estuaries and Coasts, v. 39, no. 1, p. 171-188.

Johannessen, J., and MacLennan, A., 2007, Beaches and bluffs of Puget Sound, for Puget Sound Nearshore Ecosystem: Technical Report 2007-04, 28 p.

Kaminsky, G.M., Baron, H.M., Hacking, A., McCandless, D., and Parks, D.P., 2014, Mapping and monitoring bluff erosion with boat-based lidar and the development of a sediment budget and erosion model for the Elwha and Dungeness littoral cells, Clallam County, Washington, for Washington State Department of Ecology Coastal Monitoring and Analysis Program, 44 p.

Keuler, R.F., 1988, Map showing coastal erosion, sediment supply, and longshore transport in the Port Townsend 30- by 60-minute quadrangle, Puget Sound Region, Washington: U. S. Geological Survey, scale 1:100,000, 1 sheet.

Kopp, R.E., Horton, R.M., Little, C.M., Mitrovica, J.X., Oppenheimer, M., Rasmussen, D.J., and Tebaldi, C., 2014, Probabilistic 21st and 22nd century sea-level projections at a global network of tide-gauge sites: Earth's Future, v. 2, no. 8, p. 383-406, https://doi.org/10.1002/2014EF000239.

Ladd, D., Selleck, J., and Fain, A., 2016, Geotechnical assessment and shoreline management study, for Port Gamble S'Klallam Tribe, 32 p.

MacLennan, A., Johannessen, J., Waggoner, J., Waddington, J., and Lubeck, A., 2018, Long-term bluff recession rates in Puget Sound: implications for the prioritization and design of restoration

projects, for Estuary and Salmon Restoration Program - Learning Program, Washington Department of Fish and Wildlife, 40 p.
McCollum, P., Daubenberger, H., and Phillips, S., 2016, Climate change impact assessment, for Port Gamble S'Klallam Tribe, 226 p.
Miller, I.M., Morgan, H., Mauger, G., Newton, T., Weldon, R., Schmidt, D., Welch, M., and Grossman, E., 2018, Projected sea level rise for Washington State – A 2018 assessment, a collaboration of Washington Sea Grant, University of Washington Climate Impacts Group, University of Oregon, University of Washington, and U. S. Geological survey, for the Washington Coastal Resilience Project, 24 p.
Morton, R.A., Miller, T.L., and Moore, L.J., 2004, National assessment of shoreline change: Part 1: Historical shoreline changes and associated coastal land loss along the U.S. Gulf of Mexico: U.S. Geological Survey Open-file Report 2004-1043, 45p.
NOAA Office of Coastal Management, 2017, Coastal Inundation Mapping Training: https://coast.noaa.gov/digitalcoast/training/inundationmap.html.
NOAA, 2019, Tides and Currents: https://tidesandcurrents.noaa.gov/.
OCM Partners, 2019, 2014 USACE USGS Topobathy Lidar: Puget Sound (WA), for USGS, NOAA National Centers for Environmental Information, https://inport.nmfs.noaa.gov/inport/item/50183.
Parks, D., Shaffer, A., and Barry, D., 2013, Nearshore drift-cell sediment processes and ecological function for forage fish: implications for ecological restoration of impaired Pacific Northwest marine ecosystems: Journal of Coastal Research, v. 29, no. 4, p. 984-997.
Pawlowicz, R., Beardsley, B., and Lentz, S., 2002, Classical tidal harmonic analysis including error estimates in MATLAB using T_TIDE: Computers and Geosciences, v. 28, p. 929-937.
Polenz, M., Favia, J.G., Hubert, I.J., Paulin, G.L., and Cakir, R., 2015, Geologic map of the Port Ludlow and southern half of the Hansville 7.5-minute quadrangles, Kitsap and Jefferson Counties, Washington: Washington Division of Geology and Earth Resources Map Series 2015-02, scale 1:24,000, 1 sheet, 40 p. text.
Puget Sound River History Project, 2003, T-585; Map of Port Gamble and part of the entrance to Hood's Canal, Washington Ter., 1856, Georeferenced United States Coast & Geodetic Survey Topographic Sheet T-585, Scale 1:10,000, Surveyor: Jas. S. Lawson, http://riverhistory.ess.washington.edu/tsheets/.
Pugh, D.T., and Vassie, J.M., 1978, Extreme sea levels from tide and surge probability, Proceedings 16th Conference of Coastal Engineering, Hamburg, Germany, American Society of Civil Engineers, 911–932.
Quantum Spatial, 2018, Olympic Peninsula, Washington Area 1A 3DEP LiDAR Technical Data Report, for the U. S. Geological Survey, 29 p.
Self, R.P., 1977, Longshore variation in beach sands: Nautla area, Veracruz, Mexico: Journal of Sedimentary Petrology, v. 47, no. 4, p. 1437-1443.
Serafin, K.A., Ruggiero, P., and Stockdon, H.F., 2017, The relative contribution of waves, tides, and nontidal residuals to extreme total water levels on U.S. West Coast sandy beaches: Geophysical Research Letters, v. 44, no. 4, p. 1839–1847, doi:10.1002/2016GL071020.
Shipman, H., 2001, Beach nourishment on Puget Sound: a review of existing projects and potential applications: Puget Sound Research 2001, p. 1-8.
Shipman, H., 2008, A geomorphic classification of Puget Sound nearshore landforms, for Puget Sound Nearshore Partnership, Technical Report 2008-01, 38 p.
Shipman, H., MacLennan, A., and Johannessen, J., 2014, Puget Sound feeder bluffs: coastal erosion as a sediment source and its implications for shoreline management, for Washington Department of Ecology Shorelands and Environmental Assistance Program, no. 14-06-016, 62 p.

Taggart, B.E., 1984, Net shore-drift of Kitsap County, Washington [Master's thesis]: Western Washington University, WWU Graduate School Collection, 851, 95 p., https://cedar.wwu.edu/wwuet/851.
Terrapoint, 2008, Olympic Peninsula Project Report, for Puget Sound Regional Council, v. 1, 8 p.
Thorson, R.M., 1980, Ice-sheet glaciation of the Puget Lowland, Washington, during the Vashon Stade (late Pleistocene): Quaternary Research, v. 13, no. 3, p. 303-321.
Troost, K.G., 1994, Dating earthquakes, subsidence, and sea level rise, using archaeological data at West Point, Seattle, Washington, Abstracts with Programs, 1994 Annual Meeting, The Geological Society of America, Seattle, Washington, October 24-27, 1994, p. A-157.
Troost, K.G. and Stein, J.K., 1995, Geology and geoarchaeology of West Point, 77 pp: The archaeology of West Point, edited by L.L. Larson and D.E. Lewarch.
U. S. Geological Survey, 1999, Map Accuracy Standards, USGS Fact Sheet 171-99: https://pubs.usgs.gov/fs/1999/0171/report.pdf (accessed September 2019).
Wallace, S.R., 1988, Quantification of net shore-drift rates in Puget Sound and the Strait of Juan de Fuca, Washington: Journal of Coastal Research, v. 3, no. 3, p. 395-403.
Washington State Department of Ecology, 2015, Risk Report, for Kitsap County including the Cities of Bremerton, Bainbridge, Port Orchard, Poulsbo, the Port Gamble S'Klallam Indian Reservation, the Suquamish Tribe, and Unincorporated Kitsap County, 45 p, https://fortress.wa.gov/ecy/gispublic/AppResources/SEA/RiskMAP/Kitsap/Kitsap_Project_Docs/Risk%20Report%20-%20Kitsap%20County%20-%20Final.pdf.
Washington State Department of Ecology, 2019, Shoreline Photo Viewer: https://fortress.wa.gov/ecy/shorephotoviewer/Map/ShorelinePhotoViewer (accessed October 2019).
Wnek Engineering, 2014, Site plan wall design Pt. Julia road wall, for Port Gamble S'Klallam Tribe, scale: 1:240, 1 sheet.

Puget Sound CoSMoS webpage can be found at: *https://www.usgs.gov/centers/pcmsc/science/ps-cosmos-puget-sound-coastal-storm-modeling-system?qt-science_center_objects=0#qt-science_center_objects*

7. Figures

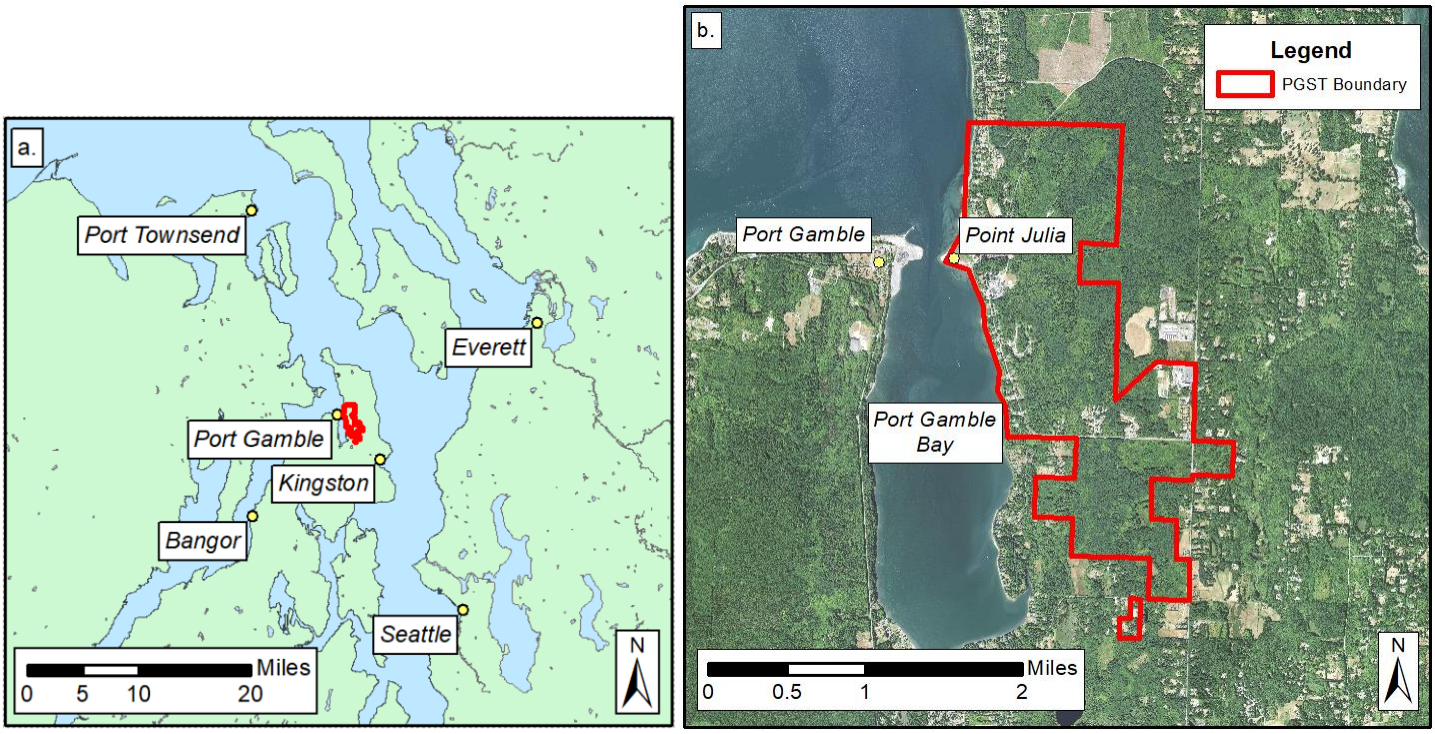

Figure 1. a) Location map. b) The project area is located on Port Gamble S'Klallam Tribe's trust land on the Kitsap Peninsula, WA. Base maps from 2017 USDA NAIP satellite imagery and Washington State Geospatial Data Archive.

Figure 2. Site map of the PGST coast. The PGST coastline is primarily bluff-backed beaches with a cuspate foreland (Point Julia). Six main streams drain the uplands forming fan deltas along the coast. Base maps from 2017 USDA NAIP satellite imagery and Washington State Geospatial Data Archive.

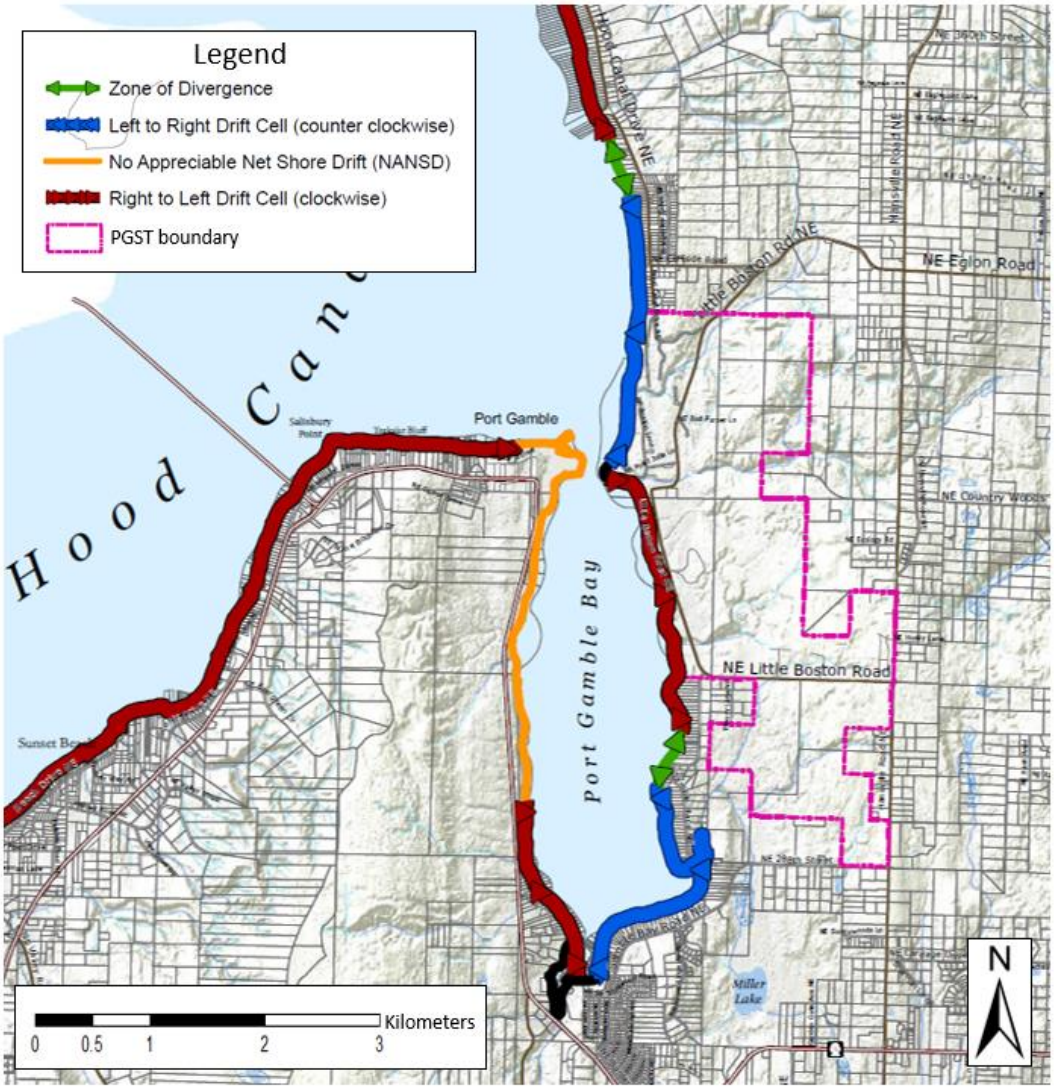

Figure 3. Drift cell map of the PGST beaches and surrounding area. Two drift cells converge at point Julia bringing sediment from the south and north. Arrows show drift direction. Map modified from Kitsap County Department of Community Development (2017). Drift cells identified and mapped by Taggart (1984).

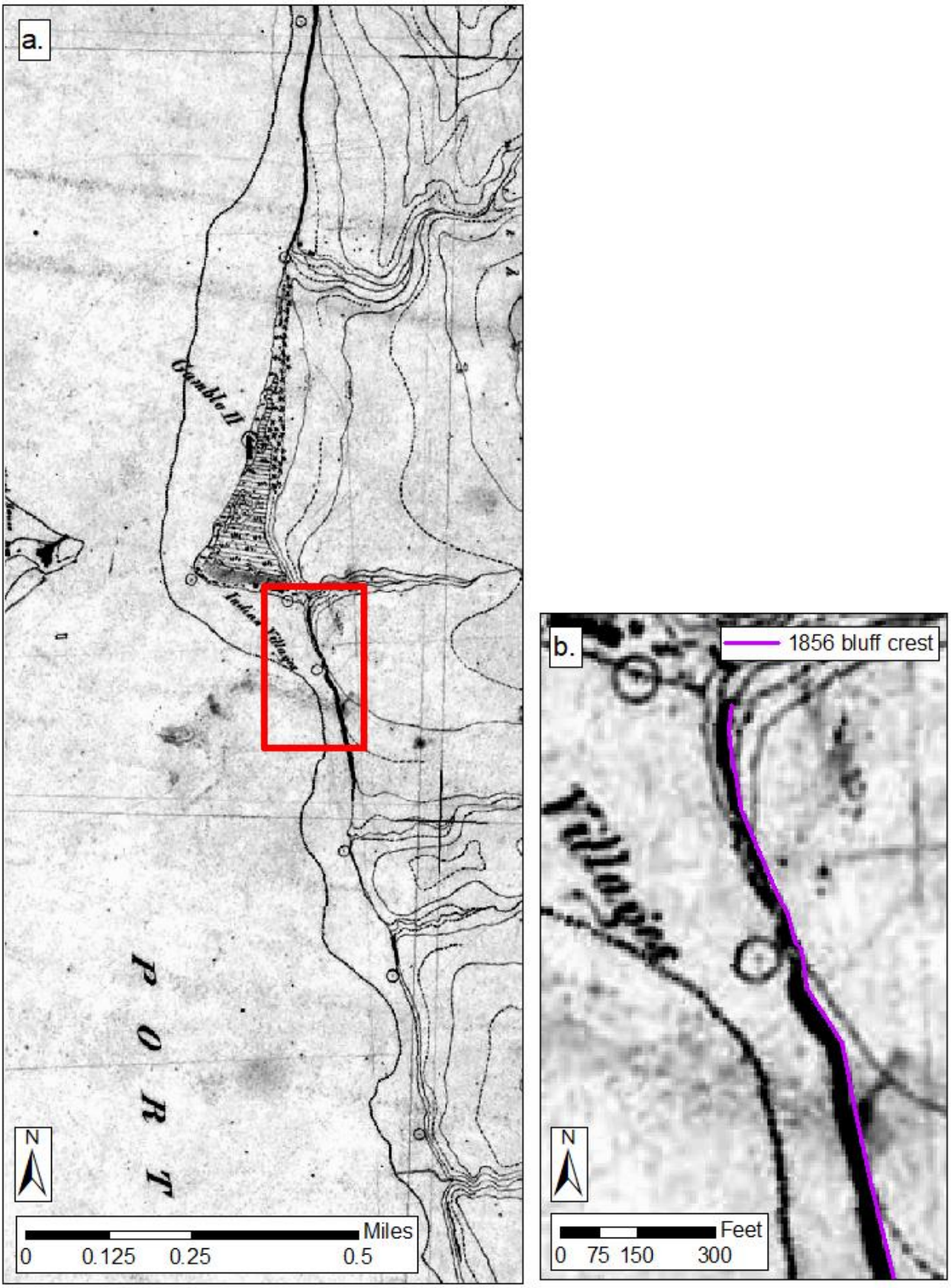

Figure 4. a) T-sheet of PGST coastline as mapped in 1856 (T-585). Four sections of bluff were mapped along the PGST coastline. Bluffs are shown as thick black lines along the coast. This T-sheet was mapped using a plane-board system. Red outline shows extent of Figure 4b. b) Bluff crest of bluff near the Tribal Center as digitized by the Puget Sound River History Project (2003).

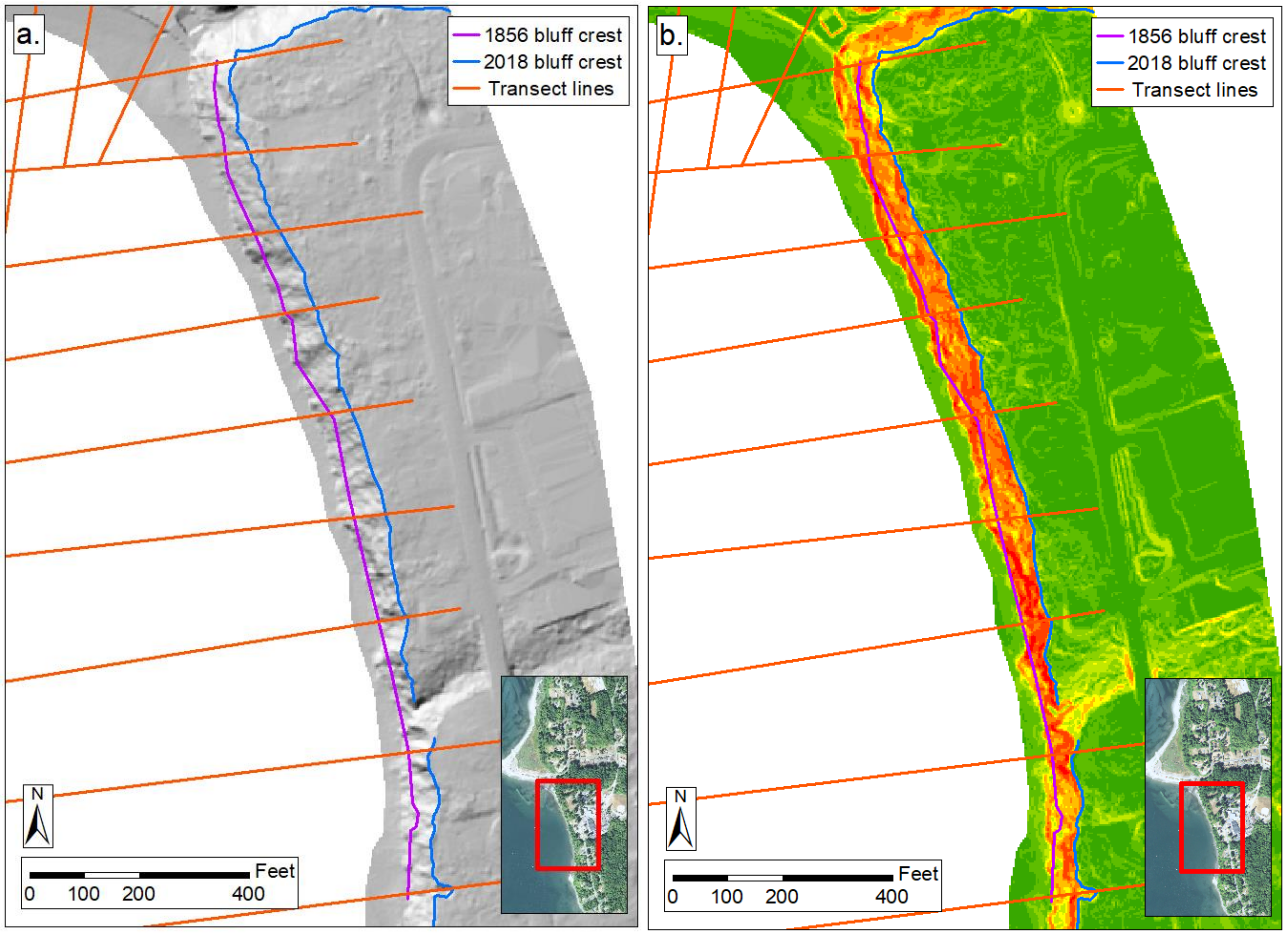

Figure 5. a) Hillshade map used to digitize bluff crests. b) Slope map used to digitize bluff crests from 2018 LiDAR data. Inset aerial imagery from 2017 USDA NAIP.

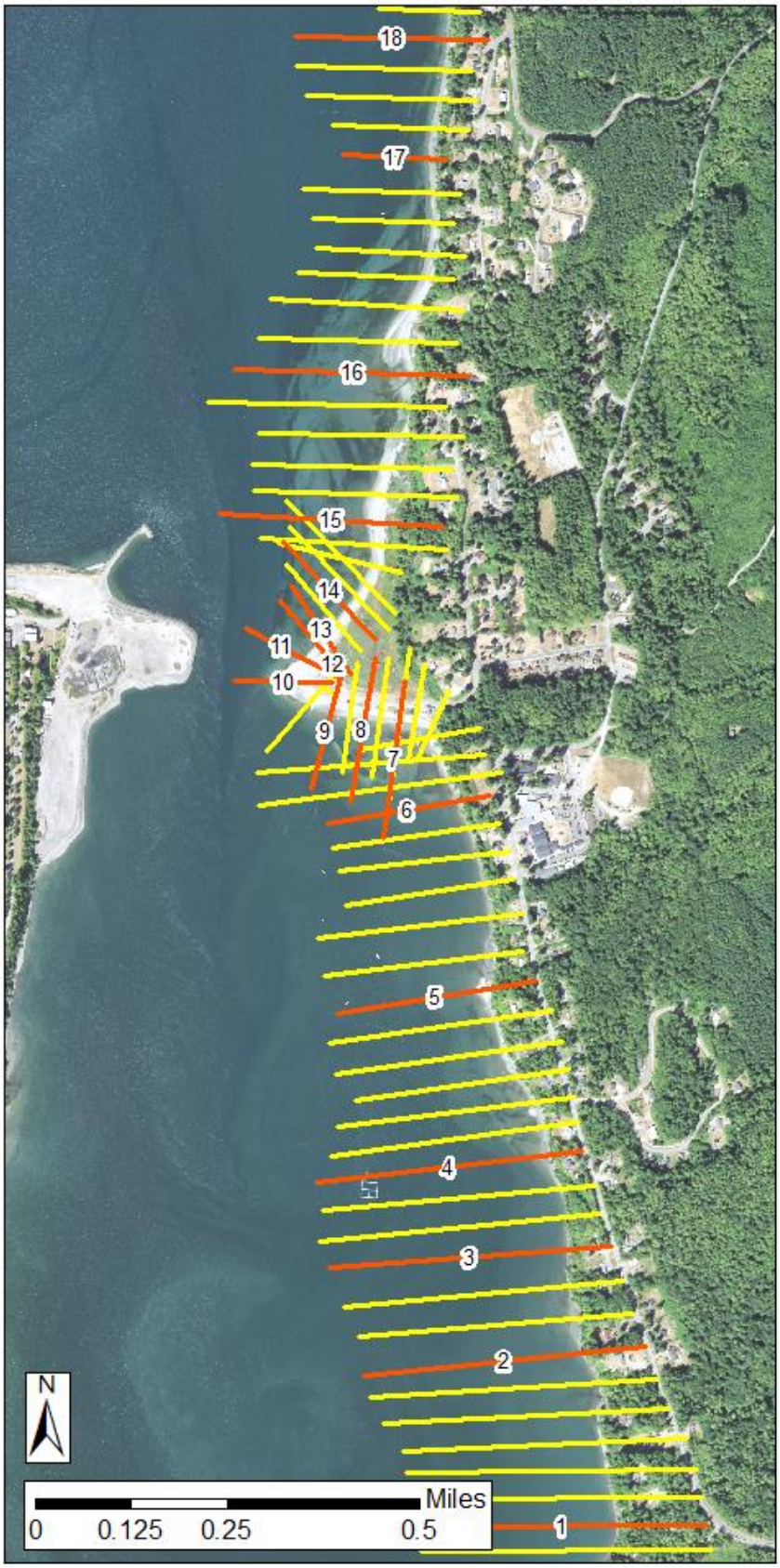

Figure 6. Shoreline transects for coastal monitoring along PGST land. Transects are spaced approximately 200 ft part with closer spacing for transects on Point Julia. "Focus reach" transects for more frequent surveying are numbered and shown in orange. Base map aerial imagery from 2017 USDA NAIP.

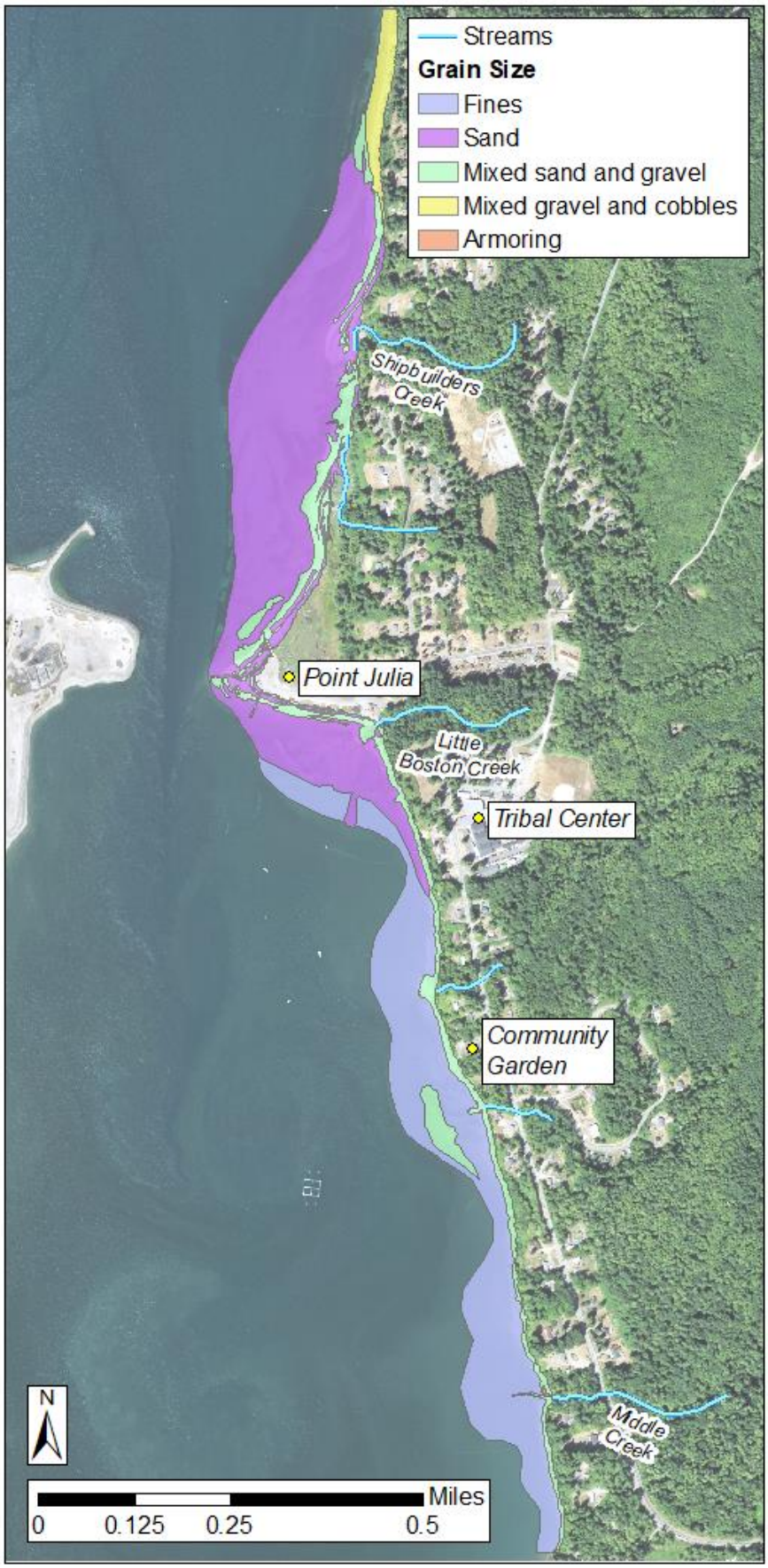

Figure 7. PGST beach grain size map. The beaches along PGST coast vary from fines (fine sand, silt, and clay) to mixed sand and gravel, up to boulders. Base map aerial imagery from 2017 USDA NAIP and 2019 PGST orthomosaic.

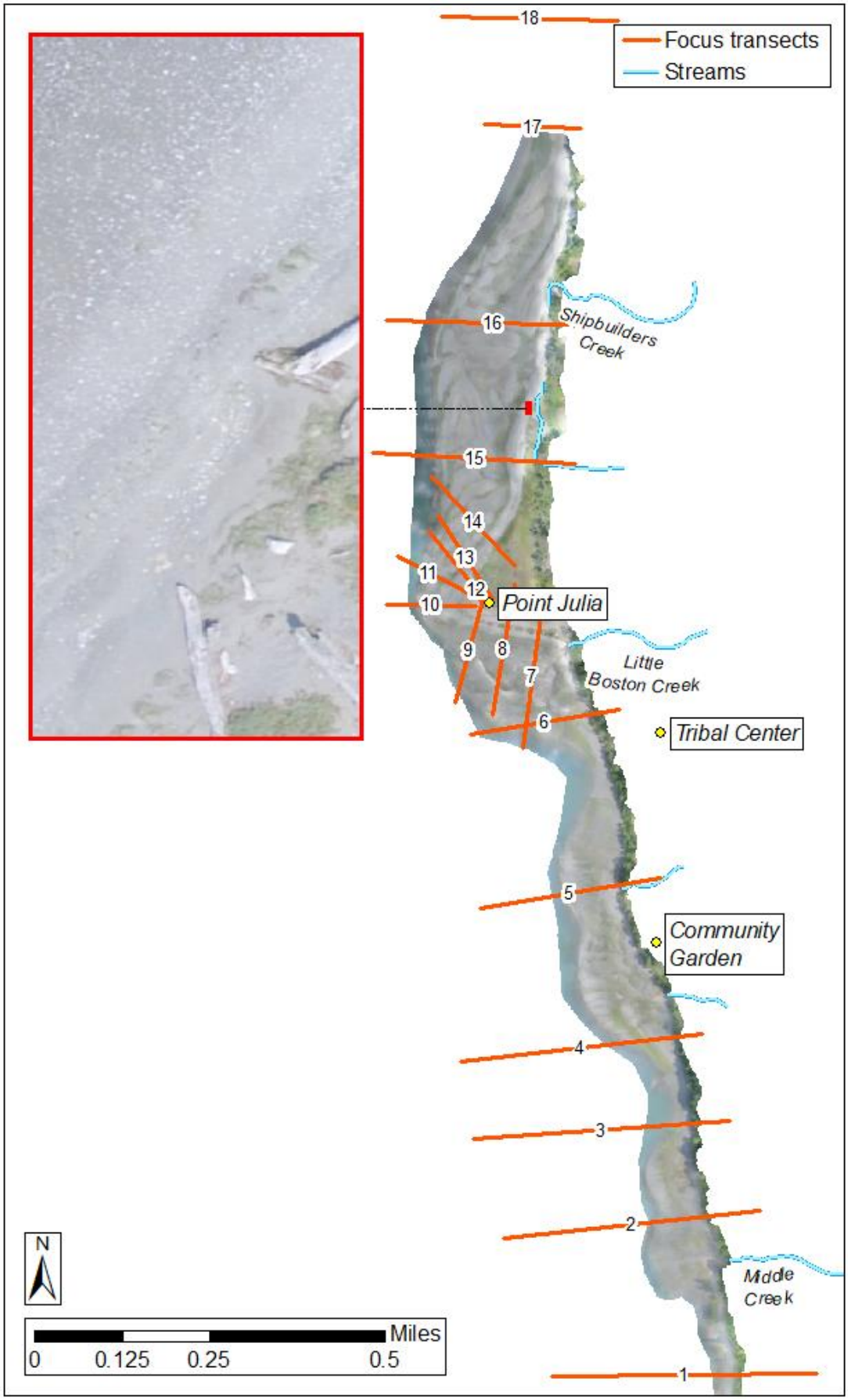

Figure 8. Orthomosaic of the PGST beaches. Orthomosaic image created in Agisoft PhotoScan using drone photos captured on July 2019. Resolution is about 0.79 in/pixel.

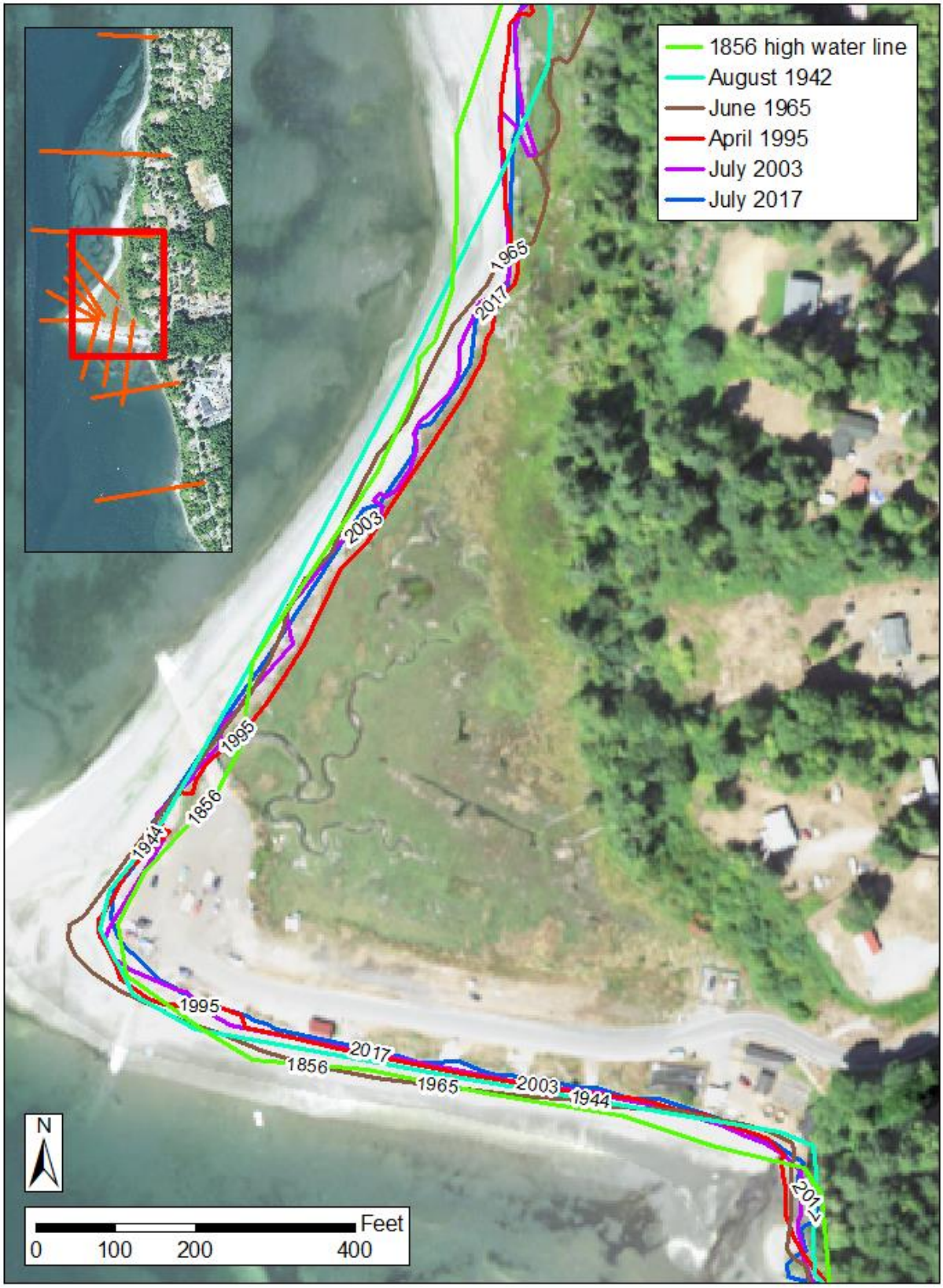

Figure 9. Shoreline change map of Point Julia. These data show a potential pattern of sea level rise with slight landward movement of the shoreline on the south side of Point Julia. I mapped shoreline from 1856 T-sheet high water line and vegetation lines from aerial imagery available at the University of Washington Libraries. Base map aerial imagery from 2017 USDA NAIP.

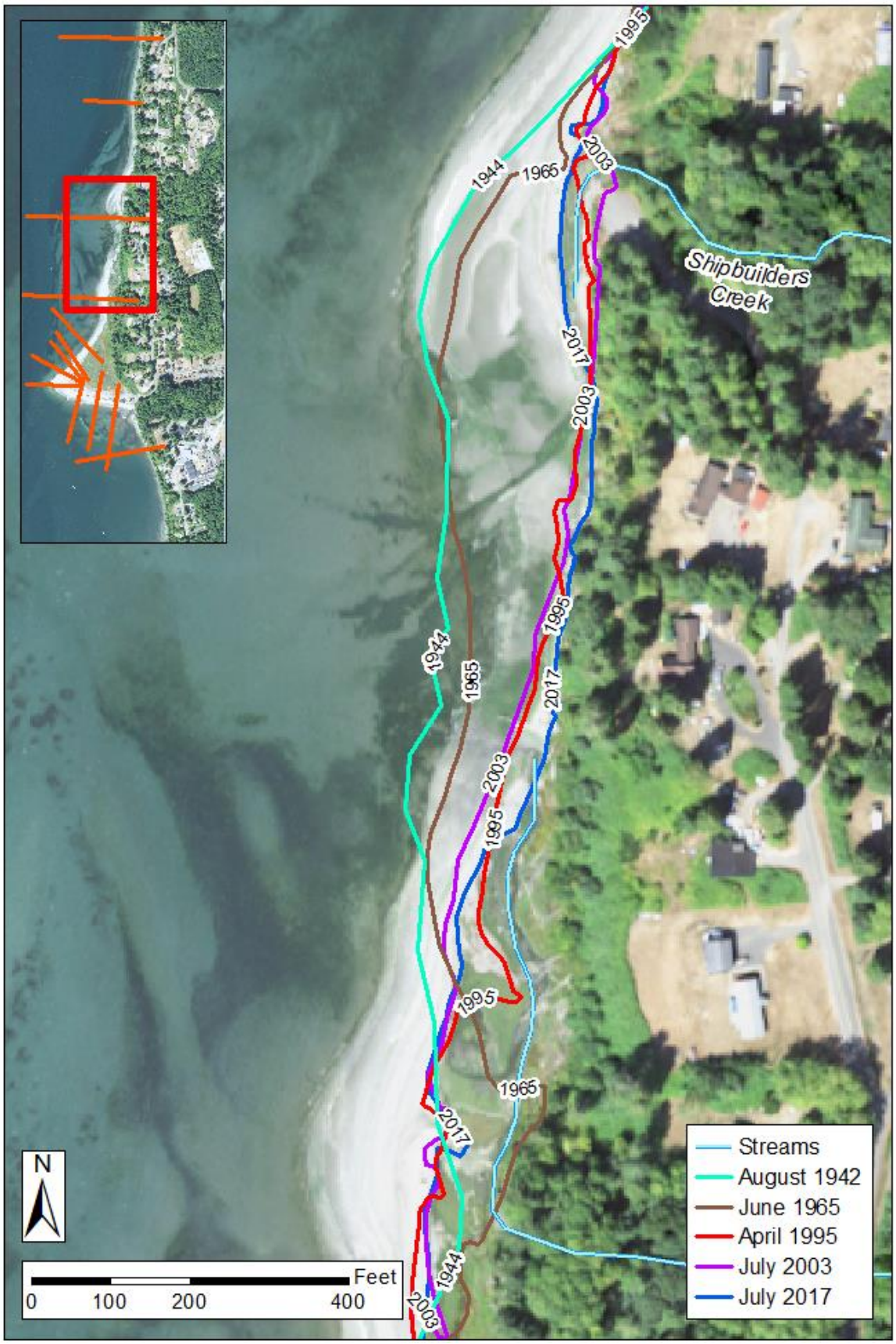

Figure 10. Shoreline vegetation change since 1942. Vegetation line was used as a proxy for shoreline to assess historic shoreline change. This area near Shipbuilders Creek shows the most significant shoreline change within the PGST coastal land and is associated with two creek mouths. Base map aerial imagery from 2017 USDA NAIP.

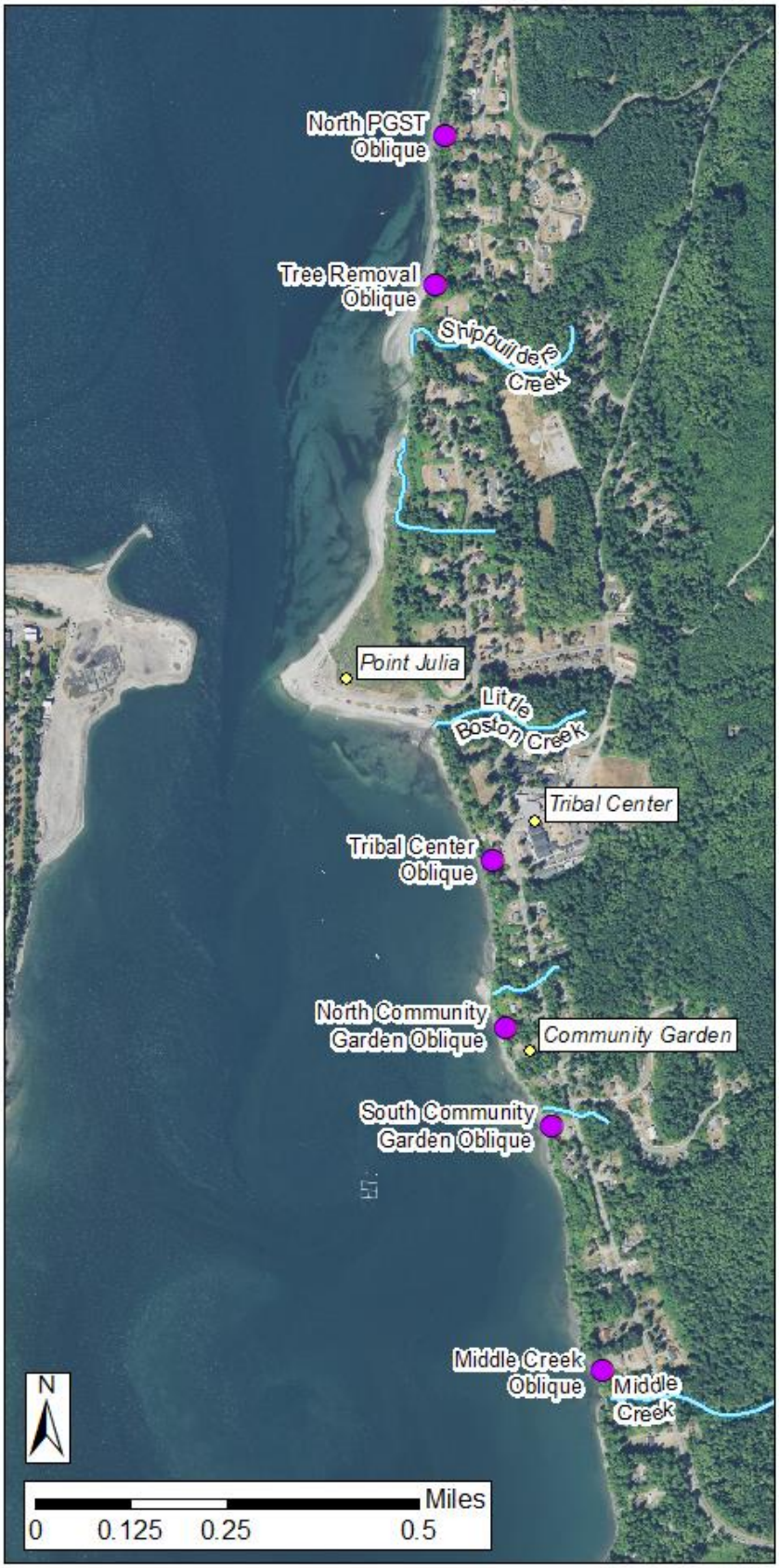

Figure 11. Location map of oblique photo sets (in subsequent figures). Oblique photos highlight six areas of change along bluffs of the PGST coastline.

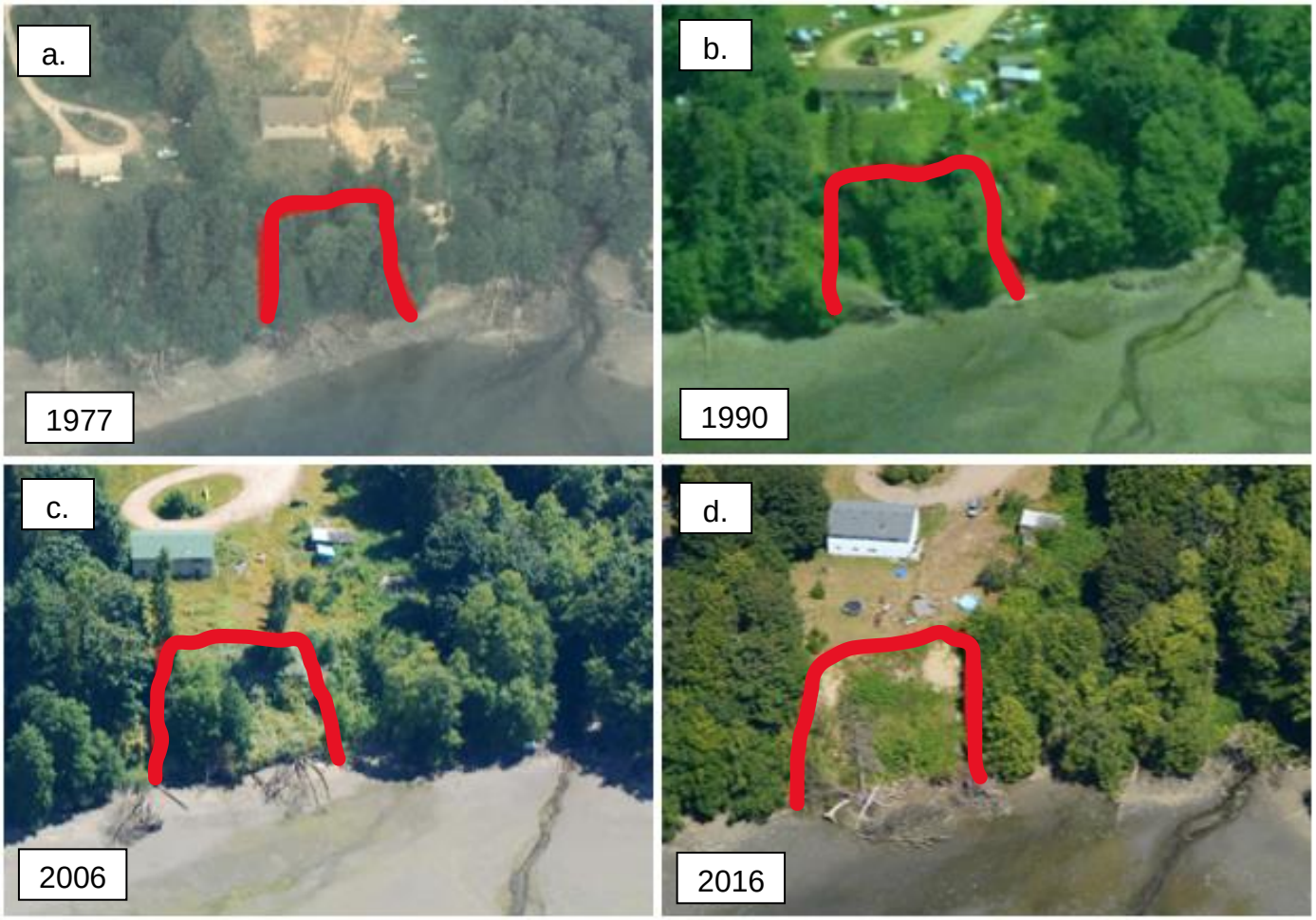

Figure 12. Oblique photo set near Middle Creek showing bluff failure possibly related to tree removal. a) 1977 oblique photo with old growth trees. b) 1990 oblique photo showing little change from 1977 photo. c) 2006 oblique photo with tree loss since 1990. d) 2016 oblique photo with significant tree loss and signs of slope failure. View to the east. Photos from WA Department of Ecology.

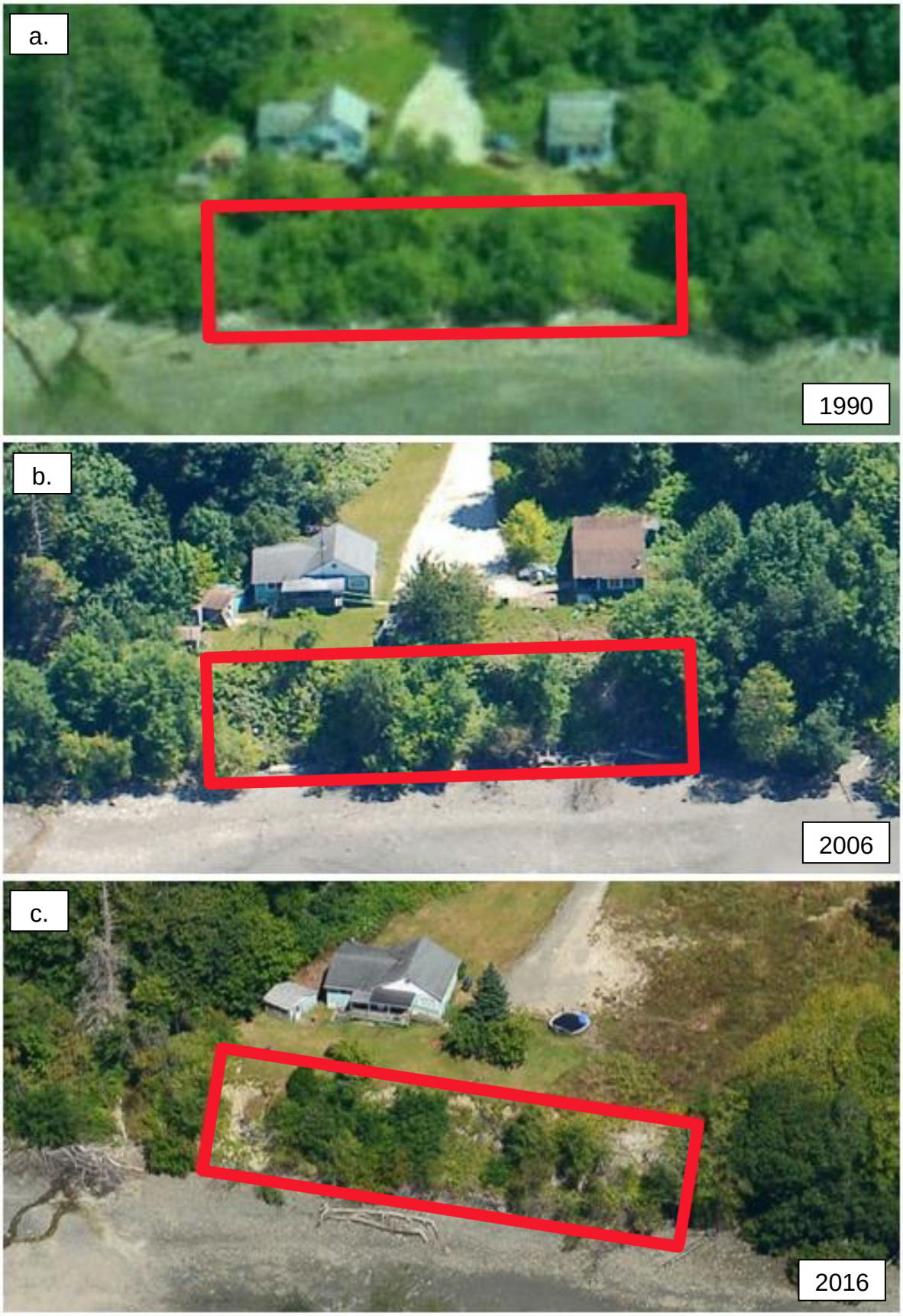

Figure 13. Oblique photos south of the community garden showing bluff erosion possibly related to tree removal. a) 1990 oblique photo with significant vegetation along the bluff. b) 2006 photo showing a loss of vegetation along the bluff. C) 2016 photo with significant loss of vegetation along the bluff and signs of slope failure. View to the east. Photos from WA Department of Ecology.

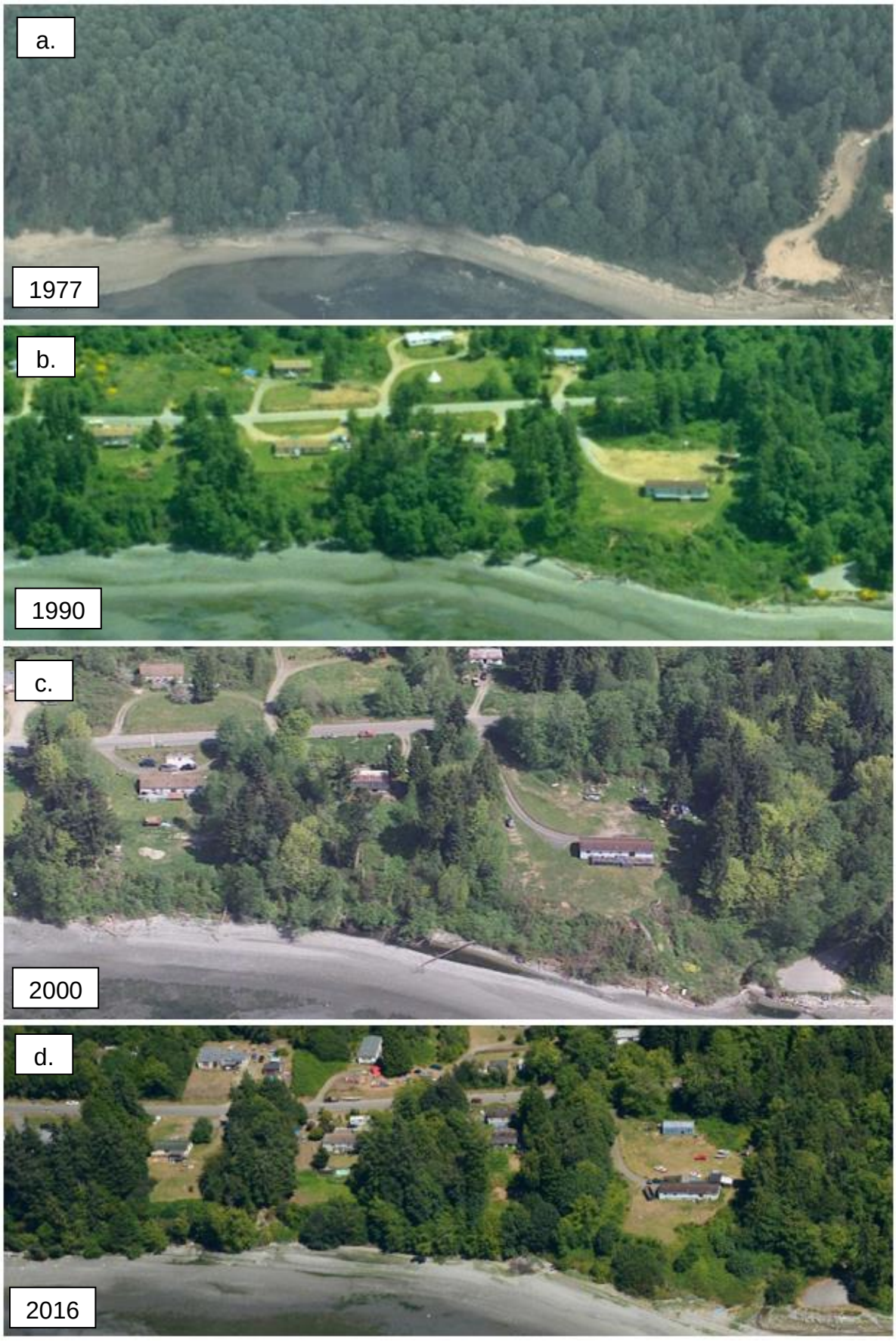

Figure 14. Tree removal along the PGST coastline since 1977. a) 1977 photo with abundant trees. b) 1990 photo with loss of trees since 1977. c) 2000 photo. d) 2016 photo. View to the east with Shipbuilders Creek outlet in the bottom right corner of the images. Photos from WA Department of Ecology.

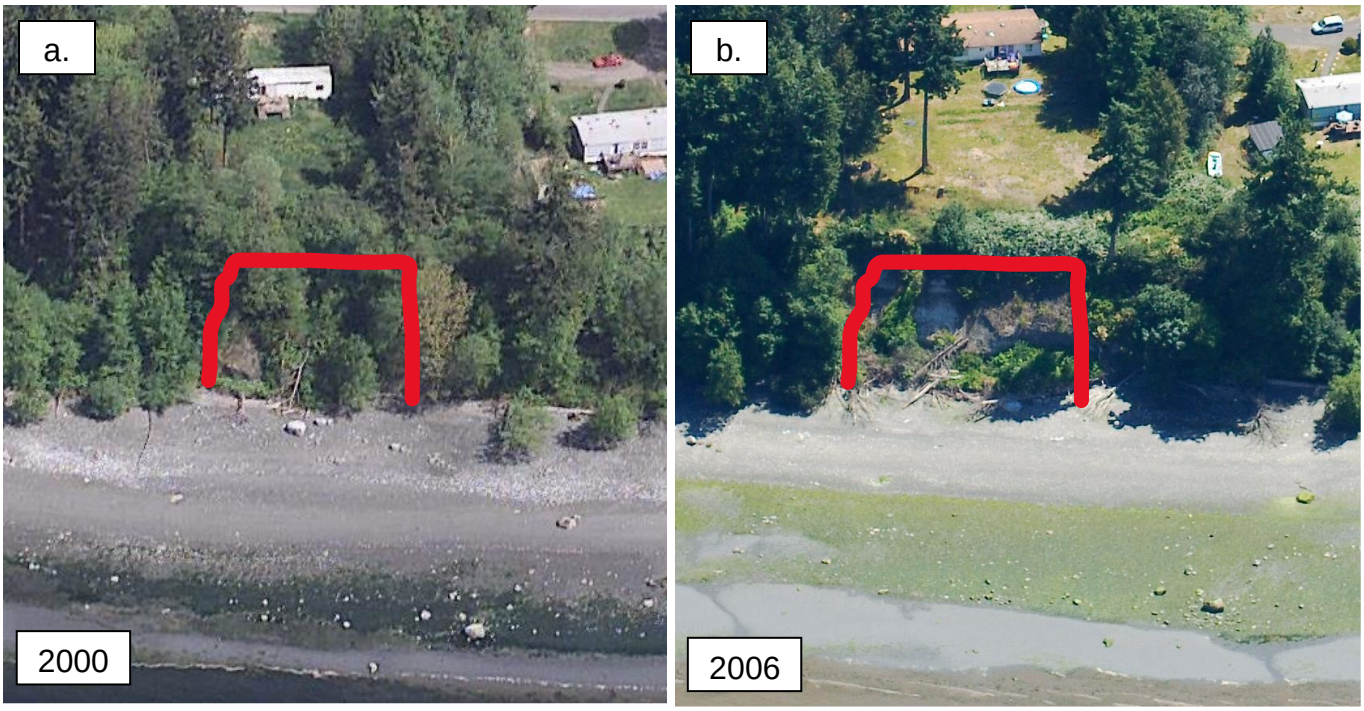

Figure 15. Bluff erosion between 2000 and 2006 on bluff north of Shipbuilders Creek. a) 2000 photo with vegetated bluff slope. b) 2006 photo with loss of vegetation and signs of slope failure. View to the east. Photos from WA Department of Ecology.

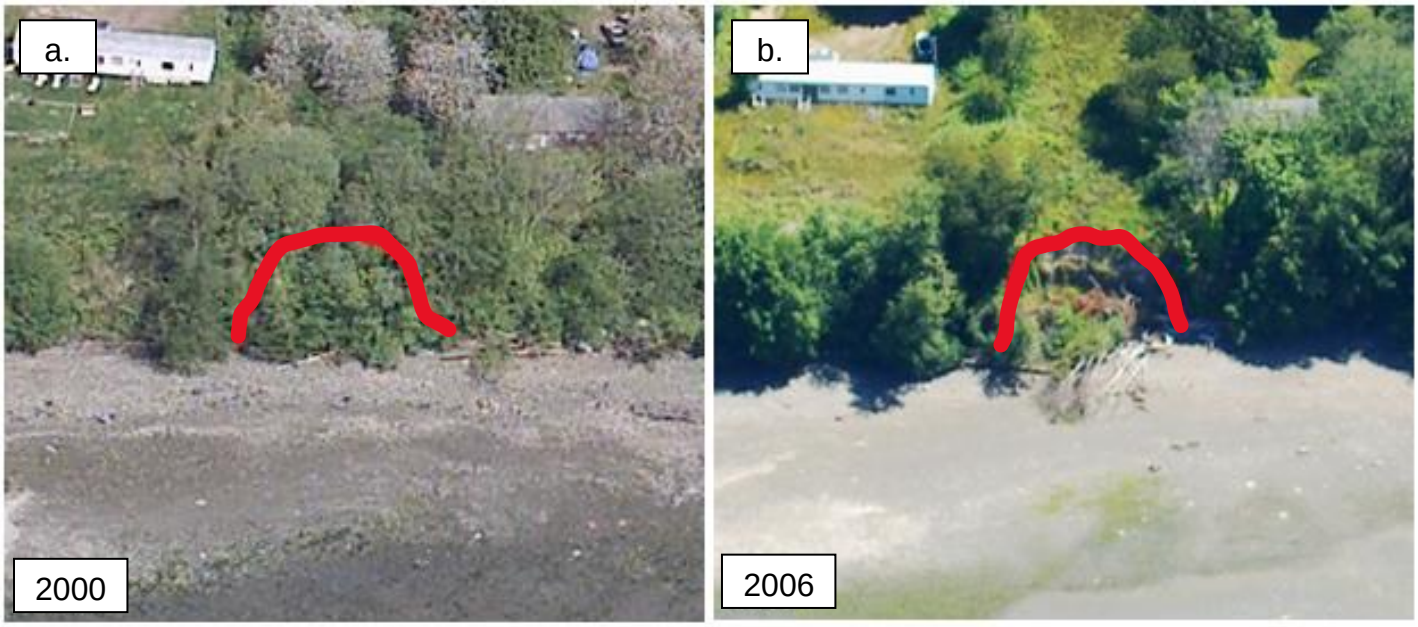

Figure 16. Bluff erosion between 2000 and 2006 on bluff north of the community garden. a) 2000 photo showing vegetated bluff prior to failure. b) 2006 photo showing bluff failure. View to the east. Photos from WA Department of Ecology.

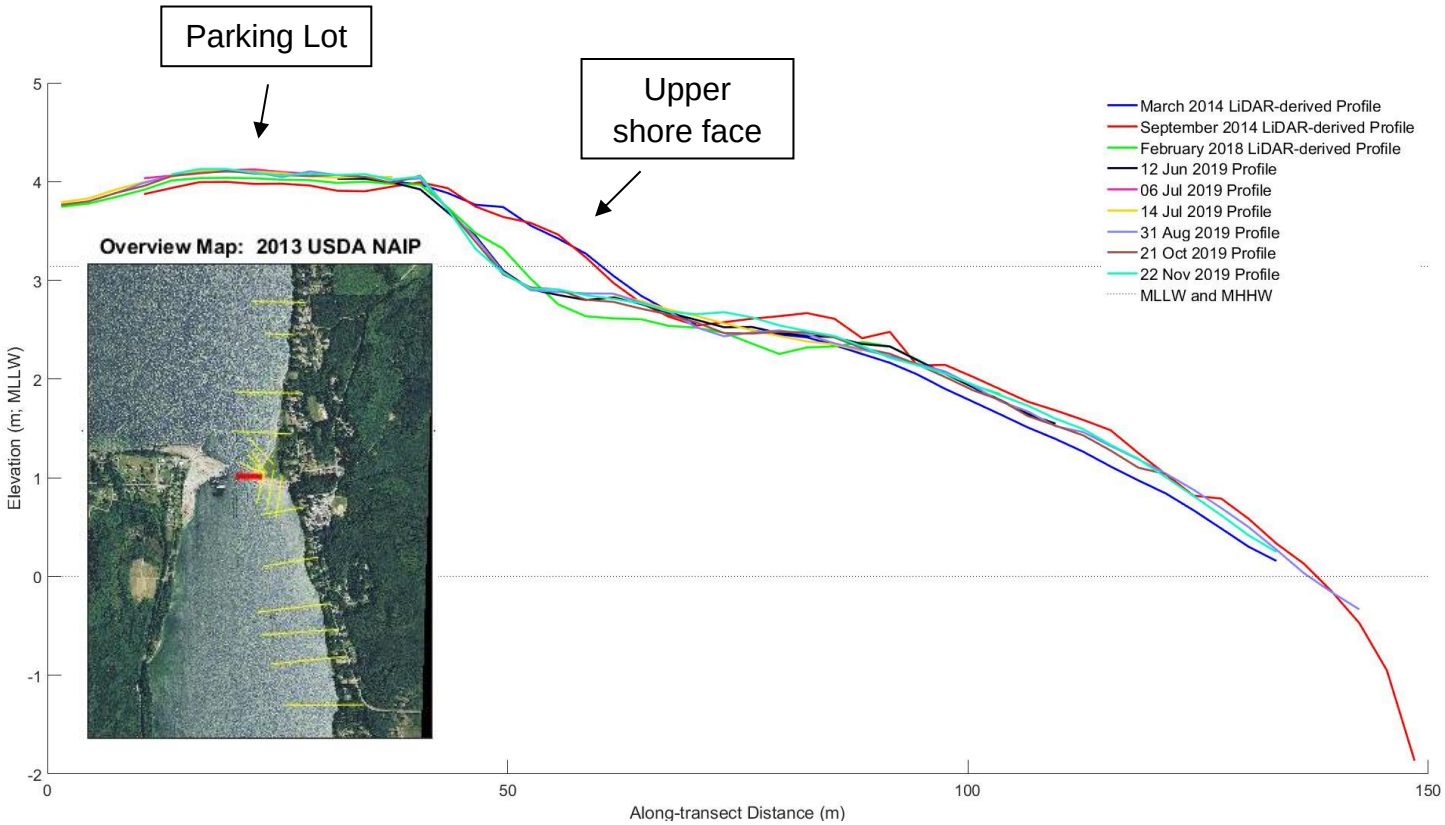

Figure 17. Shoreline profile of focus transect 10 on the tip of Point Julia. This profile showed the most significant change of all our beach profiles. The upper shoreface shows distinct changes between 2014 and 2018. We derived profiles from LiDAR data and GNSS surveying.

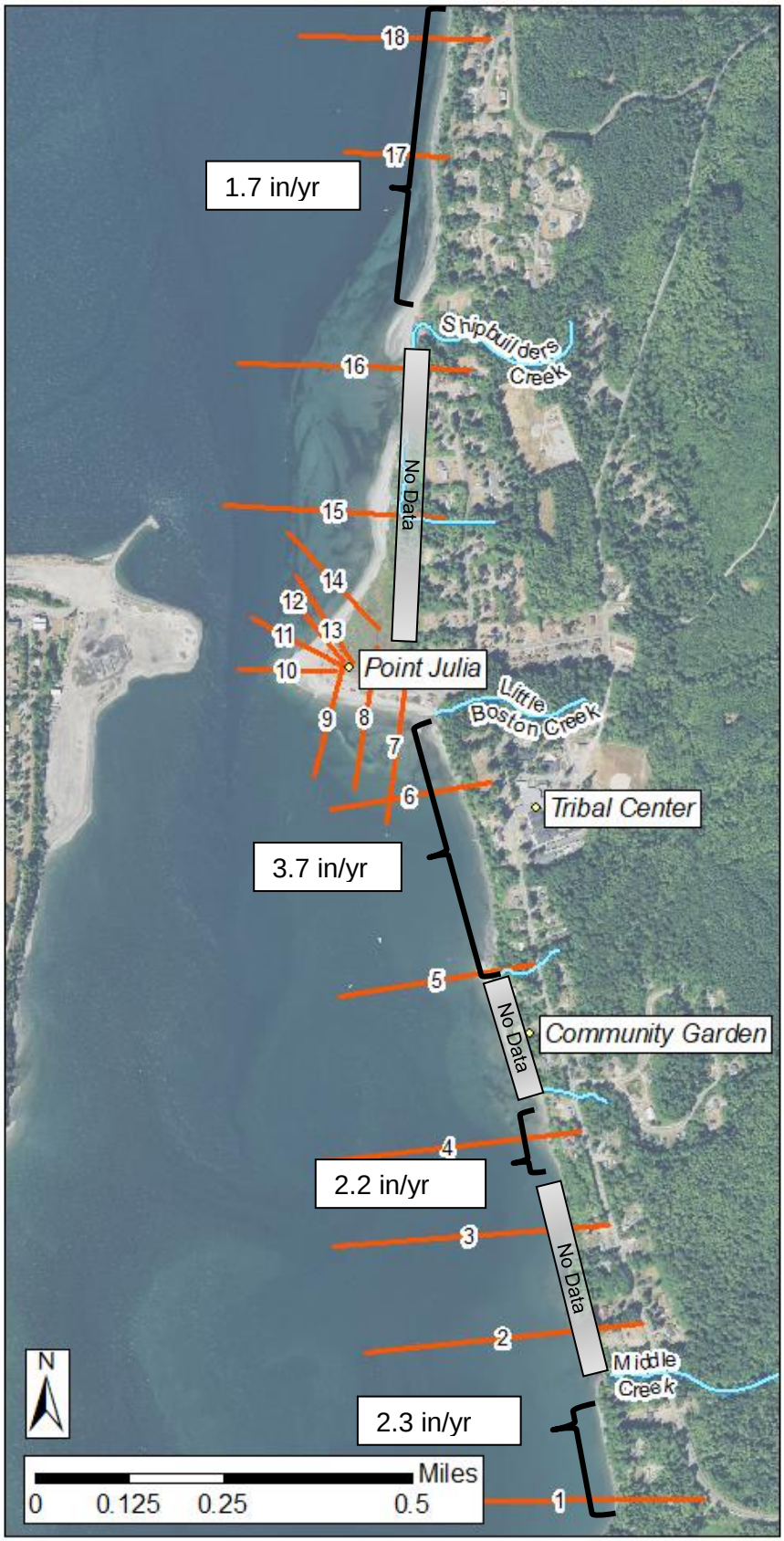

Figure 18. Calculated historical bluff erosion rates from 1856 to 2018 for the PGST coastline. Other than the erosion rate at the Tribal Center, none of the rates are greater than the uncertainty (± 2.8 in/yr). I calculated these rates based on 1856 T-sheet surveyed bluffs and 2018 LiDAR data. Base map aerial imagery from 2017 USDA NAIP.

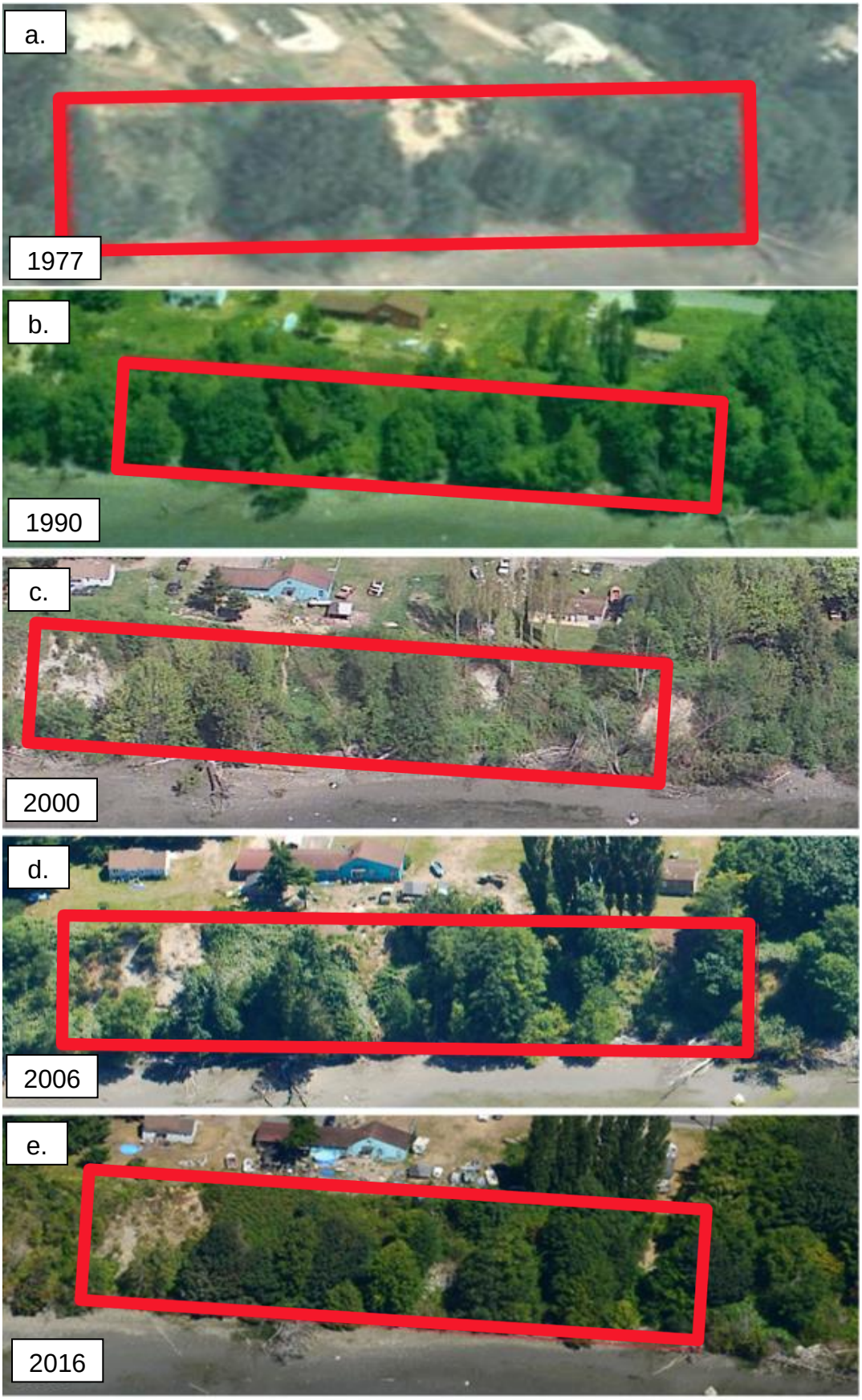

Figure 19. Oblique photos of bluff south of Point Julia near the Tribal Center. a) 1977 photo. b) 1990 photo. c) 2000 photo. d) 2006 photo. e) 2016 photo. The bluff in this area shows evidence of relatively frequent bluff erosion with exposed soil and fallen trees. View to the east. Photos from WA Department of Ecology.

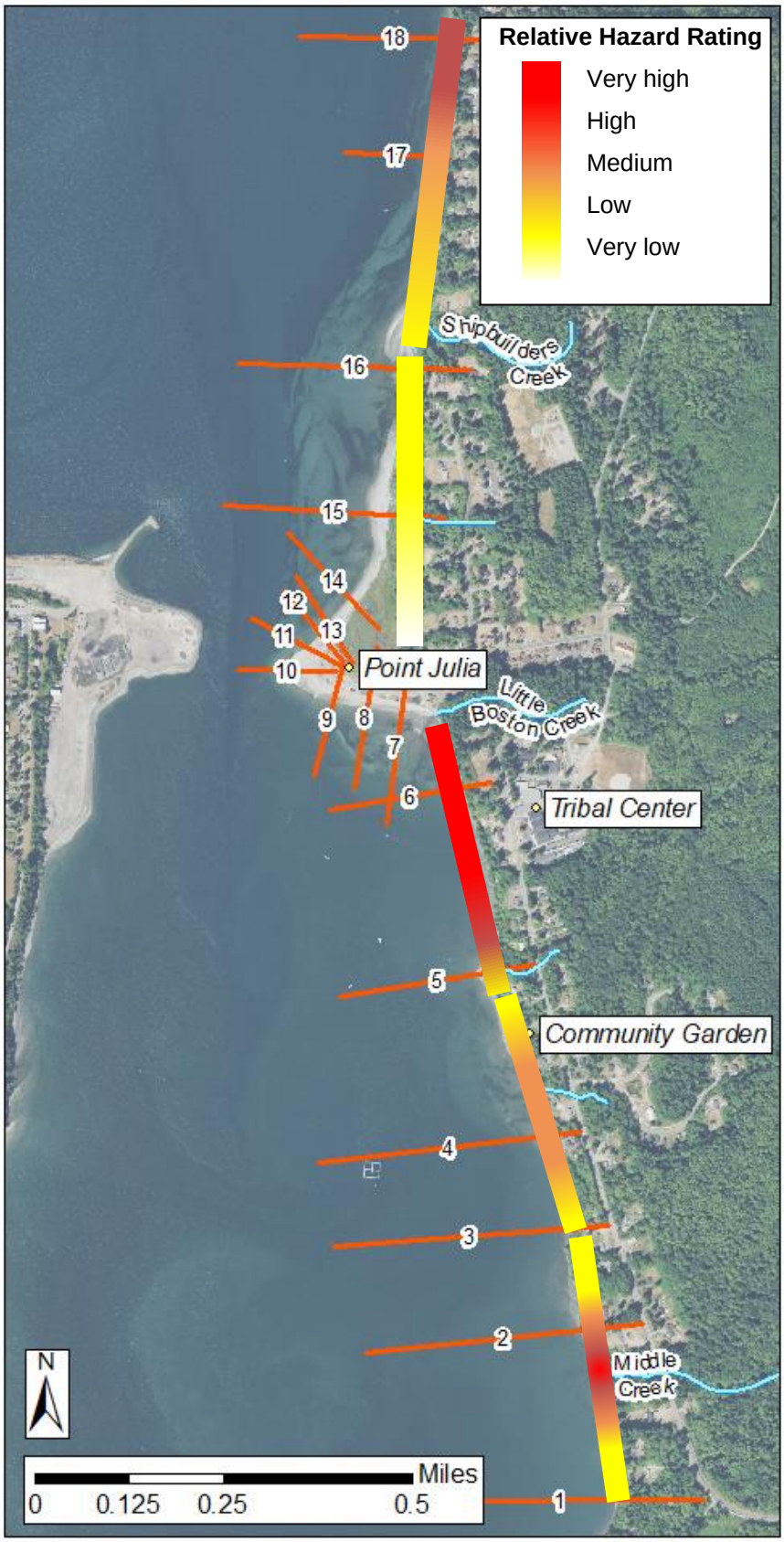

Figure 20. Bluff areas of greatest relative concern along the PGST coast. Relative ratings were determined assigning a hazard rating (1-very low hazard, 2-low hazard, 3-medium hazard, 4-high hazard, 5-very high hazard) based on historical bluff change rates, historical oblique photographs, a 2016 survey of residents, and bluff geology. These values were summed for a total hazard rating relative to other areas of the PGST coast. Base map from 2017 USDA NAIP.

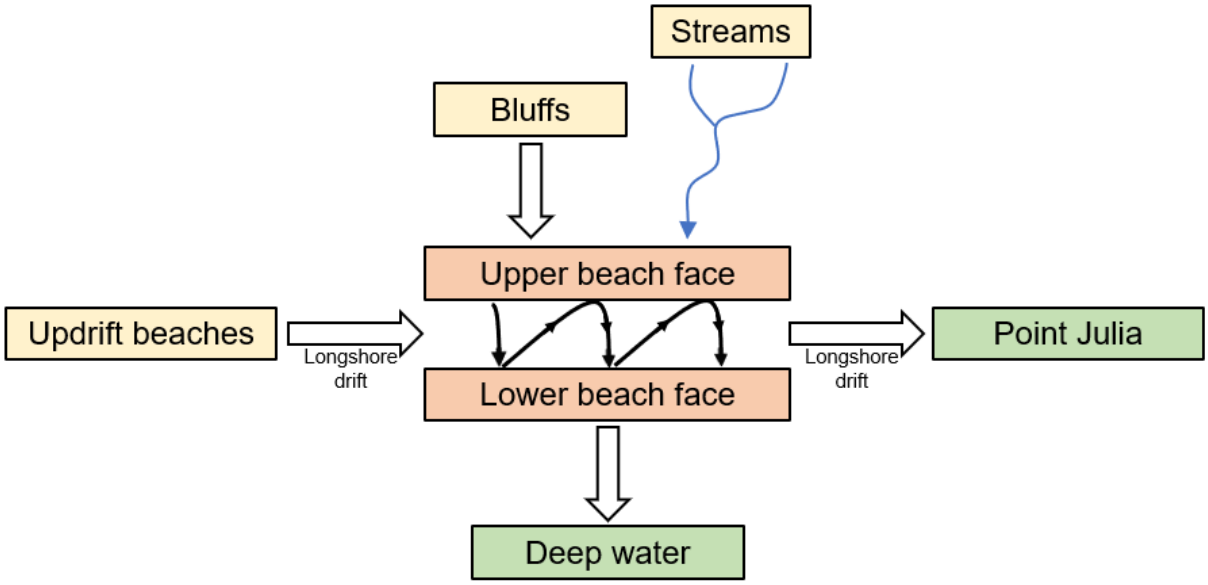

Figure 21. Conceptual model of sediment budget for the PGST beaches. This simple box model shows sediment inputs, areas of sediment transport/storage, and sediment deposition/sinks. Model modified from Shipman et al. (2014).

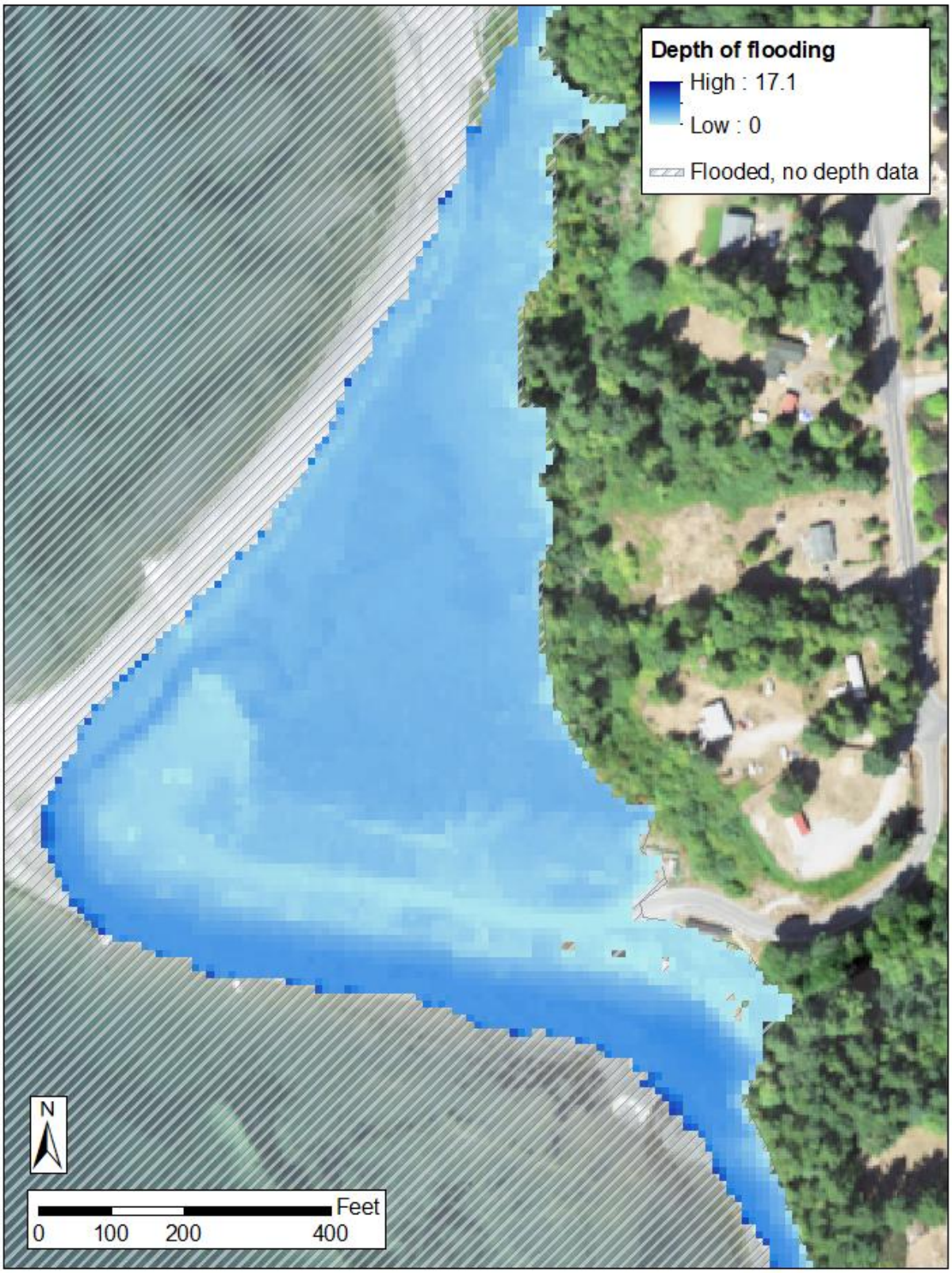

Figure 22. Base flood elevation map for Point Julia. Map shows flooding extent and depth for a 1% annual chance flood from tidal level, storm surge, and wave run up. Washington State Department of Ecology (2015) produced the data for this map using FEMA's risk assessment tool, Hazus. Base map from 2017 USDA NAIP.

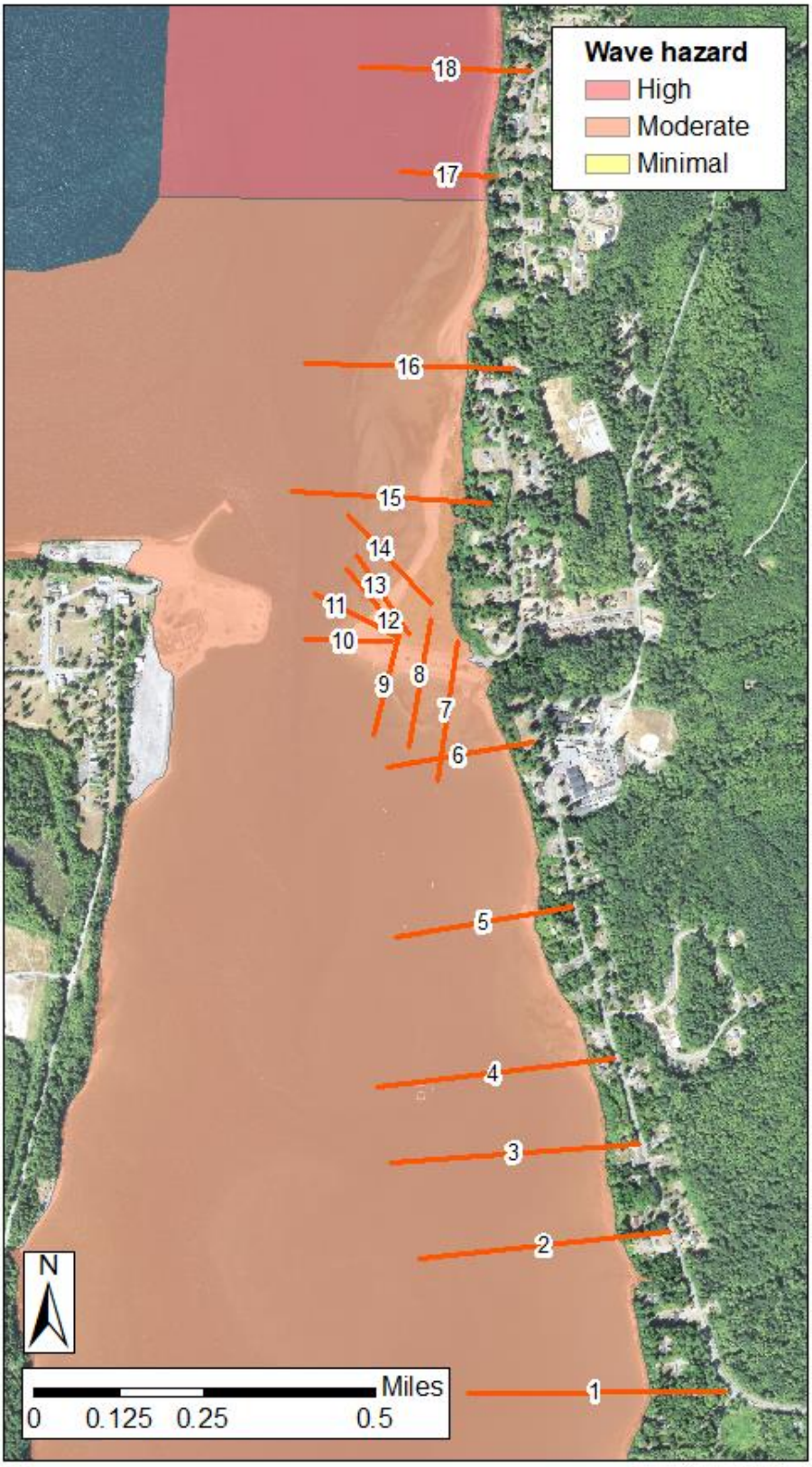

Figure 23. Wave hazard map for the PGST coastline. Most of PGST coastline has a moderate wave hazard during flooding (wave height <3 ft) with the northern part of PGST coast having a high wave hazard (wave height >3 ft). Washington State Department of Ecology (2015) produced the data for this map using FEMA's risk assessment tool, Hazus. Base map from 2017 USDA NAIP.

Figure 24. One of the Onset water loggers deployed on the tidal platform of the PGST beaches. I used the water loggers to calculate water levels along PGST beaches to compare to permanent tide gauges at Seattle and Port Townsend.

Figure 25. a) Photo overlooking Point Julia during a "king" tide event on December 26, 2018. b) Photo looking east toward the pavilion on Point Julia during the "king" tide event. c) Photo view west near the hatchery on Point Julia during the "king" tide event. d) Photo looking east toward the pavilion on Point Julia on February 17, 2020. Water level was about 5 ft above MLLW at the time of the photo (~2:45pm). e) Photo view west near the hatchery on Point Julia on February 17, 2020. Water level was about 5 ft above MLLW at the time of the photo (~2:45pm). I used this photo set to get an idea for water levels at Point Julia during extreme tide events. "King" tide photos taken by Sam Phillips ~8:00am on December 26, 2018.

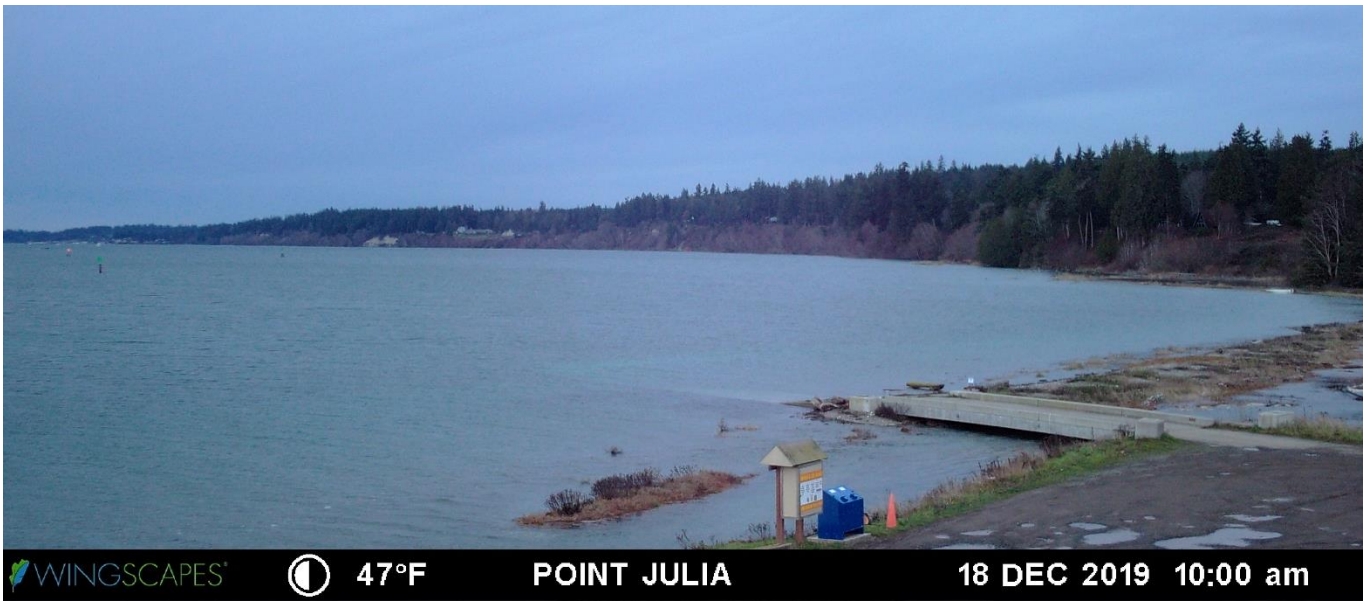

Figure 26. High tide event captured by time-lapse camera on Point Julia. This high tide flooded much of the northern beach on Point Julia. Our water loggers recorded water levels up to 12.2 ft MLLW for this event. View north.

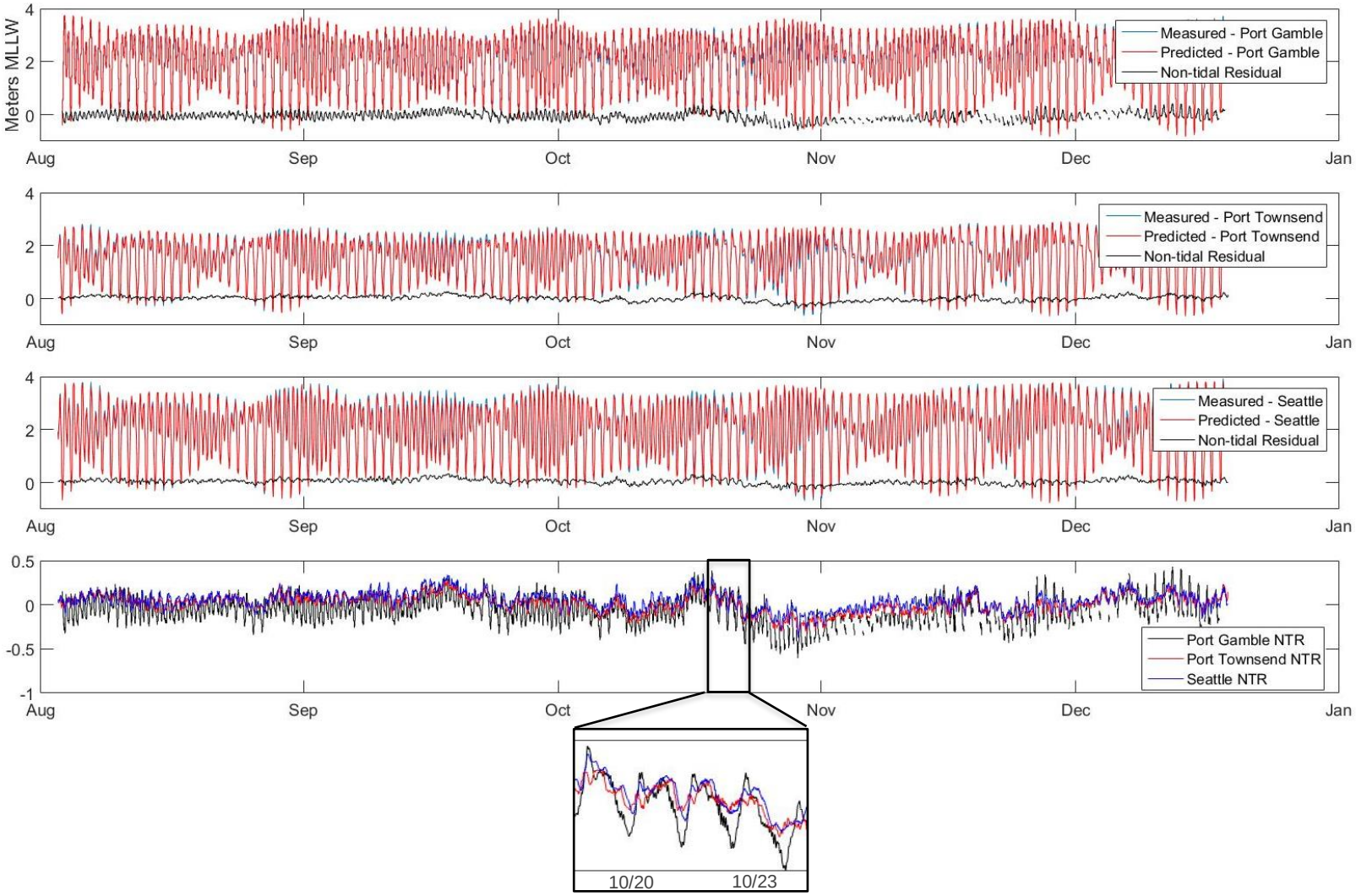

Figure 27. Plot of Port Gamble, Port Townsend, and Seattle water levels during Fall 2019. The top panel shows our measured water levels at Port Gamble from Onset Water Loggers. We predicted water levels at Bangor, WA using a harmonic tide model by Pawlowicz et al. (2002) and used this as our predicted water level at Port Gamble. Port Townsend and Seattle water level data are from NOAA Tides and Currents website. The bottom panel compares the non-tidal residual (NTR) of water levels at each site. The NTR is slightly larger at Port Gamble because the predicted water level is modelled at Bangor, WA (~13 mi from Port Gamble). Levels at Bangor, WA will be similar but not exactly the same as levels at Port Gamble. However, the overall NTR signal pattern is consistent with the NTR patterns at Seattle and Port Townsend. This suggests the ability to predict flood frequency at Port Gamble based on Port Townsend and Seattle water level, NTR, and flood frequency predictions.

Figure 28. Waves breaking on Point Julia during a slightly breezy period (gusts up to 6 mph at Port Townsend, WA) on November 19, 2019. View north from time-lapse camera.

8. Appendix A: Agisoft Processing Report

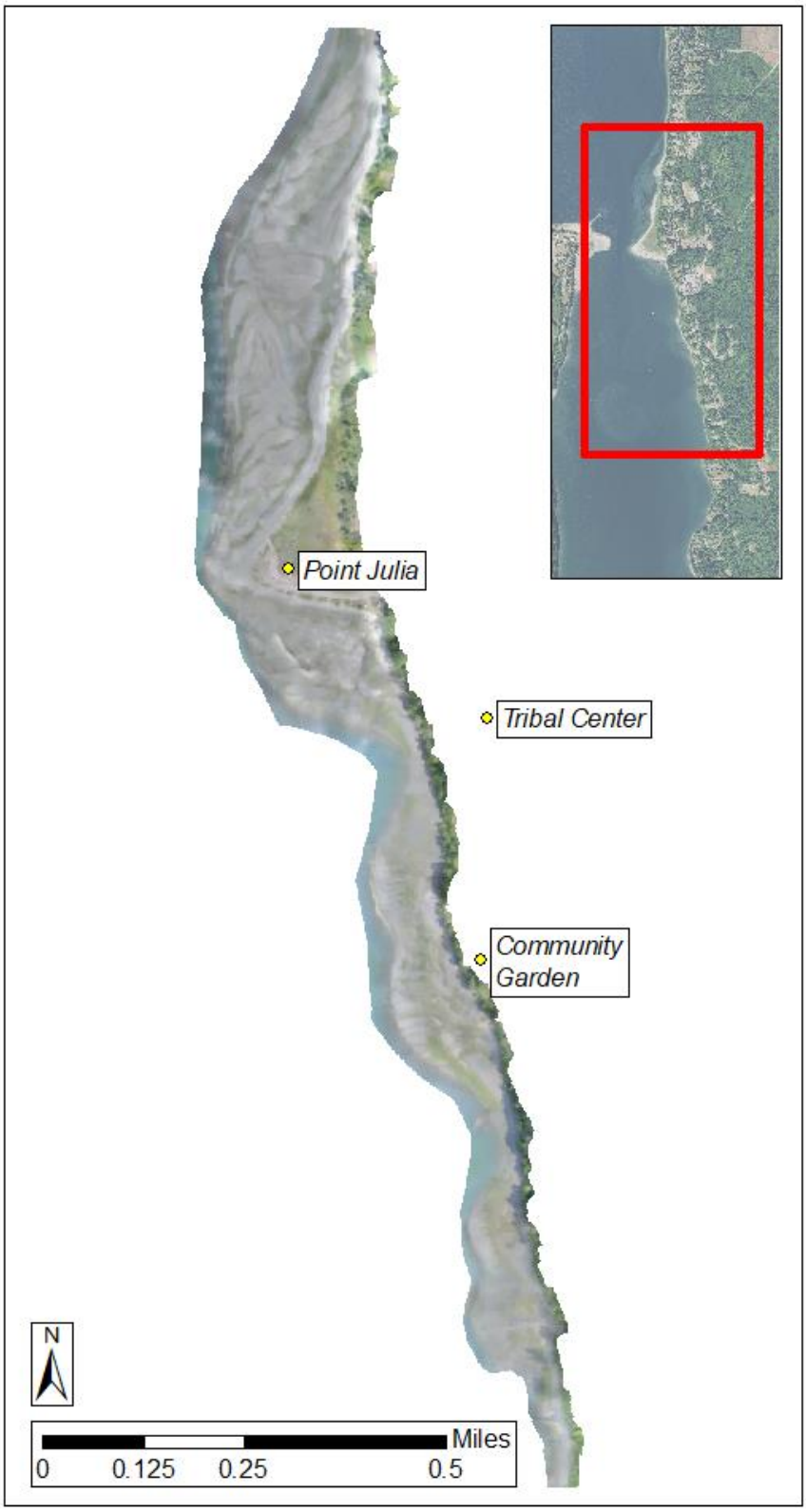

Figure A1. Orthomosaic of PGST beaches. Orthomosaic image created in Agisoft PhotoScan using drone photos captured on July 2019. Resolution is about 0.79 in/pixel.

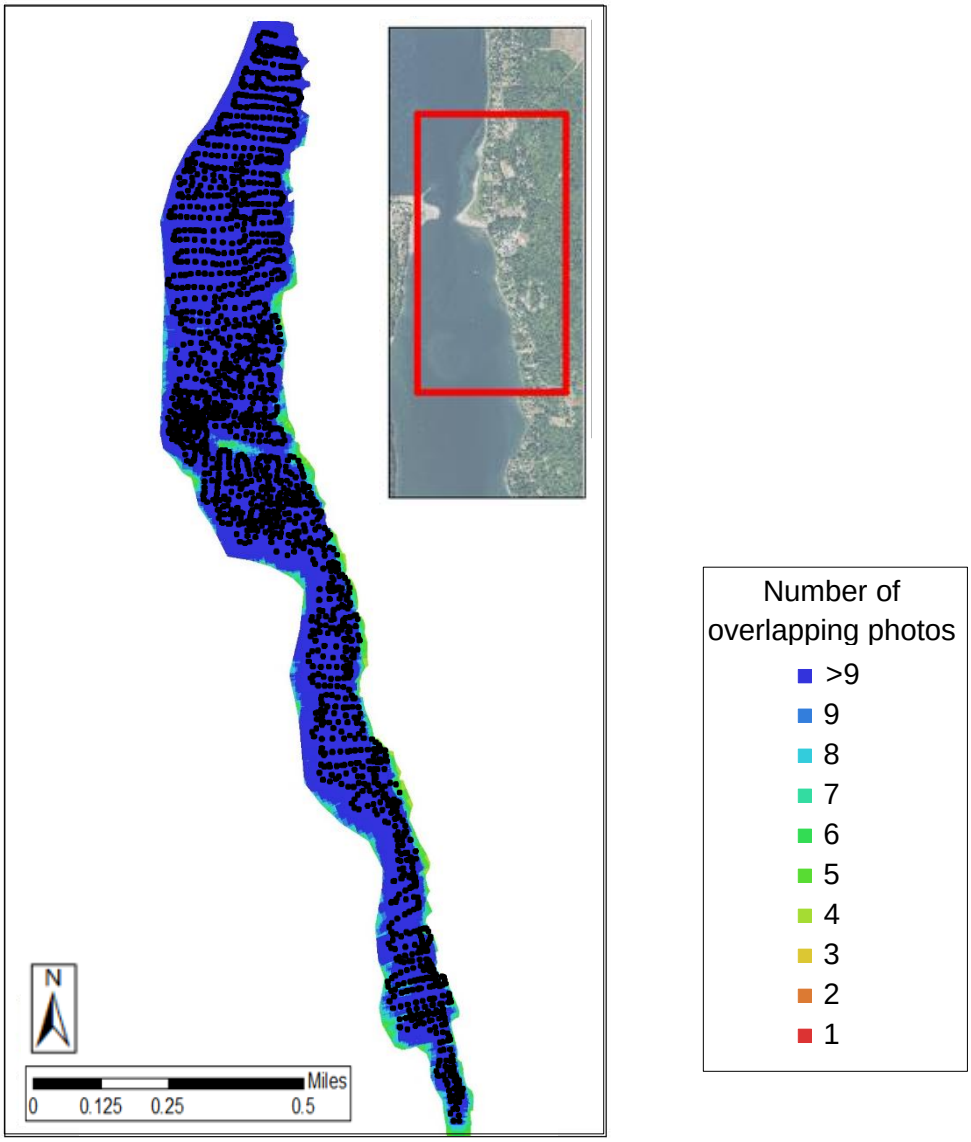

Figure A2. Camera locations and image overlap. Colors show the number of overlapping images at that location. Black dots show position of camera for each photo (2,514 total images).

Table A1. Orthomosaic survey and camera information

Flying altitude:	49.5 m	Camera stations:	2,289
Ground resolution:	1.84 cm/pix	Tie points:	9,414,254
Coverage area:	0.654 km²	Projections:	36,529,767
Number of images:	2,514	Reprojection error:	1.23 pix
Camera model:	FC300X (3.61 mm)	Resolution:	4000 x 3000
Focal length:	3.61 mm	Pixel size:	1.56 x 1.56 µm
Precalibrated:	No		

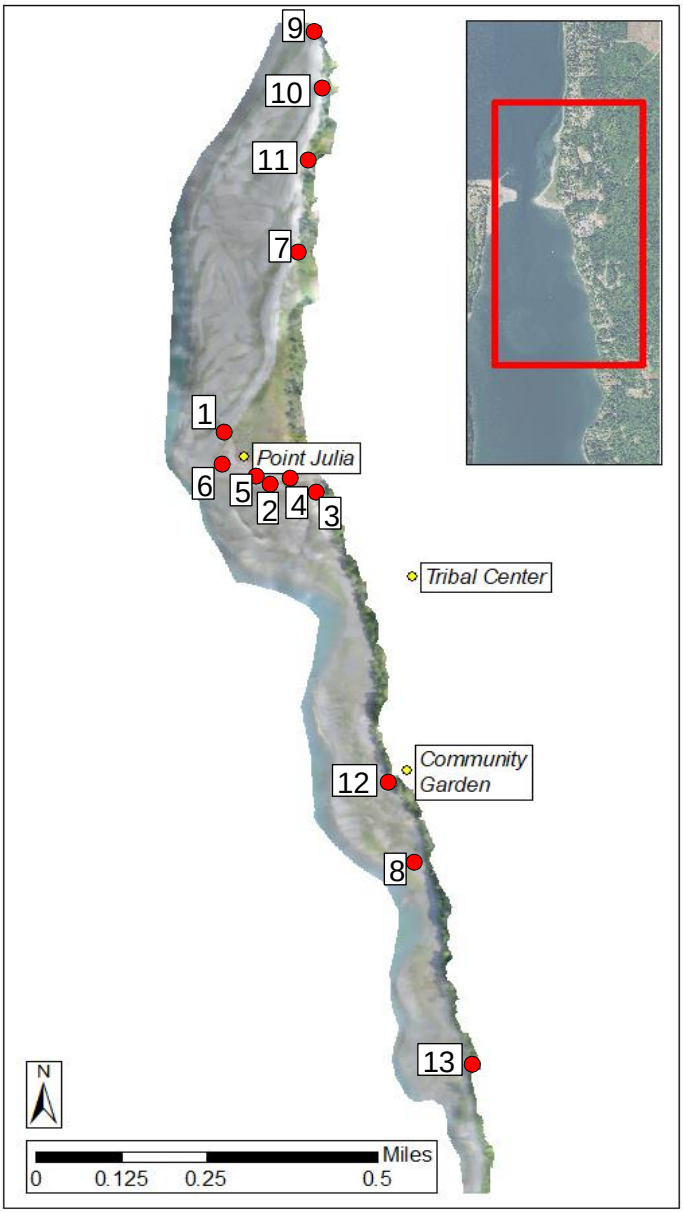

Figure A3. Ground control points. These ground control points were used to improve the georeferencing of the orthomosaic.

Table A2. Ground control point Root means square error values

Count	X error (cm)	Y error (cm)	Z error (cm)	XY error (cm)	Total (cm)	Image (pix)
13	4.59454	3.40681	3.7513	5.7198	6.84021	1.816

Table A3. Ground control points

Label	X error (cm)	Y error (cm)	Z error (cm)	Total (cm)	Image (pix)
1	2.68438	-6.89624	-0.249147	7.40447	1.220 (22)
2	-0.726877	4.68262	-6.3212	7.90018	1.739 (15)
3	7.96596	2.73248	4.42763	9.51456	1.077 (5)
4	-0.929698	-2.87845	2.17581	3.72612	1.234 (10)
5	-3.41952	-2.62776	-5.64118	7.10078	3.180 (8)
6	-3.94654	6.16527	5.19319	8.97523	1.010 (15)
7	-4.29925	-0.544853	0.35447	4.34811	1.832 (17)
8	-0.0912953	0.29179	-1.22585	1.2634	2.721 (36)
9	-11.4194	-2.63689	6.40029	13.3536	0.133 (2)
10	1.07151	1.41379	2.89291	3.3935	0.801 (14)
11	4.97139	-3.34453	-1.70964	6.23085	0.847 (14)
12	-0.587256	-0.391283	2.40584	2.50719	1.448 (6)
13	-0.0397647	-0.23877	-0.343687	0.420372	0.929 (4)
Total	**4.59454**	**3.40681**	**3.7513**	**6.84021**	**1.816**

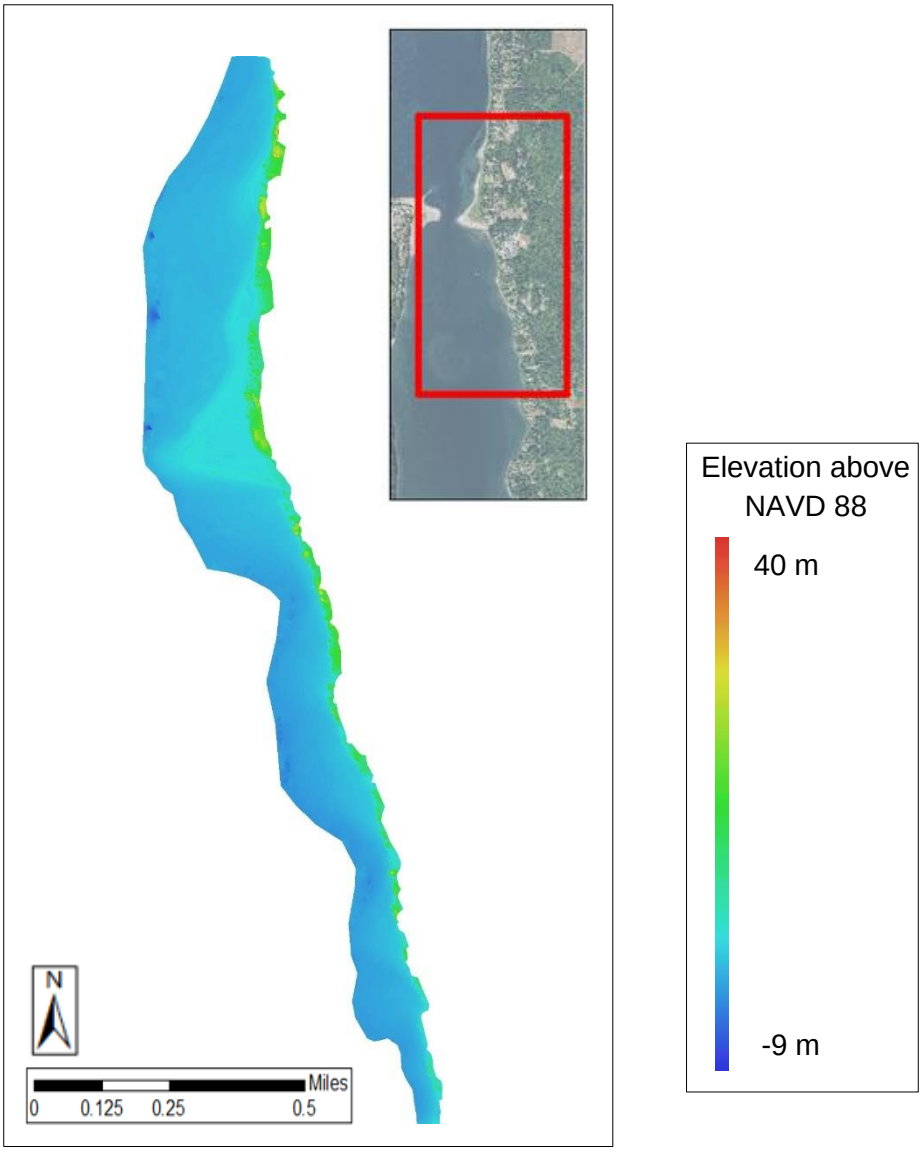

Figure A4. Reconstructed digital elevation model (DEM). Resolution is 3.68 cm/pix. Point density is 738 points/m^2.

Table A4. Agisoft processing parameters

General	
Cameras	2514
Aligned cameras	2289
Markers	13
Coordinate system	NAD83(2011) (EPSG::6318)
Point Cloud	
Points	9,414,254 of 11,994,838
RMS reprojection error	0.311224 (1.23232 pix)
Max reprojection error	102.806 (436.384 pix)
Mean key point size	3.93397 pix
Effective overlap	4.31587
Alignment parameters	
Accuracy	High
Pair preselection	Generic
Key point limit	60,000
Tie point limit	0
Constrain features by mask	No
Adaptive camera model fitting	Yes
Matching time	9 hours 51 minutes
Alignment time	6 hours 12 minutes
Optimization parameters	
Parameters	f, b1, b2, cx, cy, k1-k4, p1, p2
Optimization time	16 minutes 14 seconds
Dense Point Cloud	
Points	532,410,539
Reconstruction parameters	
Quality	High
Depth filtering	Aggressive
Depth maps generation time	1 days 22 hours
Dense cloud generation time	13 hours 50 minutes
DEM	
Size	45,604 x 106,559
Coordinate system	NAD83(2011) (EPSG::6318)
Reconstruction parameters	
Source data	Dense cloud
Interpolation	Enabled
Processing time	26 minutes 19 seconds
Orthomosaic	
Size	90,928 x 212,917
Coordinate system	NAD83(2011) (EPSG::6318)
Channels	3, uint8
Blending mode	Mosaic
Reconstruction parameters	
Surface	DEM
Enable color correction	No
Processing time	39 minutes 44 seconds
Software	
Version	1.2.6 build 2834
Platform	Windows 64 bit

9. Appendix B: PGST Shoreline Profiles

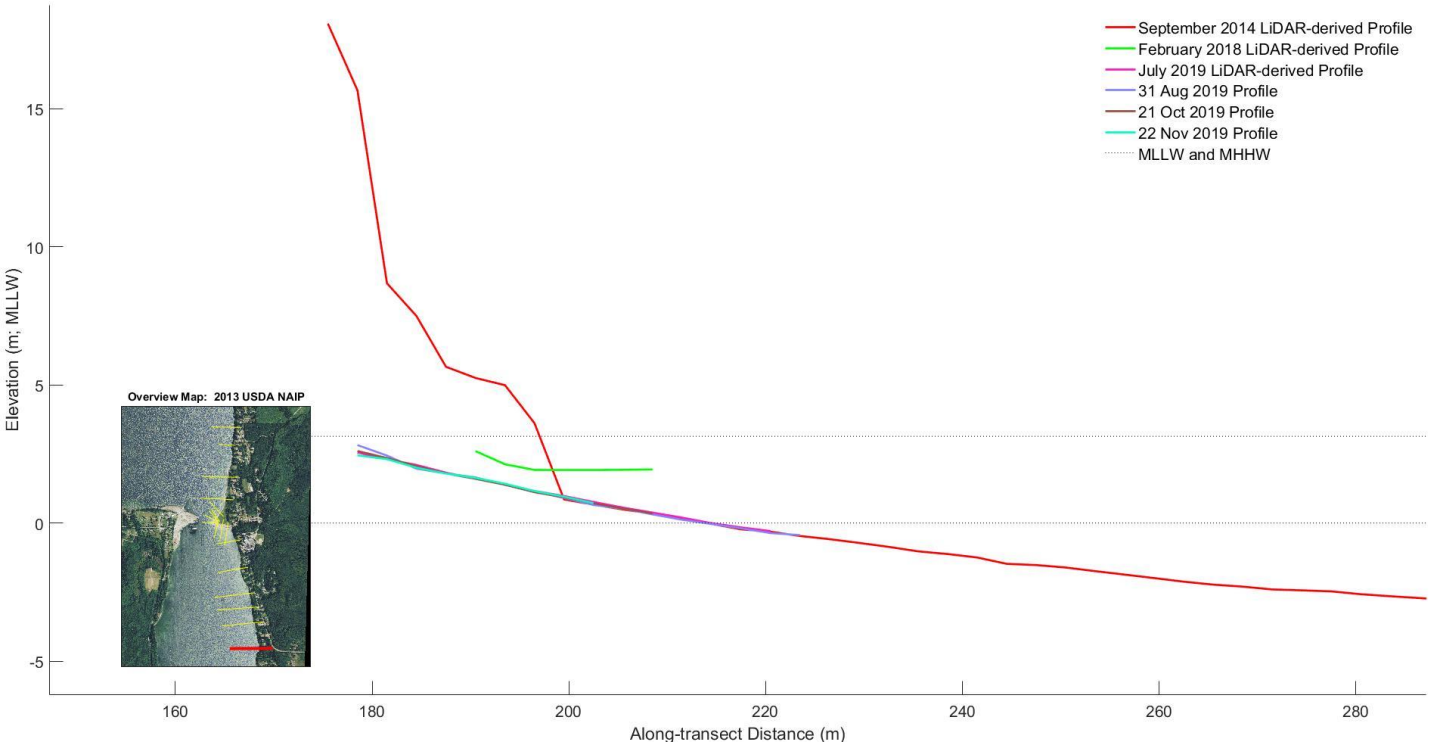

Figure B1. Shoreline profile of Focus transect 1 on the south end of PGST coastline. We derived profiles from LiDAR data and GNSS surveying.

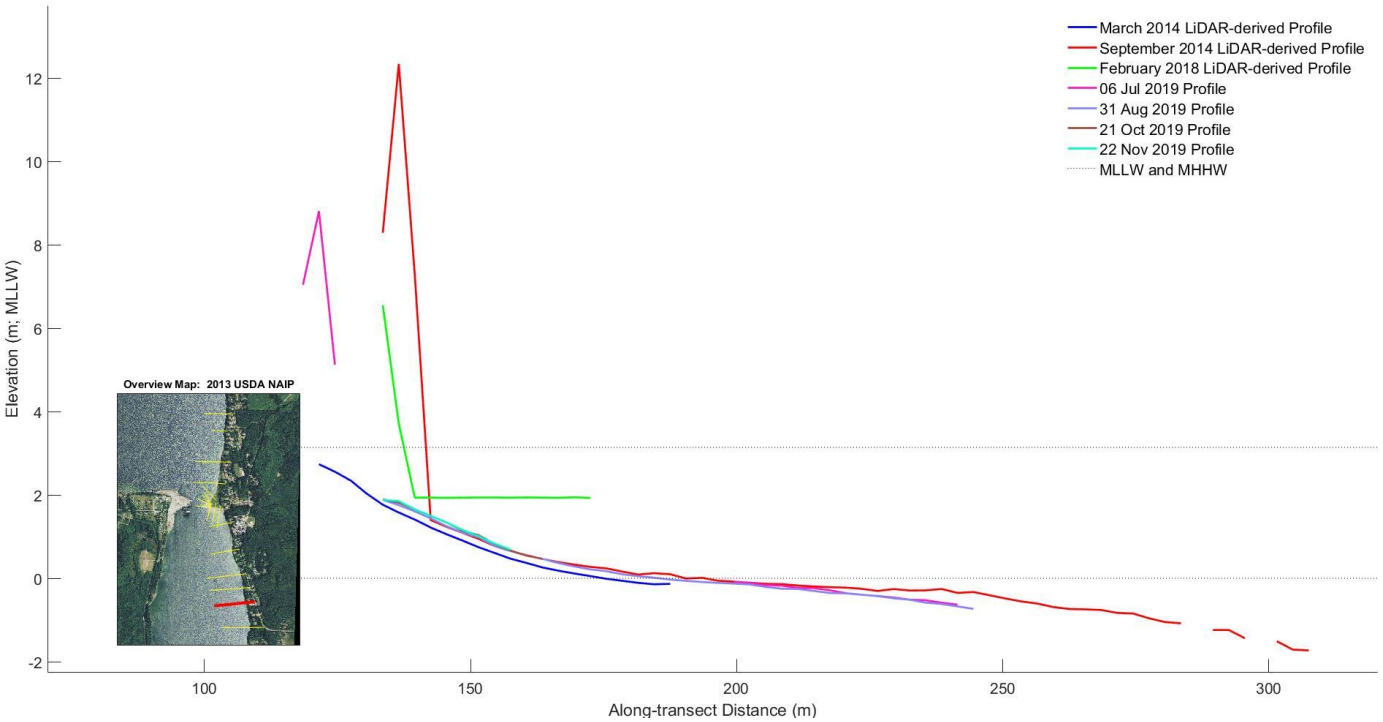

Figure B2. Shoreline profile of Focus transect 2. We derived profiles from LiDAR data and GNSS surveying.

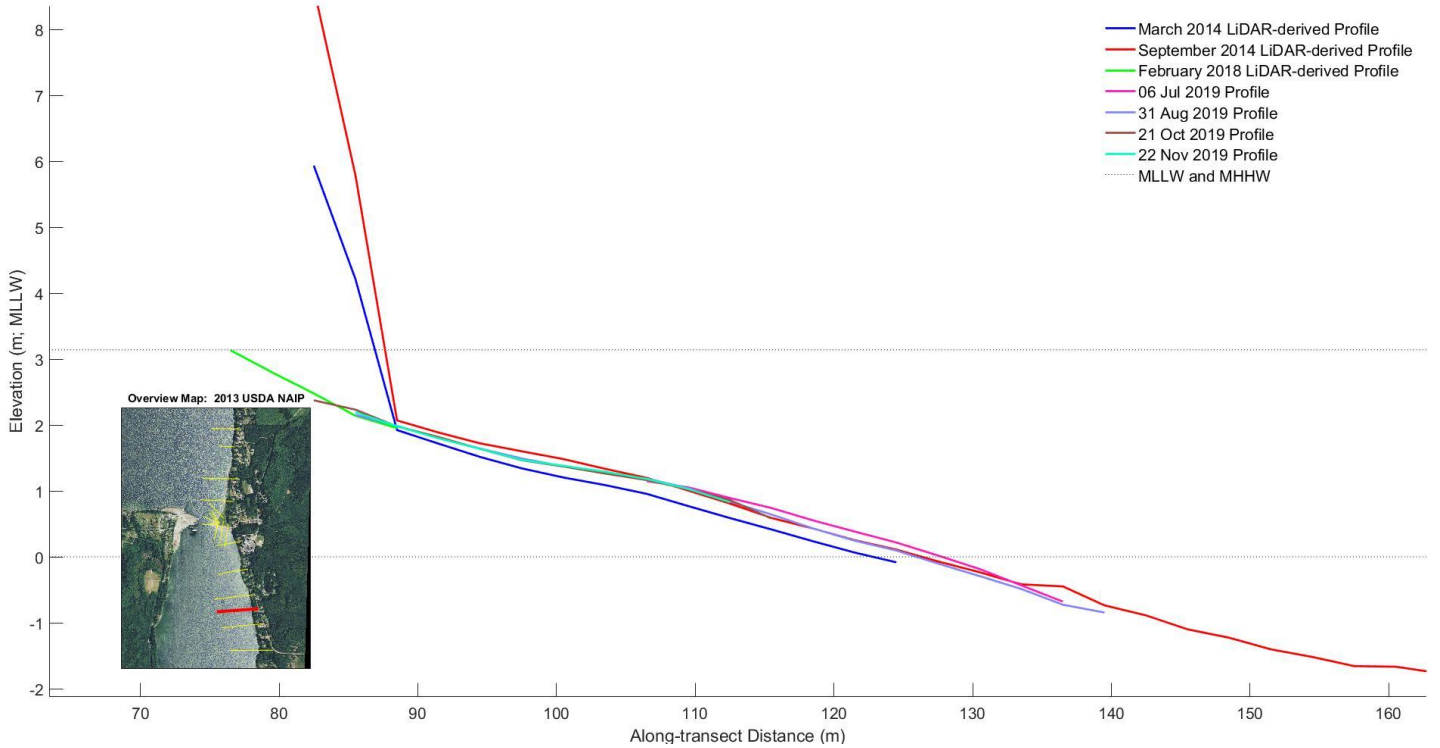

Figure B3. Shoreline profile of Focus transect 3. We derived profiles from LiDAR data and GNSS surveying.

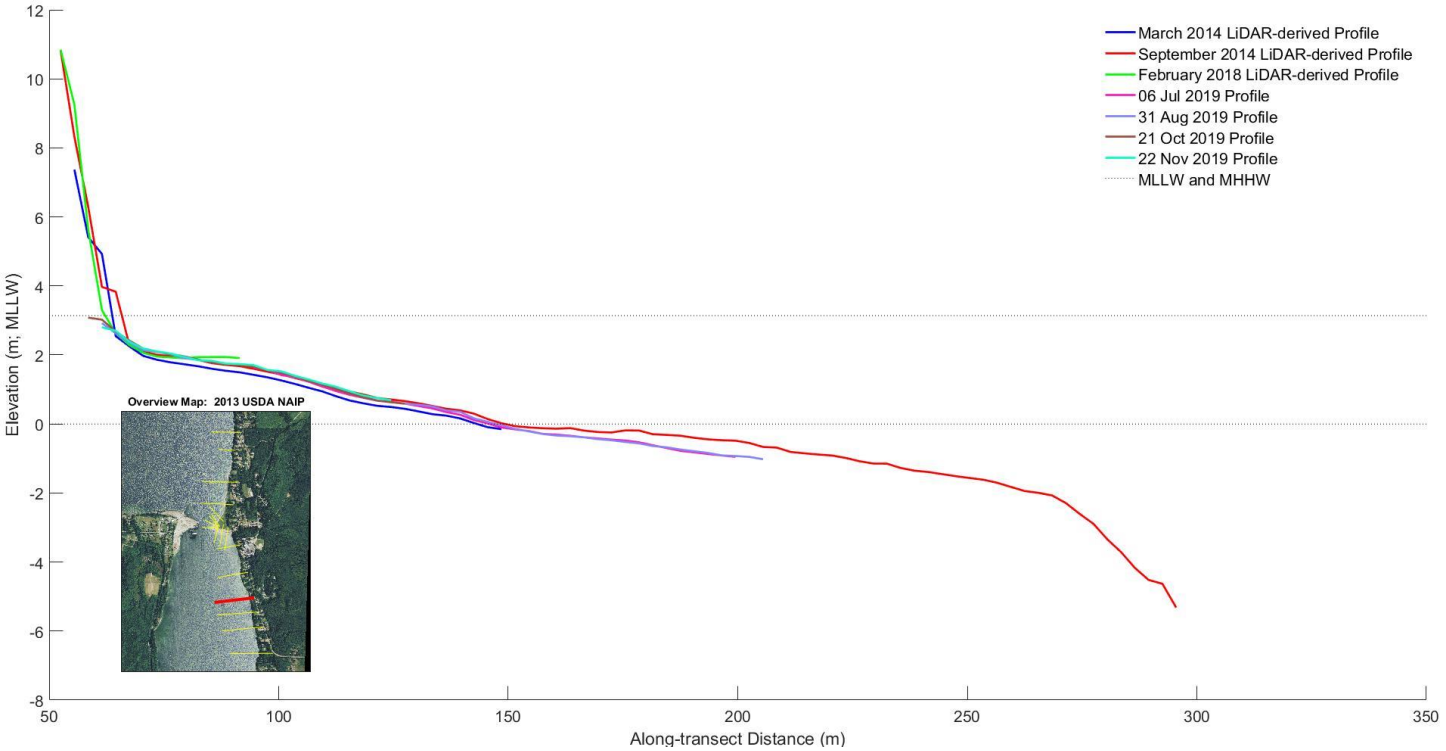

Figure B4. Shoreline profile of Focus transect 4. We derived profiles from LiDAR data and GNSS surveying.

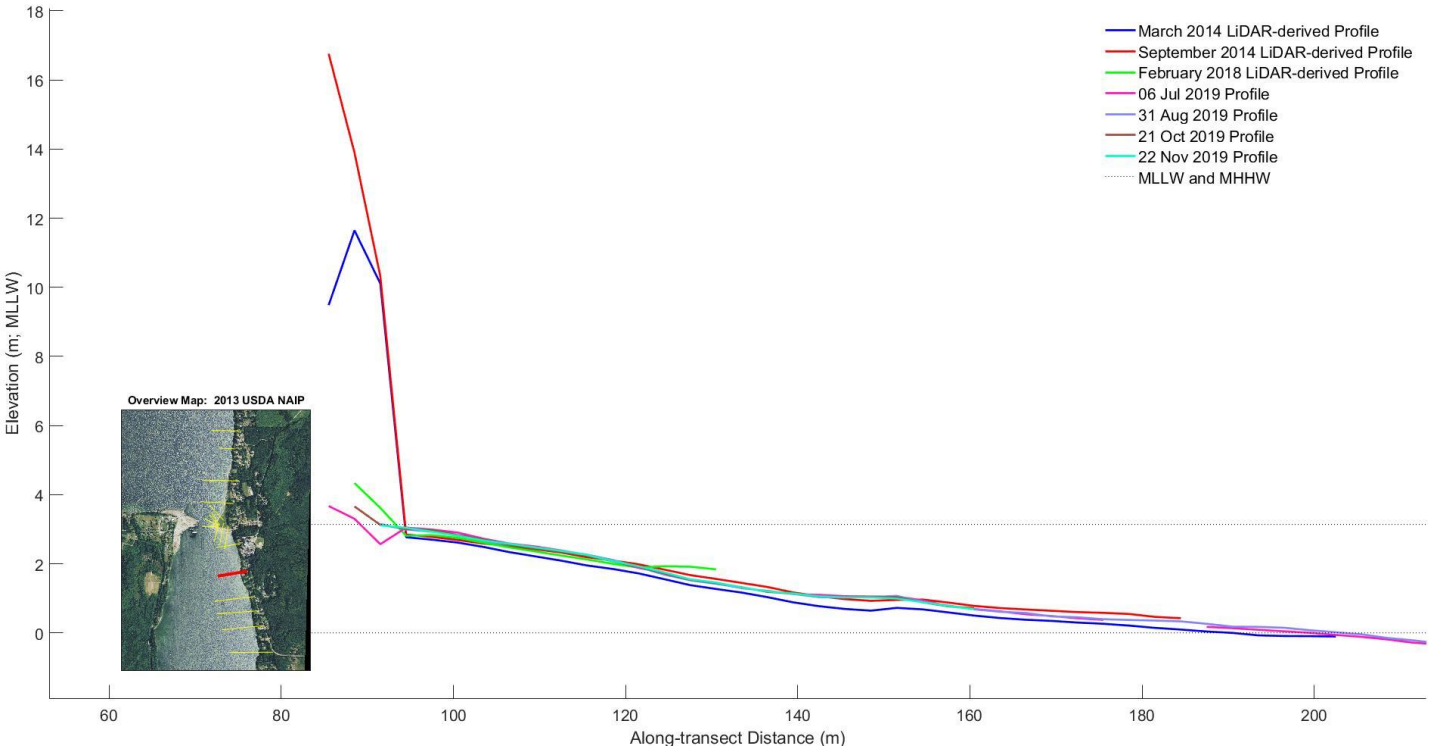

Figure B5. Shoreline profile of Focus transect 5. We derived profiles from LiDAR data and GNSS surveying.

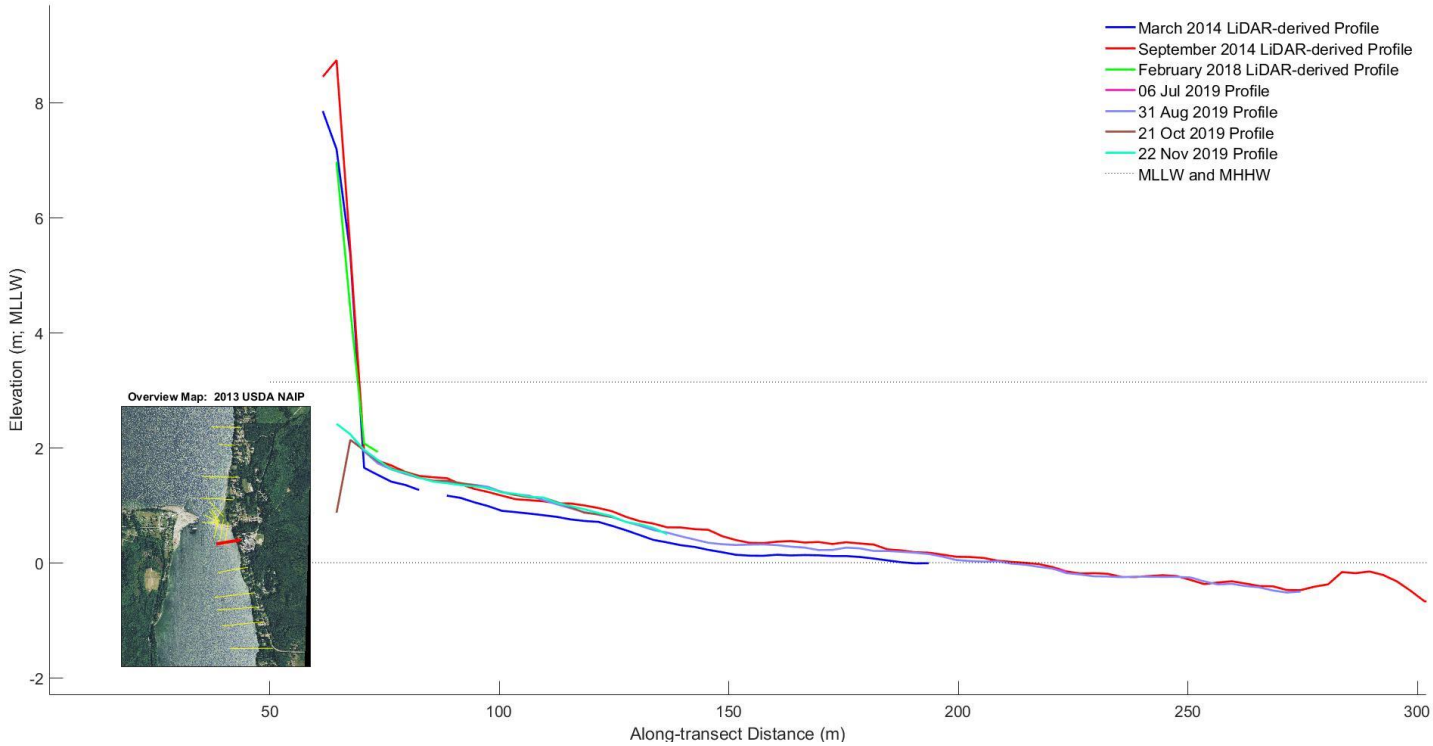

Figure B6. Shoreline profile of Focus transect 6 near the base of the cemetery. We derived profiles from LiDAR data and GNSS surveying.

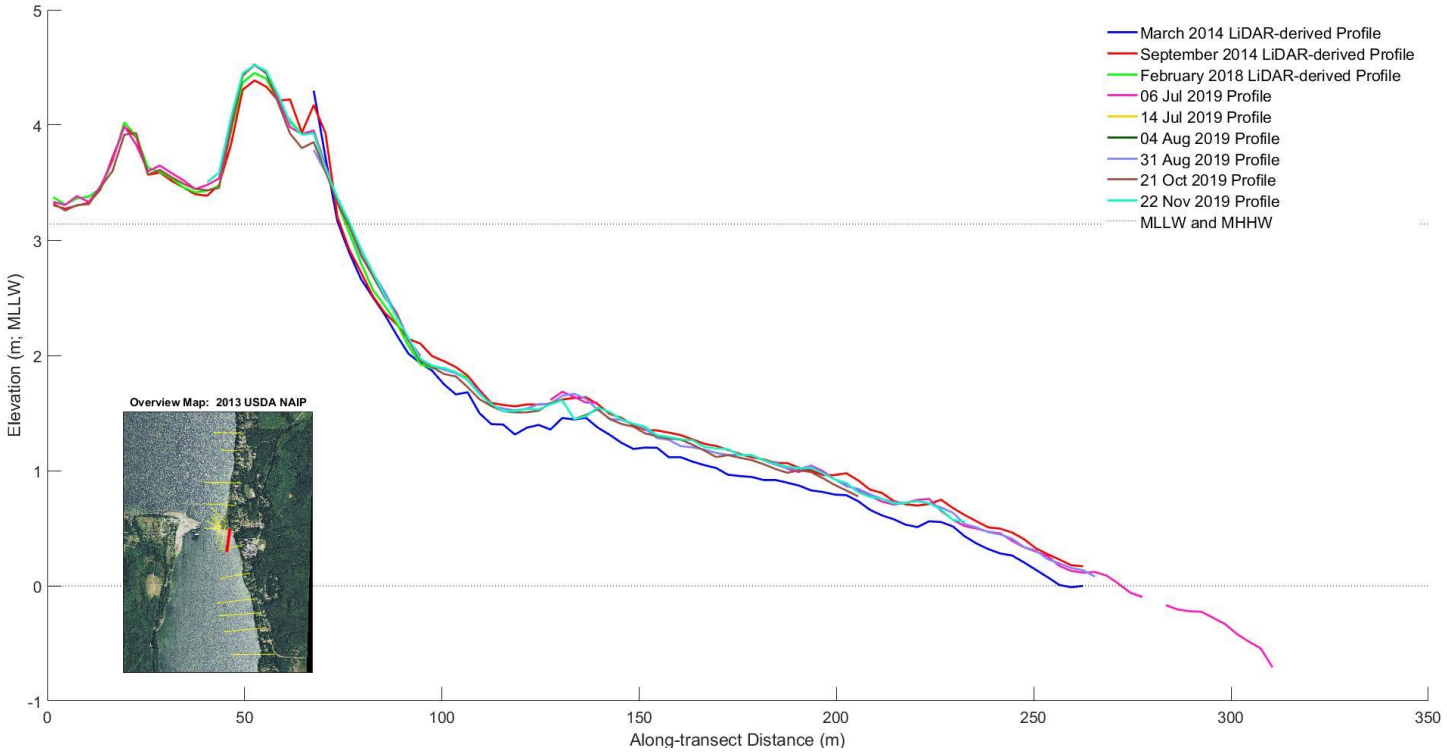

Figure B7. Shoreline profile of Focus transect 7 on the south side of Point Julia. We derived profiles from LiDAR data and GNSS surveying.

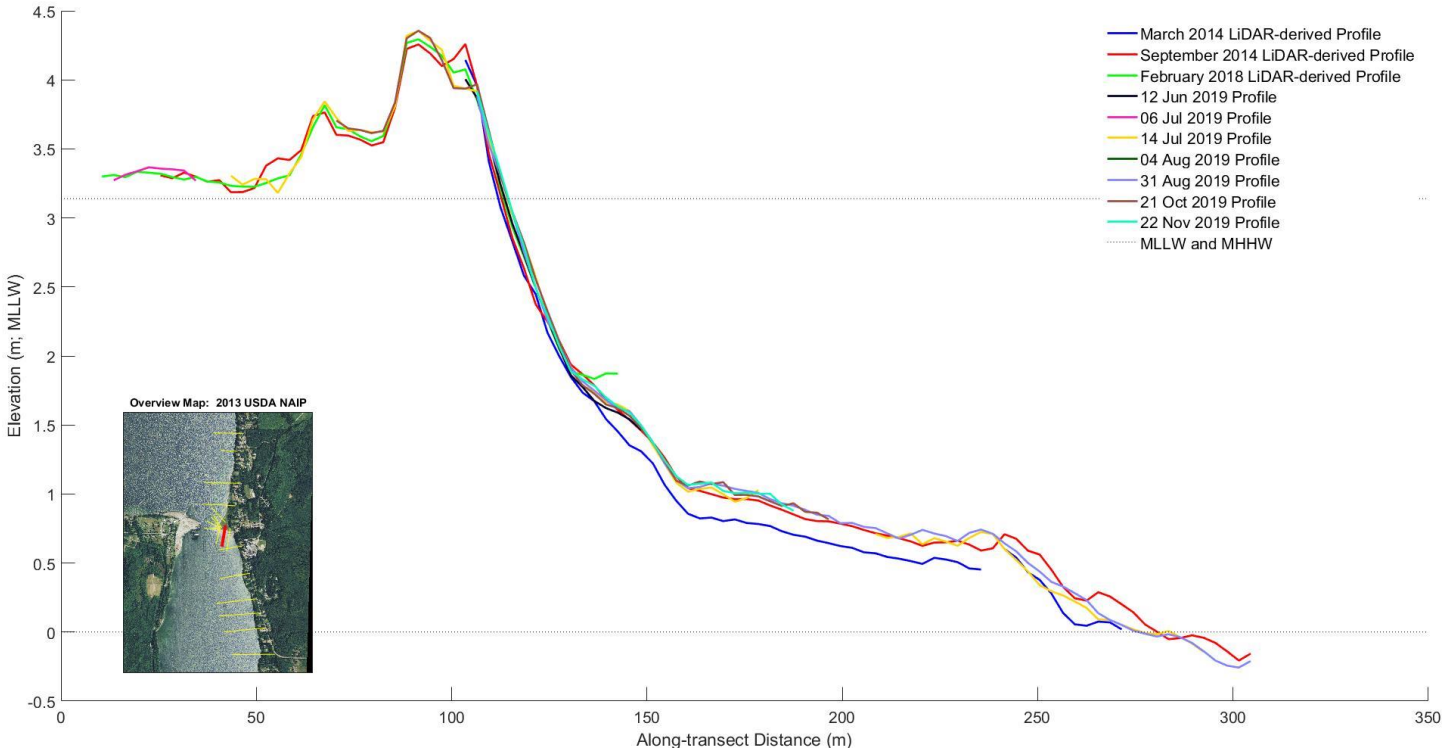

Figure B8. Shoreline profile of Focus transect 8 on the south side of Point Julia. We derived profiles from LiDAR data and GNSS surveying.

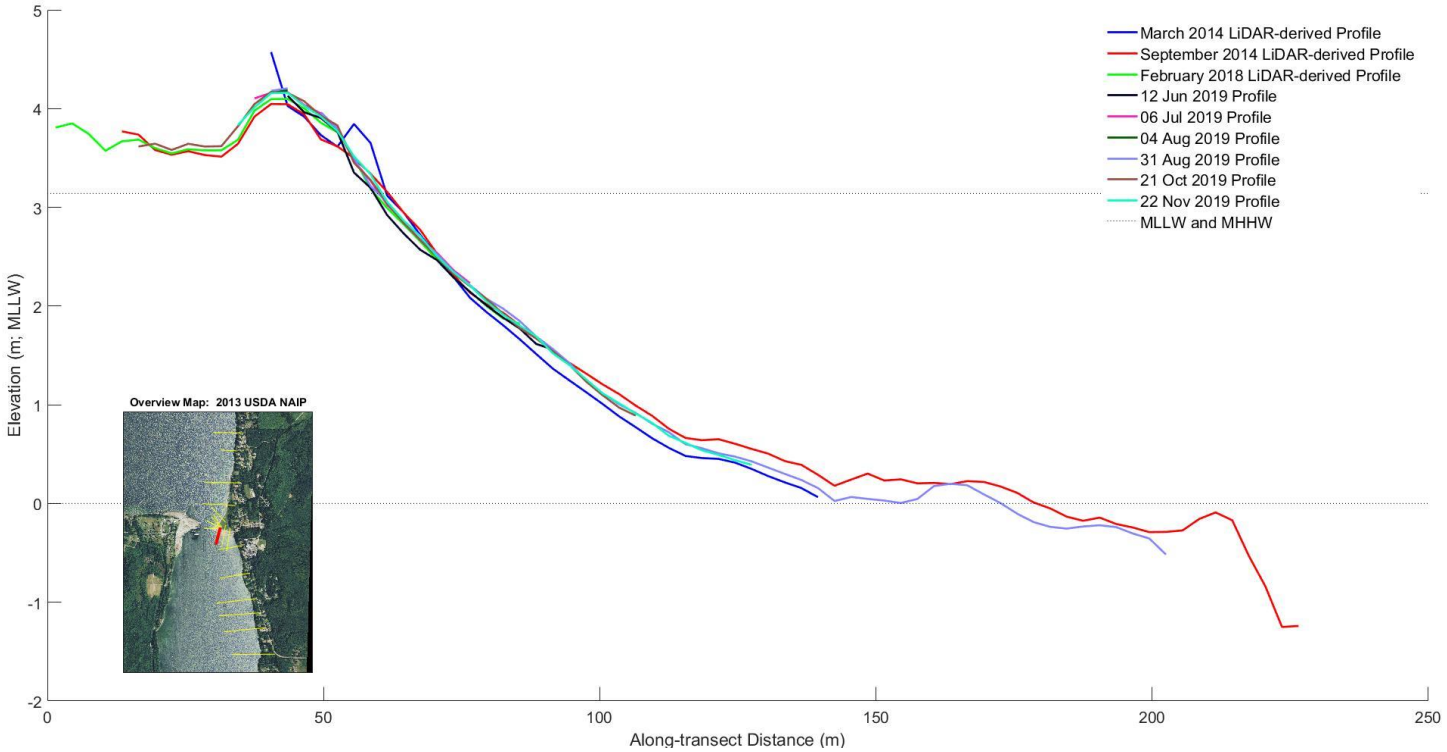

Figure B9. Shoreline profile of Focus transect 9 near the south boat ramp on Point Julia. We derived profiles from LiDAR data and GNSS surveying.

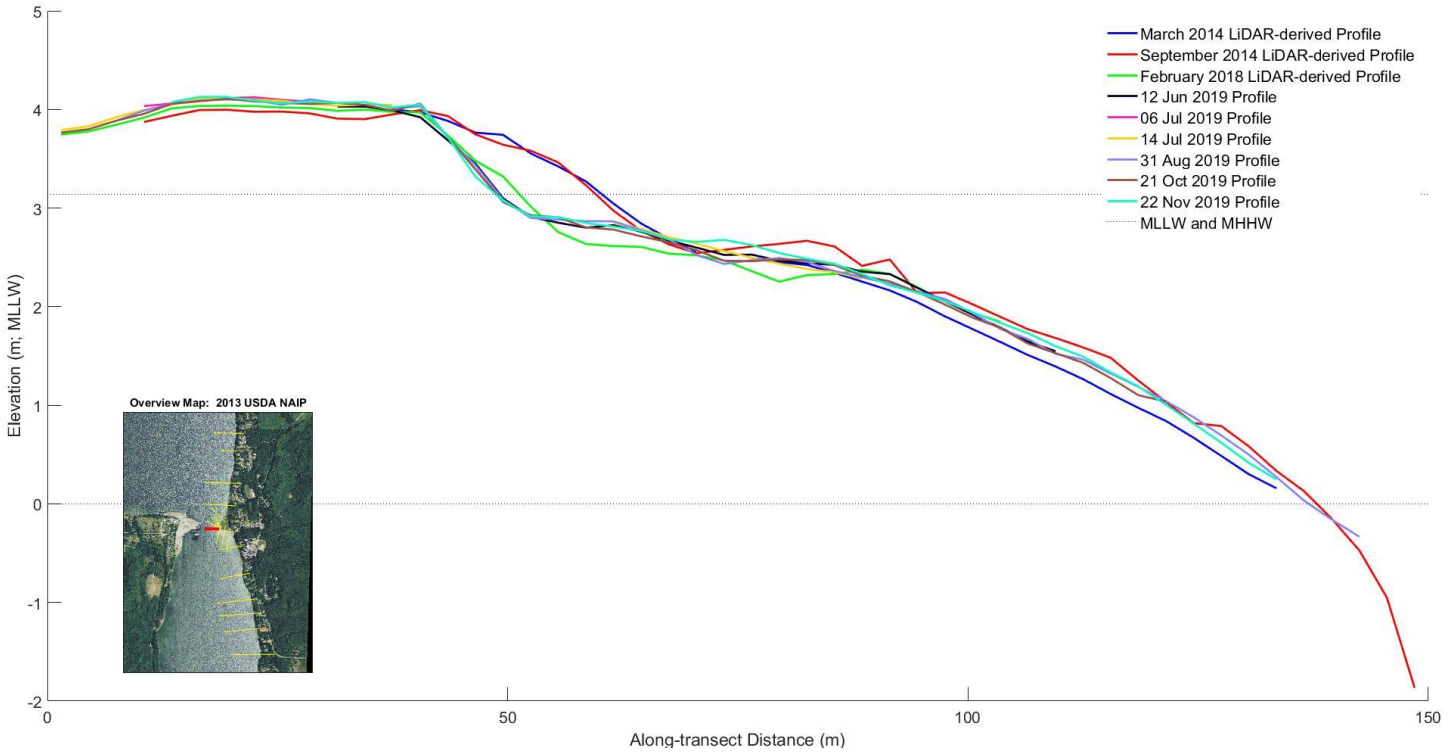

Figure B10. Shoreline profile of Focus transect 10 on the tip of Point Julia. This profile showed the most significant change of all our beach profiles. The upper shoreface shows distinct changes between 2014 and 2018. We derived profiles from LiDAR data and GNSS surveying.

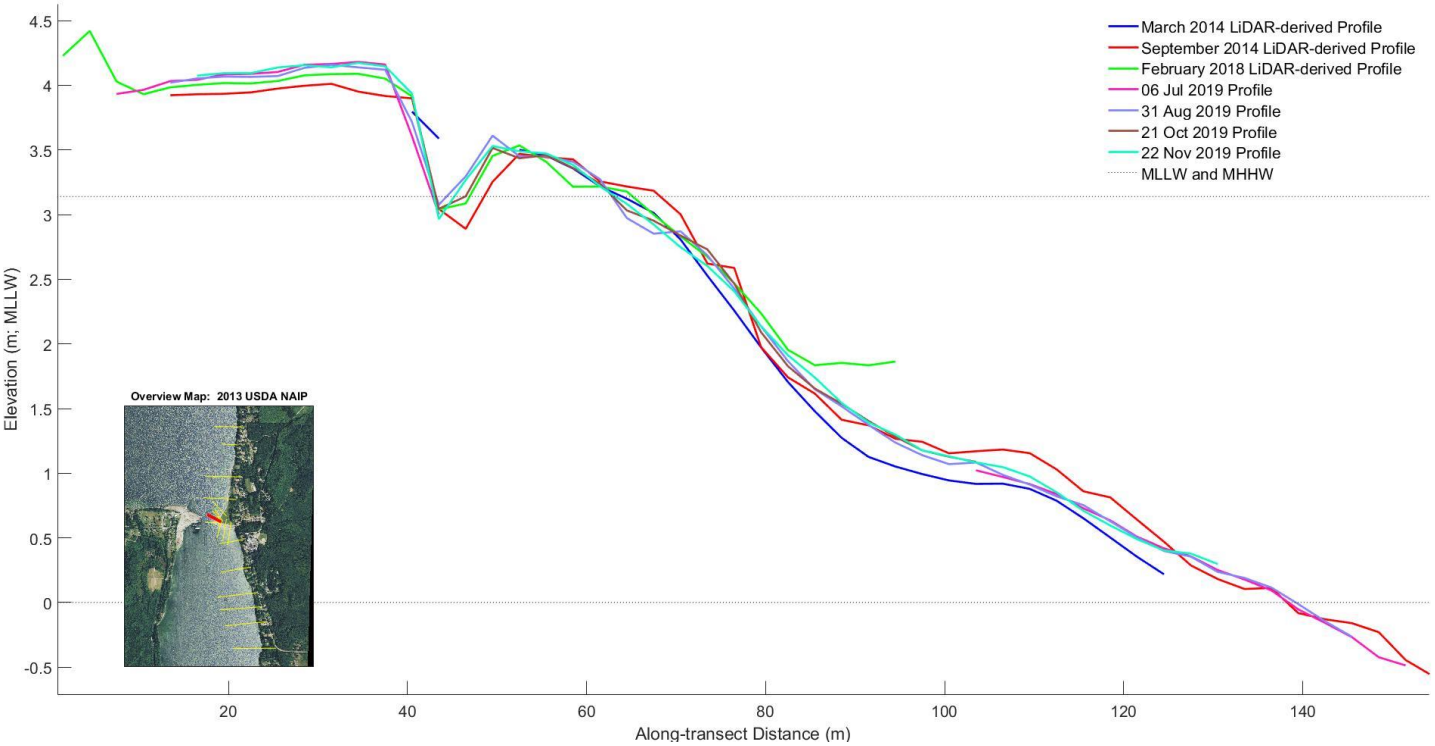

Figure B11. Shoreline profile of Focus transect 11 on the north side of Point Julia. We derived profiles from LiDAR data and GNSS surveying.

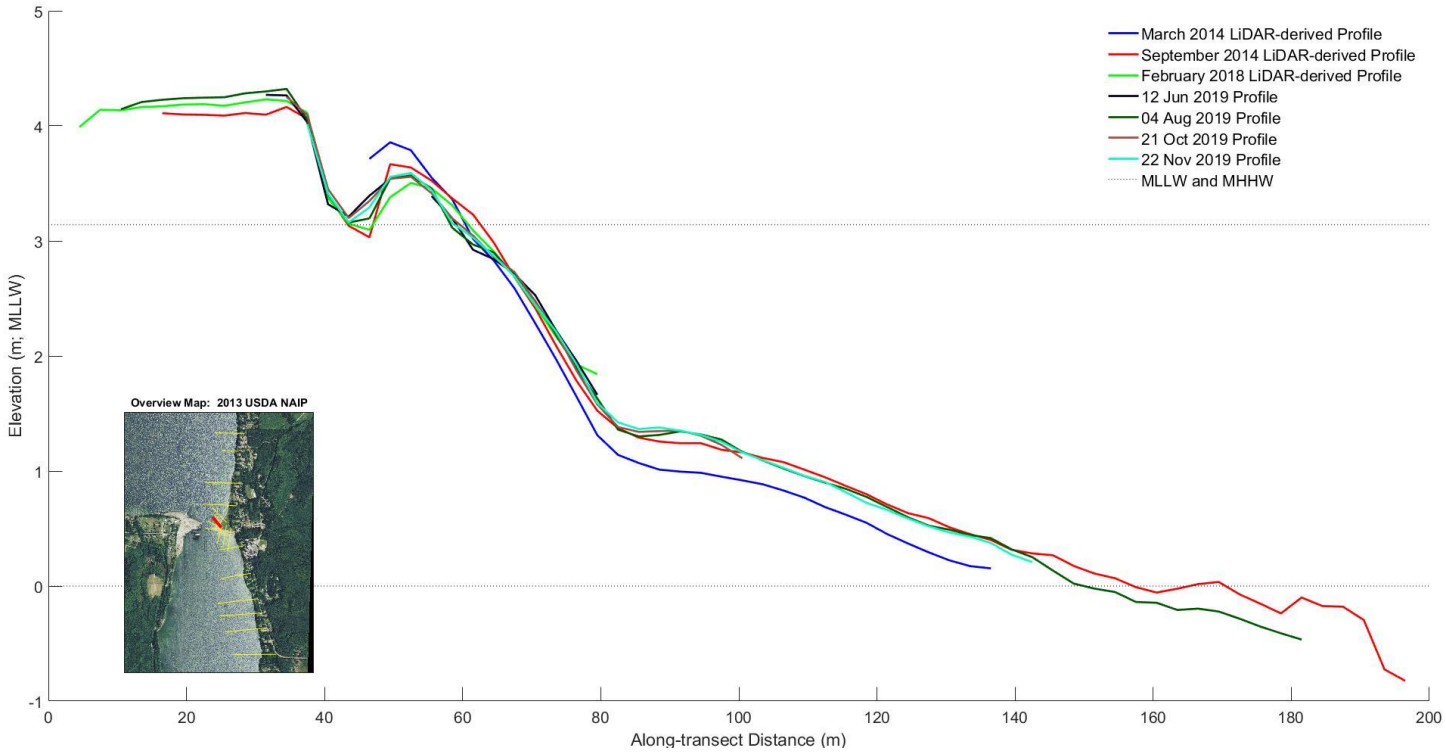

Figure B12. Shoreline profile of Focus transect 12 on the south side of the north boat ramp on Point Julia. We derived profiles from LiDAR data and GNSS surveying.

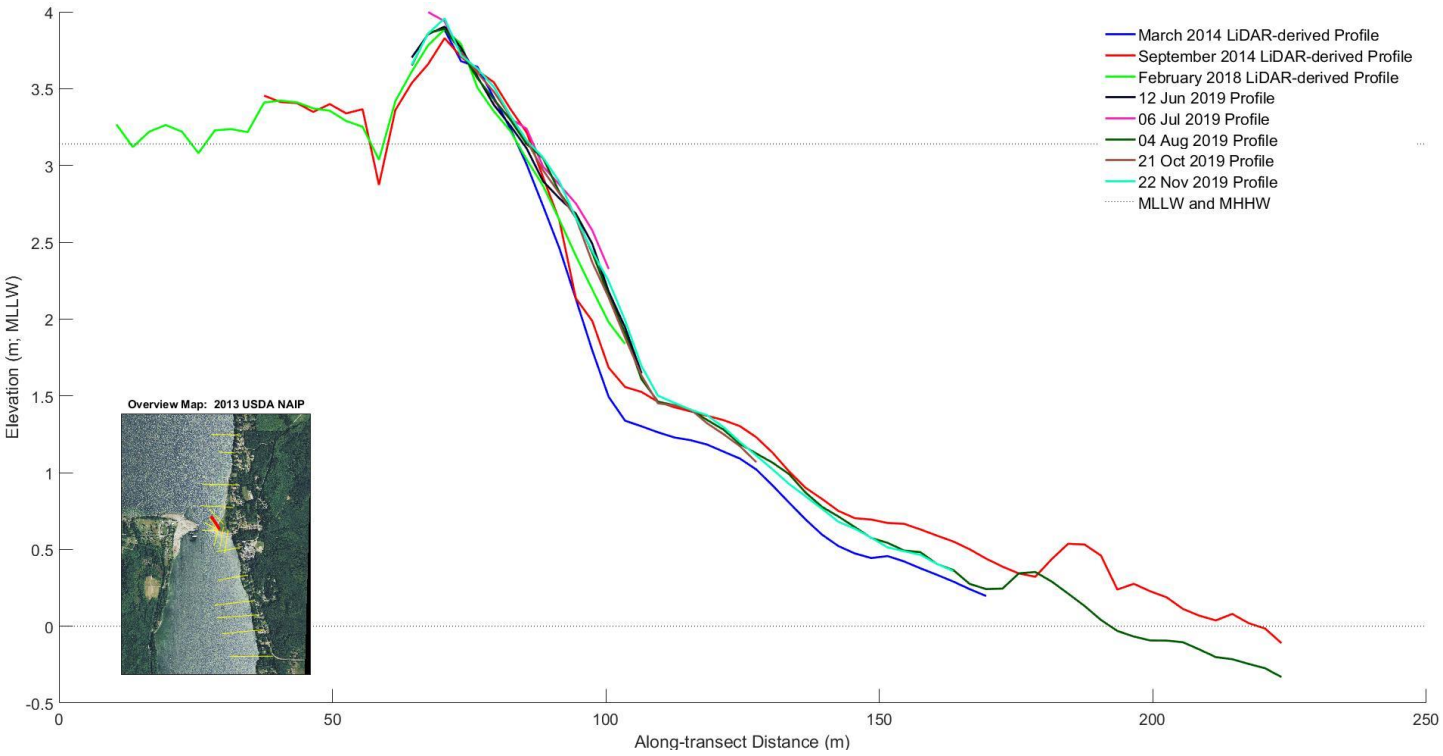

Figure B13. Shoreline profile of Focus transect 13 on the north side of the north boat ramp on Point Julia. We derived profiles from LiDAR data and GNSS surveying.

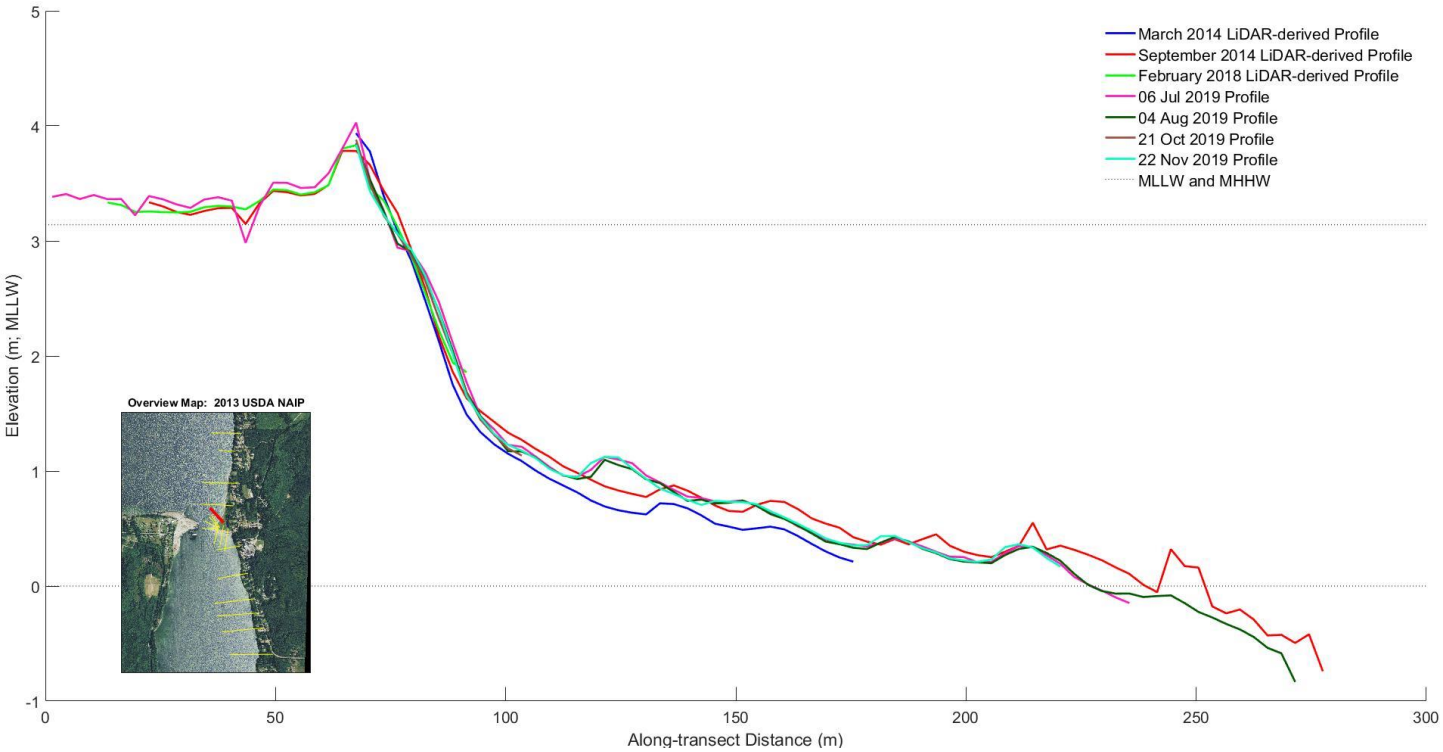

Figure B14. Shoreline profile of Focus transect 14 on the north side of Point Julia. We derived profiles from LiDAR data and GNSS surveying.

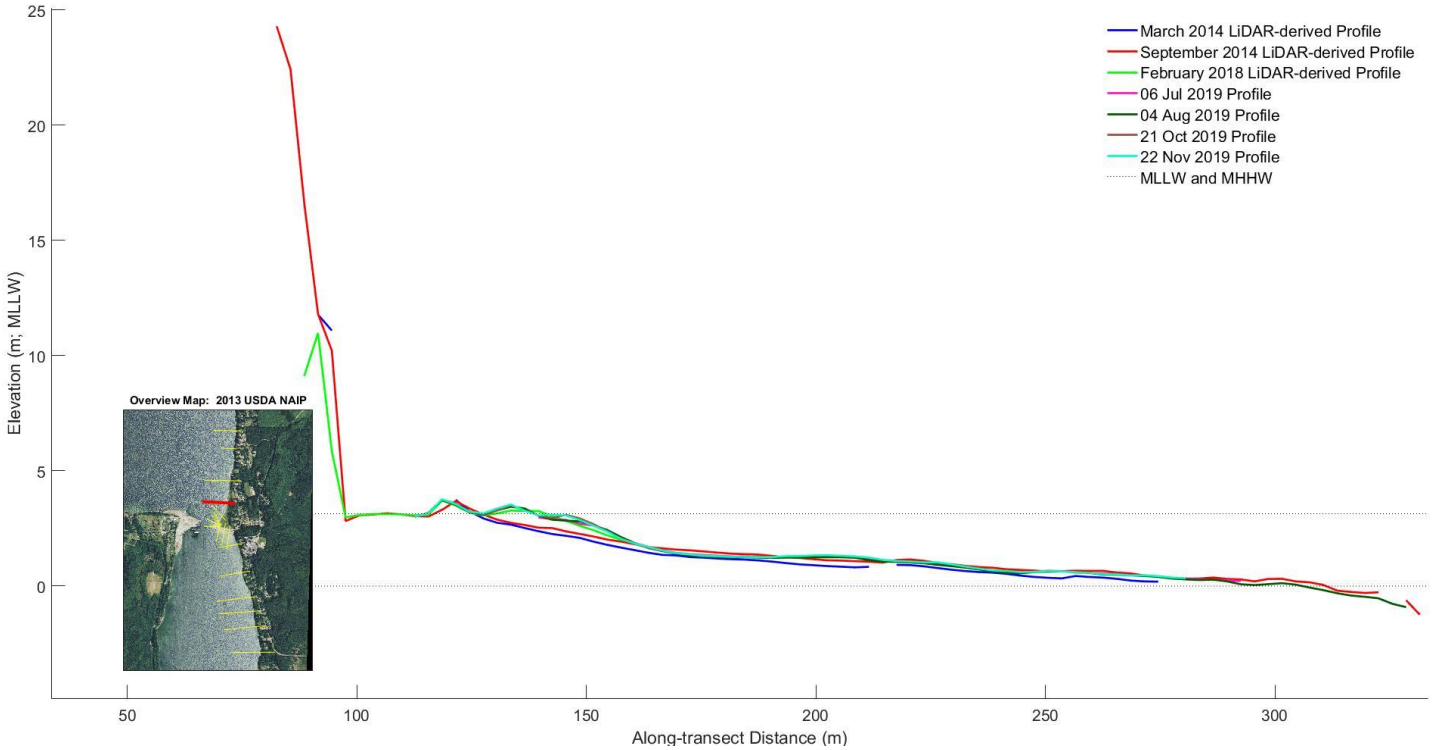

Figure B15. Shoreline profile of Focus transect 15, north of Point Julia. We derived profiles from LiDAR data and GNSS surveying.

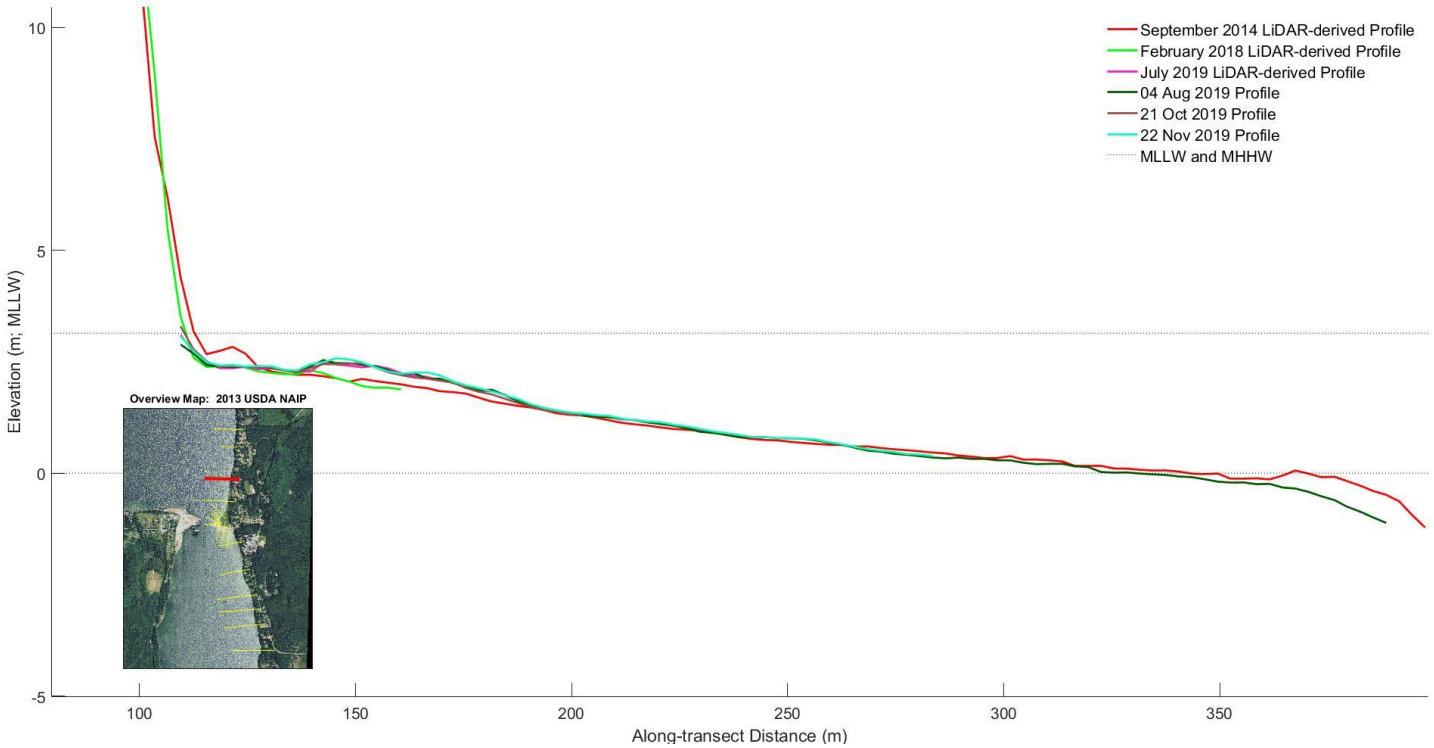

Figure B16. Shoreline profile of Focus transect 16 near the mouth of Shipbuilders Creek. We derived profiles from LiDAR data and GNSS surveying.

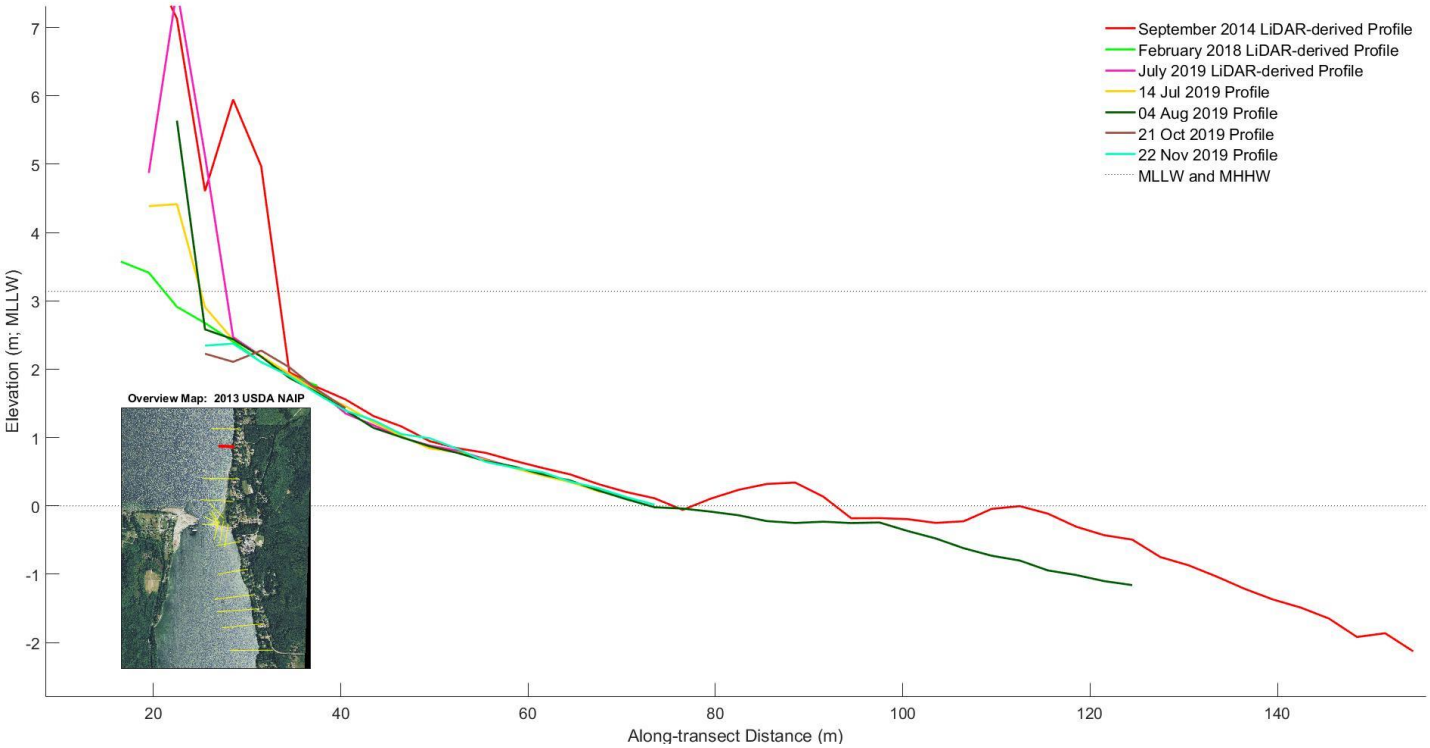

Figure B17. Shoreline profile of Focus transect 17. We derived profiles from LiDAR data and GNSS surveying.

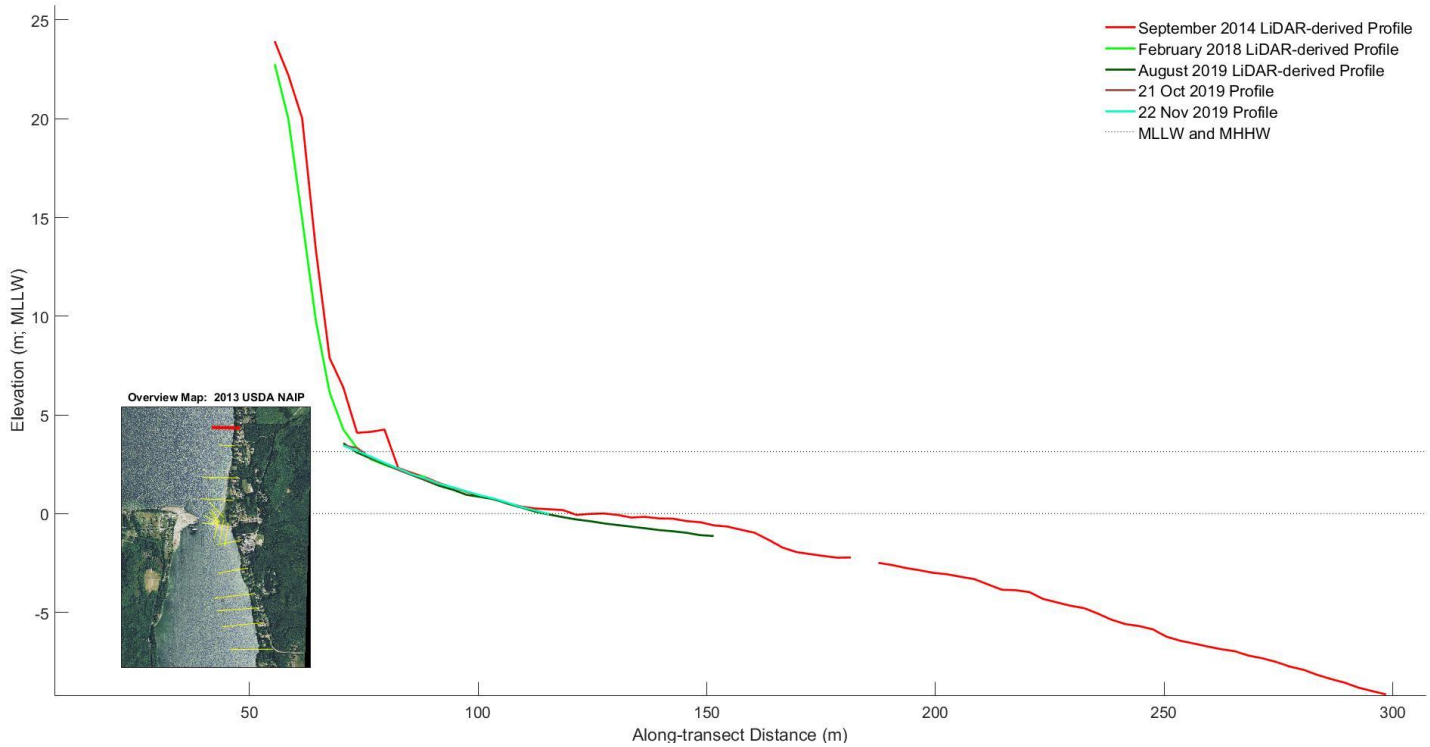

Figure B18. Shoreline profile of Focus transect 18 on the north side of PGST shoreline. We derived profiles from LiDAR data and GNSS surveying.

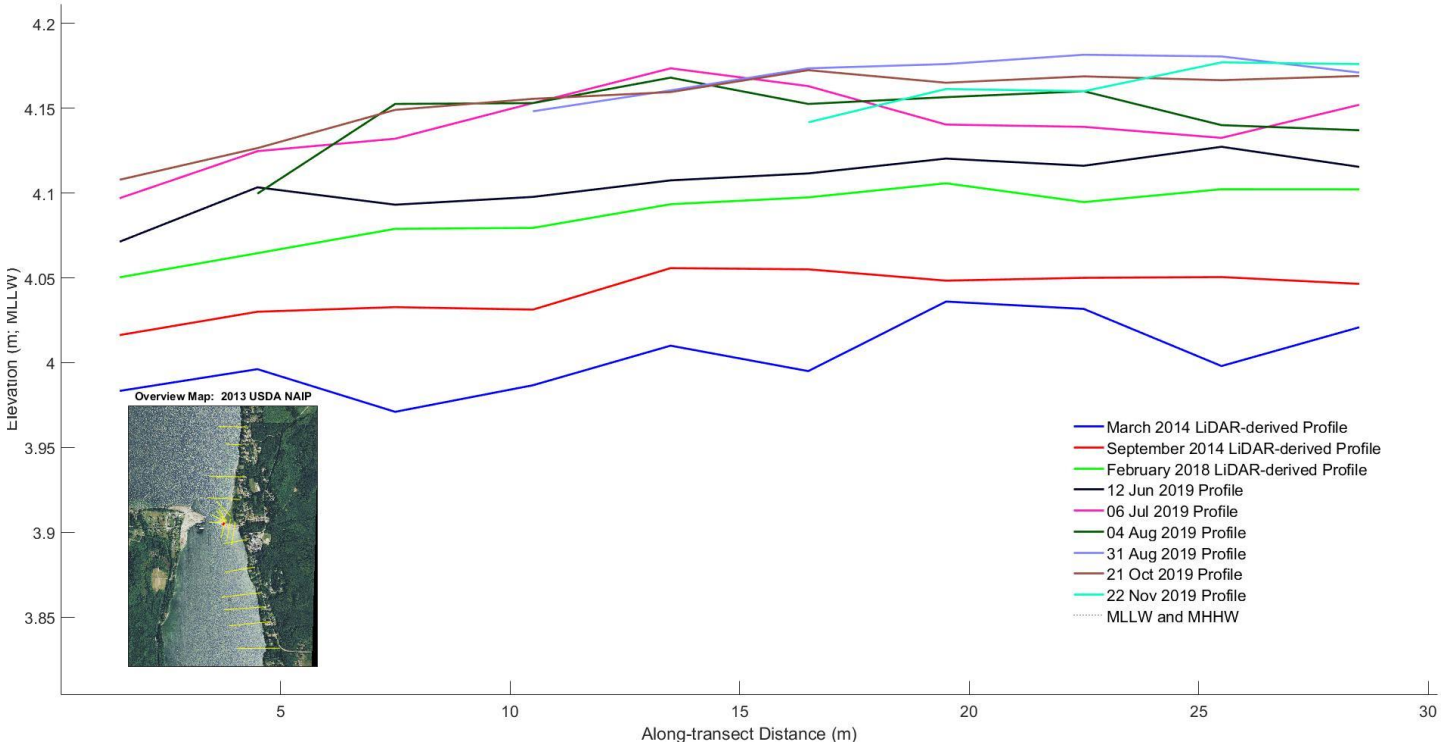

Figure B19. Quality control profile of the road on Point Julia. We used this profile to assess quality and differences between each LiDAR and GNSS survey data set.

10. Appendix C: PGST Coastal Flooding Maps

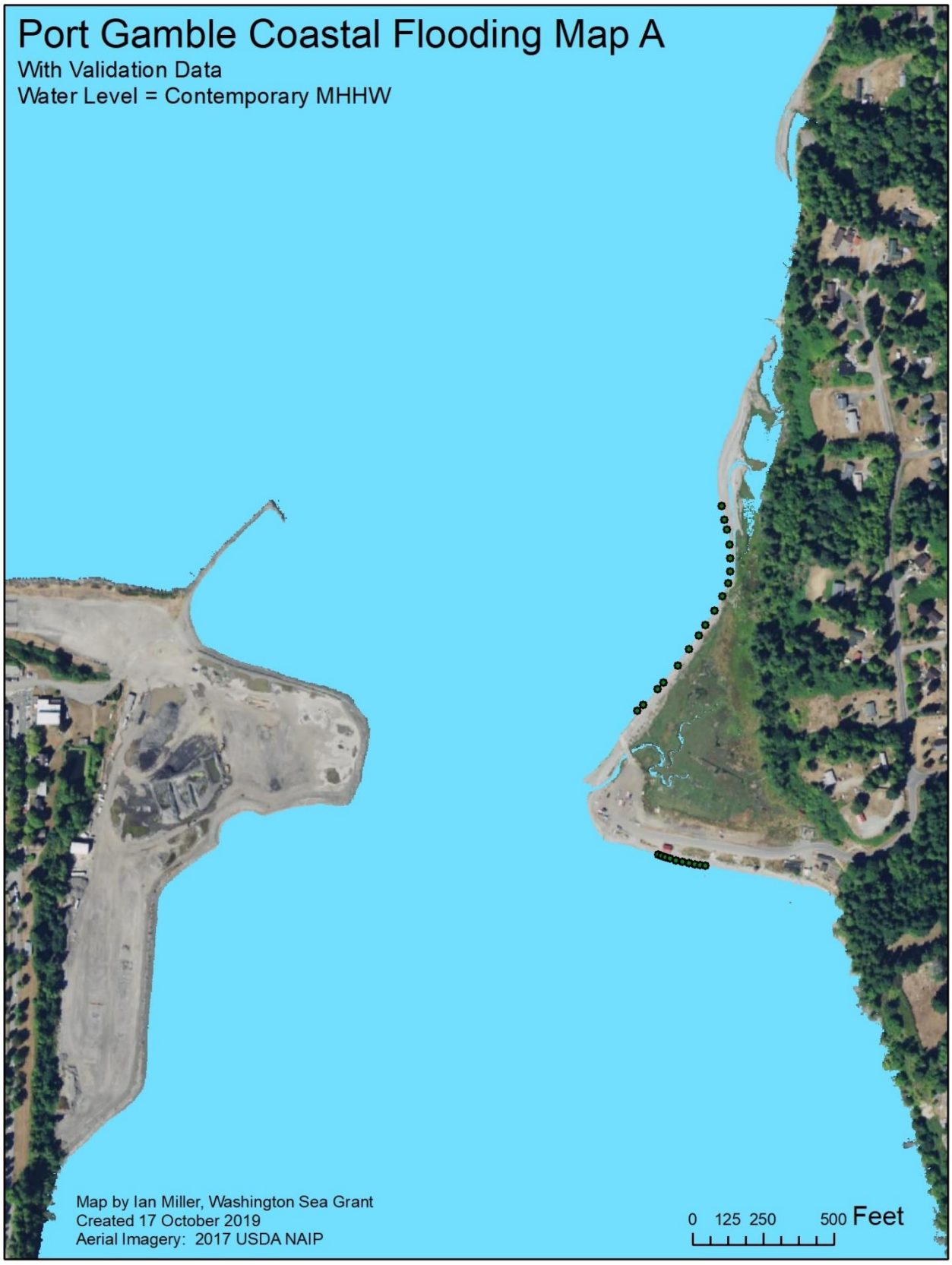

Figure C1. Inundation map showing current flooding extent of Point Julia at current Mean Higher High Water (8.446 ft NAVD 88). Points along Point Julia show the wrack line as surveyed by Sam Phillips in Fall 2019.

Figure C2. Inundation map showing estimated flooding extent of Point Julia at current MHHW plus 1 foot.

Figure C3. Inundation map showing estimated flooding extent of Point Julia at current MHHW plus 2 feet.

Figure C4. Inundation map showing estimated flooding extent of Point Julia at current MHHW plus 3 feet.

Figure C5. Inundation map showing estimated flooding extent of Point Julia at current MHHW plus 4 feet.

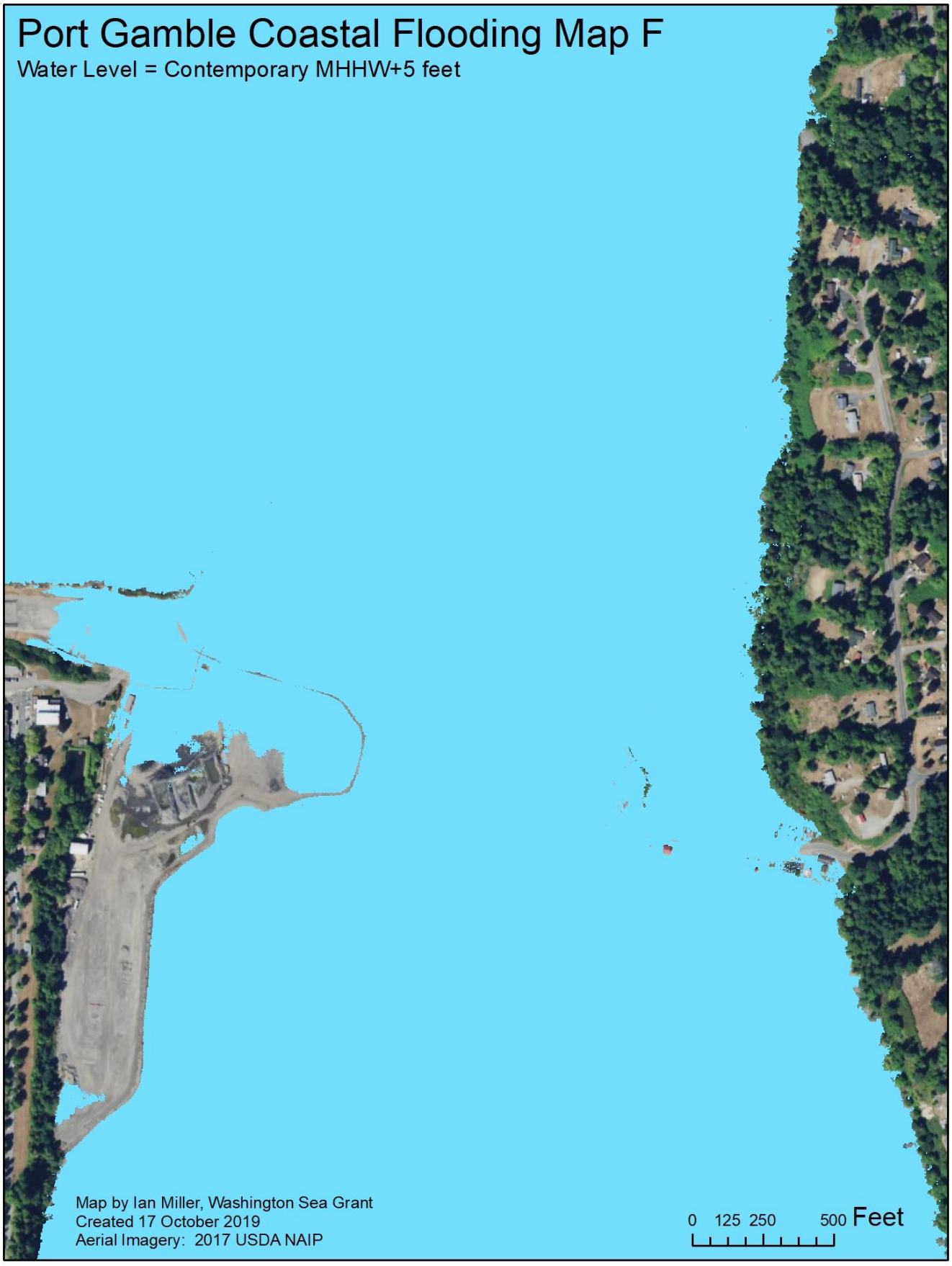

Figure C6. Inundation map showing estimated flooding extent of Point Julia at current MHHW plus 5 feet.

Figure C7. Inundation map showing estimated flooding extent of Point Julia at current MHHW plus 6 feet.

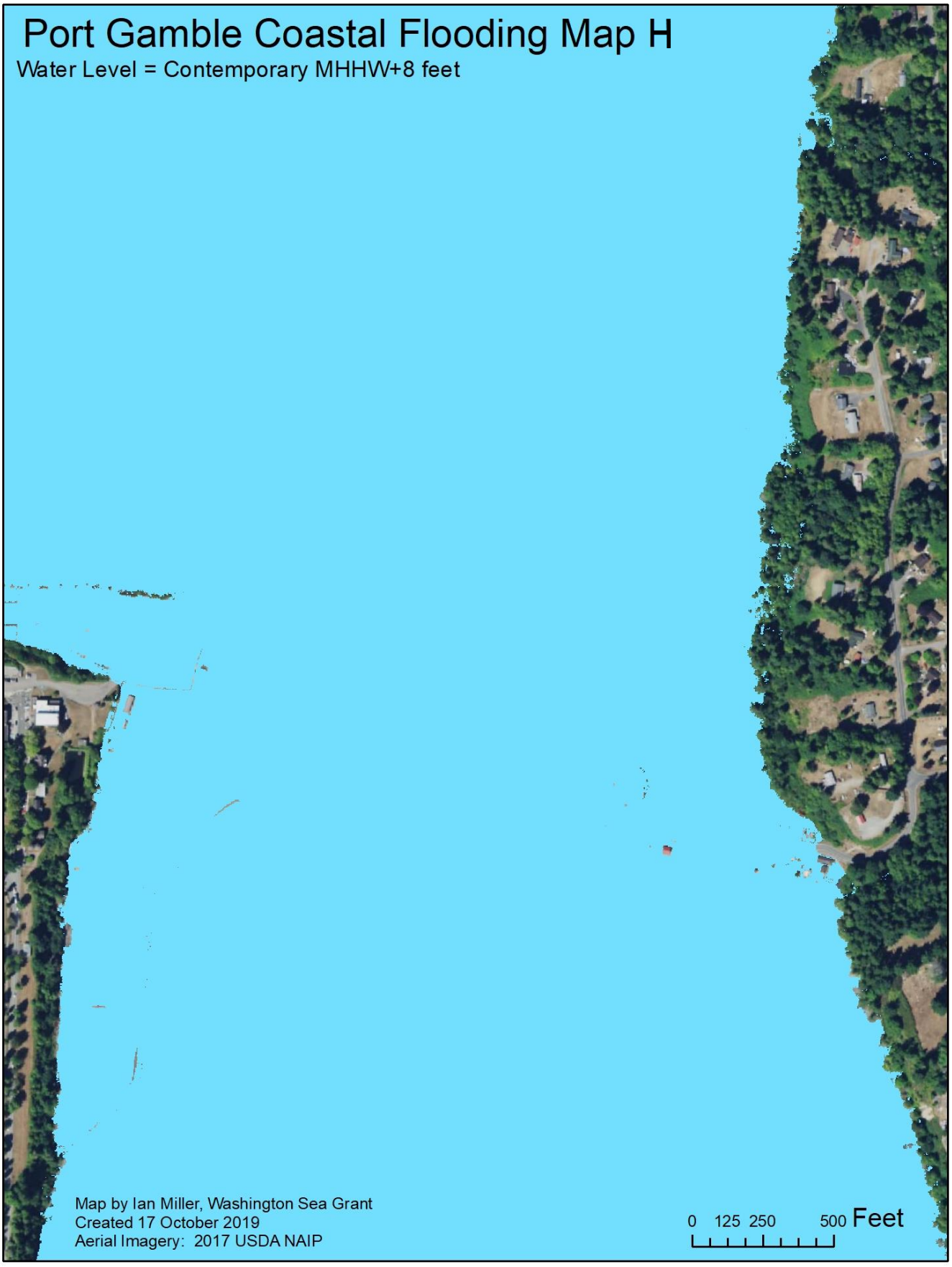

Figure C8. Inundation map showing estimated flooding extent of Point Julia at current MHHW plus 8 feet.

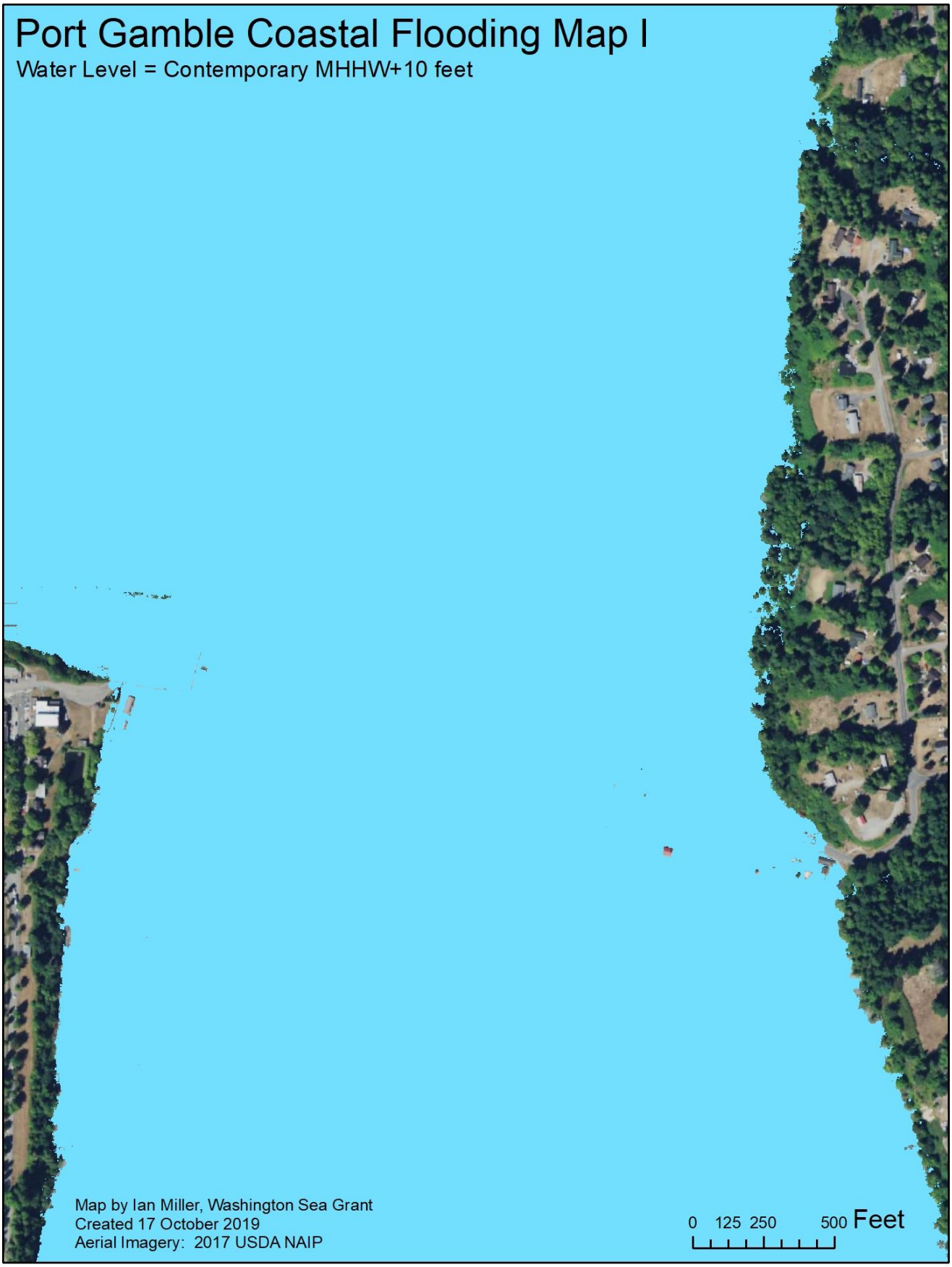

Figure C9. Inundation map showing estimated flooding extent of Point Julia at current MHHW plus 10 feet.